PT - 4601

FREE - SPACE MICROWAVE POWER TRANSMISSION STUDY COMBINED PHASE III AND FINAL REPORT

Technical Report

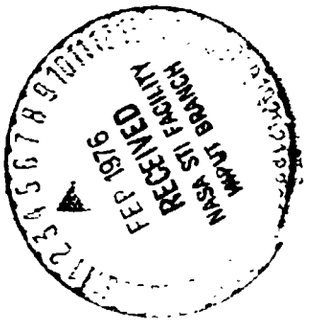

Microwave Tube Operation
Waltham, Massachusetts 02154

RAYTHEON

RAYTHEON COMPANY
Microwave and Power Tube Division
Waltham, Massachusetts

COMBINED PHASE III AND FINAL REPORT

FREE-SPACE MICROWAVE POWER TRANSMISSION STUDY

Report Period: December 9, 1969 - July 31, 1974

Prepared for

Marshall Space Flight Center
Huntsville, Alabama

Under Contract No. NAS-8-25374

Prepared by W. C. Brown, Program Manager

PT-4601
10 September 1975

FOREWORD

This is a final report for a contractual effort on free-space microwave power transmission carried out for the Marshall Space Flight Center during the period from December 9, 1969 to July 31, 1974. The work carried out under this contract represents a major contribution to the technology of free-space power transmission. In particular, the result of this effort has led to the acceptance of the fact that ordinary dc electrical power can be transferred from one point to another with high efficiency by first converting the dc power into microwave power at the transmitting point, forming an efficient microwave beam for transferring the power, and then absorbing this microwave power and converting it back into dc power at the receiving point. The highly efficient behavior of such a power transfer system has not been intuitively accepted because many component and interface efficiencies must be multiplied together to obtain the overall efficiency of the system. Surprisingly, with the selection of the proper technology, it has been found that all of the component efficiencies can be very high.

With general acceptance that efficient transfer of power is possible, it is expected that other basic advantages of a microwave power transmission system will be recognized. These basic advantages include two unique features: the absence of a need for a physical medium for transferring the power from one point to another, and the fact that the energy conversion systems require little material mass. It is a combination of these two features which makes certain new concepts such as the satellite solar power station of practical significance.

The original interest at Marshall Space Flight Center that led to a study of a microwave power transmission system was in connection with an astronomical observatory in which power was to be transmitted from a central manned station to a co-orbiting daughter satellite.[1,2] As a result of this interest, Mr. W. Robinson of NASA-MSFC investigated[3] the state of the art of microwave power transmission and found that a significant amount of experimental work had been done and reported upon.[4,5,6,7,8] Subsequently, W. Brown of the Raytheon Company gave a laboratory type demonstration of microwave power transmission to the MSFC director and his staff in October, 1968.

A contract was subsequently given to Raytheon Company for a system study in December, 1969.

Early in the study, it became apparent that the basic technology needed a considerable amount of upgrading, and this aspect received he bulk of attention in subsequent work. In particular, the efficiency of the reception and rectification part of the system received a great deal of attention. Eventually, this was improved to the point where other portions of the system were limiting the efficiency. Improvements were then made in efficient microwave beam launching. As a result of this effort an overall dc to dc efficiency in excess of 50% was achieved.

In the future the applications of microwave power transmission may be greatly different than those envisaged in 1969 when the effort covered by the following report began. However, the improvements in the technology achieved under the MSFC sponsorship are basic to all applications, new or old, and constitute a major forward thrust in the technology of microwave power transmission.

ACKNOWLEDGMENTS

The initiation of the work described in this report was made possible through the foresight of Dr. Ernst Stuhlinger and the encouragement of Dr. Werner von Braun. The conduct and direction of the effort to a successful conclusion is credited in large measure to Dr. William Johnson and William Robinson, Jr. Thanks are extended to Eugene Eves for his technical contributions.

TABLE OF CONTENTS

LIST OF ILLUSTRATIONS

LIST OF ILLUSTRATIONS (Cont'd)

LIST OF ILLUSTRATIONS (Cont'd)

LIST OF ILLUSTRATIONS (Cont'd)

LIST OF ILLUSTRATIONS (Cont'd)

ABSTRACT

This report presents the results of the contracted portion of a study effort on the technology of free-space power transmission by microwave beam supported by the Marshall Space Flight Center of the National Aeronautics and Space Administration in the time period from December, 1969 to July, 1974. A description of the steps that were taken to increase the overall dc to dc efficiency of microwave power transmission from 15% to over 50% is given.

Included in this overall efficiency were the efficiencies of the dc to microwave conversion, the microwave transmission itself, and the microwave to dc conversion. Improvements in launching the microwave beam with high efficiency by means of a dual-mode horn resulted in 95% of the output of the microwave generator reaching the receiving area. Emphasis was placed upon successive improvements in reception and rectification of the microwave power, resulting in the design of a rectenna device for this purpose whose efficiency was 75%. The test procedures and the hardware developed under this effort were the basis for later tests certified by the Jet Propulsion Laboratory in which an overall dc to dc efficiency of 54% was achieved.

1.0 SUMMARY

1.1 Introduction

This report is the third of a series[9, 10] of reports of a comprehensive and summary nature written under contract number NAS-8-25374. The new material in this report covers the period of June 30, 1972 to July 31, 1974. However, because this report will also be the last one under this contract, important work completed in other phases will either be summarized or be included as appendices to provide a single reference for the total contractual effort.

The major accomplishments of this study may be summarized as follows:

1. Several demonstrations of successively improved overall efficiency of a microwave power transmission system, defined as the ratio of the dc power output of the system to the dc power input.

2. Several basic improvements in rectenna design including (a) more efficient and more powerful GaAs Schottky-barrier diodes; (b) low-pass microwave filter input to the rectenna element; (c) development of a simplified but efficient half-wave rectifier circuit; (d) start of the development of a computer program which takes the fine structure of the rectenna element and the rectifier into consideration; (e) design of a rectenna to use in a high overall efficiency system and to maximize the amount of useful experimental data.

3. Improved method of more efficiently launching the microwave beam.

4. The development of a design procedure for a microwave beam transmission system of arbitrary transmission efficiency and transmission distance in which a point-source of microwave power is used to excite the system.

5. A new design procedure for a low-cost ellipsoidal reflector.

These accomplishments are now described in greater detail:

1.2 Overall Microwave Power Transmission Efficiency Improvements

It is believed that the succession of experiments and demonstrations indicating steady progress in overall microwave power transmission efficiency represents the major accomplishment of this study. An improvement in overall efficiency is the ultimate technical criterion because it reflects not only improvements in efficiency in the parts of the system but also improvements in the interfaces between these parts. High overall dc to dc efficiency is considered a necessary objective for microwave power transmission technology since in nearly all applications ordinary electrical power is available at the transmitting end and ordinary electrical power is wanted at the receiving end. In the context in which we use it, the term ordinary electrical power may be either dc power or 60 cycle ac; the routine conversion between these two forms of ordinary electrical power is not considered a part of the microwave power transmission system.

To understand the nature of the improvements that have been made, it is desirable to break up a microwave power transmission system into the following three major parts as shown in Figure 1 and indicated below:

1. Conversion of dc power to microwave power.

2. Transfer of microwave power from the output of the microwave generator to the receiving point.

3. Collection and rectification of the microwave power at the receiving end.

For convenience, the efficiencies associated with these principal elements will be referred to as η_g, η_t, and η_r, respectively.* Thus, the overall efficiency of the system is $\eta = \eta_g \eta_t \eta_r$.

* Each of these efficiencies breaks down into a set of subefficiencies which are strictly defined and which are needed for detailed study of a microwave power transmission system. For a definition of these efficiencies, see Reference 11.

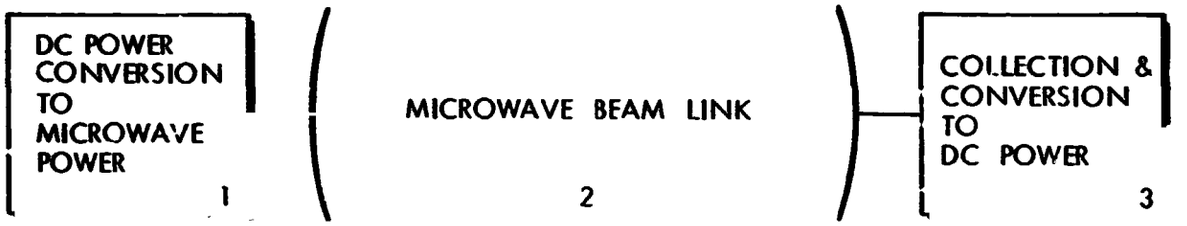

Figure 1. Elements of a Free-Space Microwave Power Transmission System

Before discussing the efficiency results, it may be desirable to point out that the efficiency of the conversion of dc power to microwave power has not been of prime concern to this study. Although we found it expedient in our tests to use off-the-shelf magnetrons which were not particularly efficient, there is experimental data on CW crossed field devices that indicates an efficiency of at least 85% can be obtained.[12, 13, 14] Further, the interface between the microwave generator and the antenna feed is not at all critical. The study, therefore, concentrated on that part of the system beginning at the terminals of the microwave generator and ending at the dc output at the receiving end. That was the portion of the system needing development effort and where obtaining high efficiency was in doubt. Therefore, in presenting the results, the combined transmission and collection rectification efficiency is presented along with the overall dc to dc efficiency.

We have also included in the results certified measurements that were made after the conclusion of the contract. These measurements which were made on the system after the addition of a few modifications to modestly improve the efficiency were certified by Quality Assurance personnel from Jet Propulsion Laboratory in response to a desire expressed for certified measurements by Dr. William Johnson of MSFC and Samuel Fordyce of the Communications Directorate at NASA headquarters.[15] These results are included here because of their very close association with the MSFC work and because they aid the credibility of the other results that are presented.

Figure 2 indicates the progress that has been made in the efficiency of microwave power transmission as a function of time. The overall dc to dc efficiency has increased from 15% in 1963 to 54% in 1975. And the combined transmission and collection efficiency (the ratio of the dc output from the rectenna to the rf power out of the microwave generator source) has increased from 25% to 78%. It is interesting to observe that if a microwave generator of 85% efficiency (a reasonable value to expect from a tube specifically designed at 2450 MHz for this kind of application) had been available, an overall dc to dc efficiency of 66% would have been realized.

With Figure 2 as a reference to identify the successive developments, it may be of interest to review the high points of these successive developments.

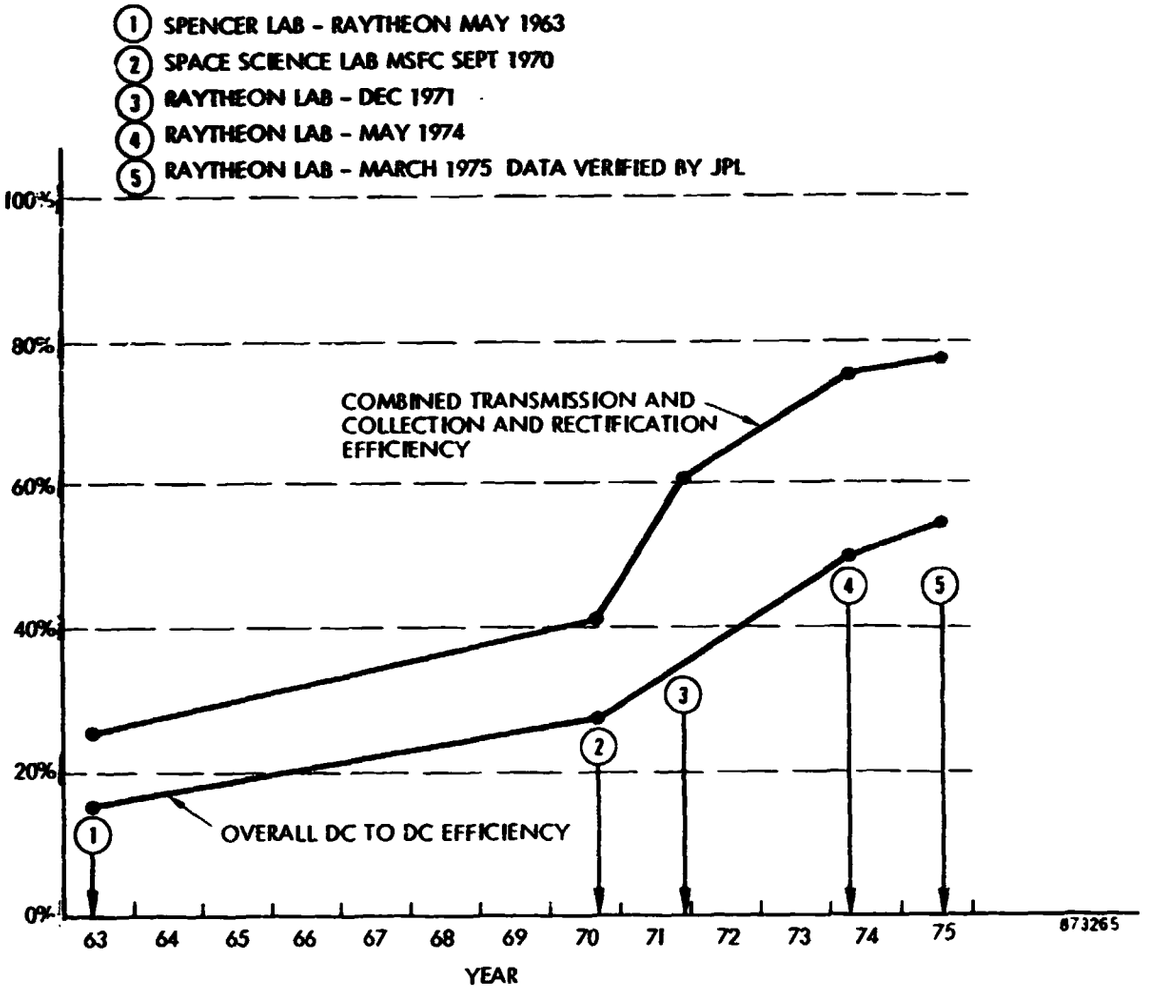

Figure 2. Progress in the Efficiency of Free-Space Microwave Power Transmission as a Function of Time

The point of departure for efficiency improvement was the microwave power transmission system tested at Spencer Laboratory[5] of the Raytheon Company in 1963. A photograph of this set up is shown in Figure 3. The approach used conventional transmitting and receiving apertures, and a close-spaced thermionic diode as a rectifier. From the standpoint of high efficiency, the results clearly demonstrated the inability of the receiving aperture to match the incoming beam pattern with good efficiency, and the limited capability of the close-spaced diode rectifier.

The next measurement of overall efficiency was on a system assembled at Raytheon and transported to Marshall Space Flight Center where the overall efficiency measurements were made in 1970.[16] This system is shown in Figure 4. As shown in Figure 4, the system uses a completely new type of receiving device called the "rectenna". The rectenna device had been conceived and developed in the intervening period of time for a helicopter application.[17] Although the rectenna was in an early stage of development, it had the potential to match efficiently to any pattern of incoming radiation. It also utilized solid state rectifiers which also had the potential for very high efficiency. Although there was an improvement in the overall efficiency with this arrangement, and the rectenna was an exciting innovation, there were two defects in the system. One of these was the large amount of power contained in the side lobes of the power radiated from the horn. The other was a large amount of power reflected from the rectenna.

The next effort was devoted to correcting these defects.[18] The deficiency of the radiating horn was corrected with the design and construction of a dual mode horn.[19] The reflected power from the rectenna was greatly reduced by placing the elements closer together. A better geometry of the system was also established by making the rectenna in circular form to match the circular pattern of the beam. These changes had the impact of increasing the combined transmission and collection and rectification efficiency from 41% to 61%, and pointed the way toward further improvement by taking full advantage of the gaussian illumination pattern of the dual-mode horn and the circular format of the rectenna. The test set up for this development stage is shown in Figure 5.

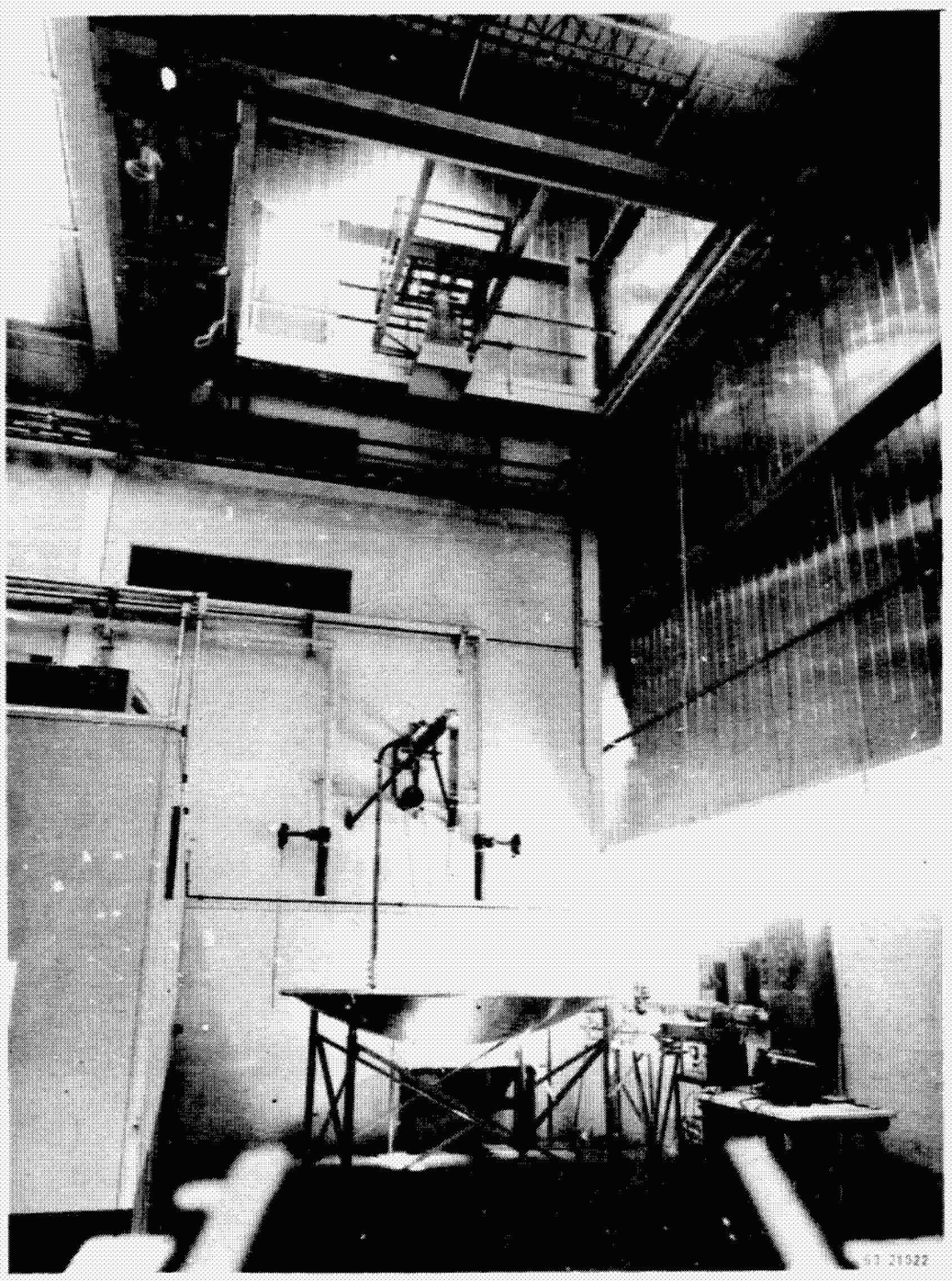

Figure 3. First demonstration of the efficient transfer of meaningful amounts of power by a microwave beam, at Spencer Laboratory of Raytheon Company, in May 1963. Ratio of dc power output of the rectifier (close-spaced thermionic diode) to rf power output of the magnetron was 25%. DC power output was 100 watts. Microwave frequency was 3 GHz.

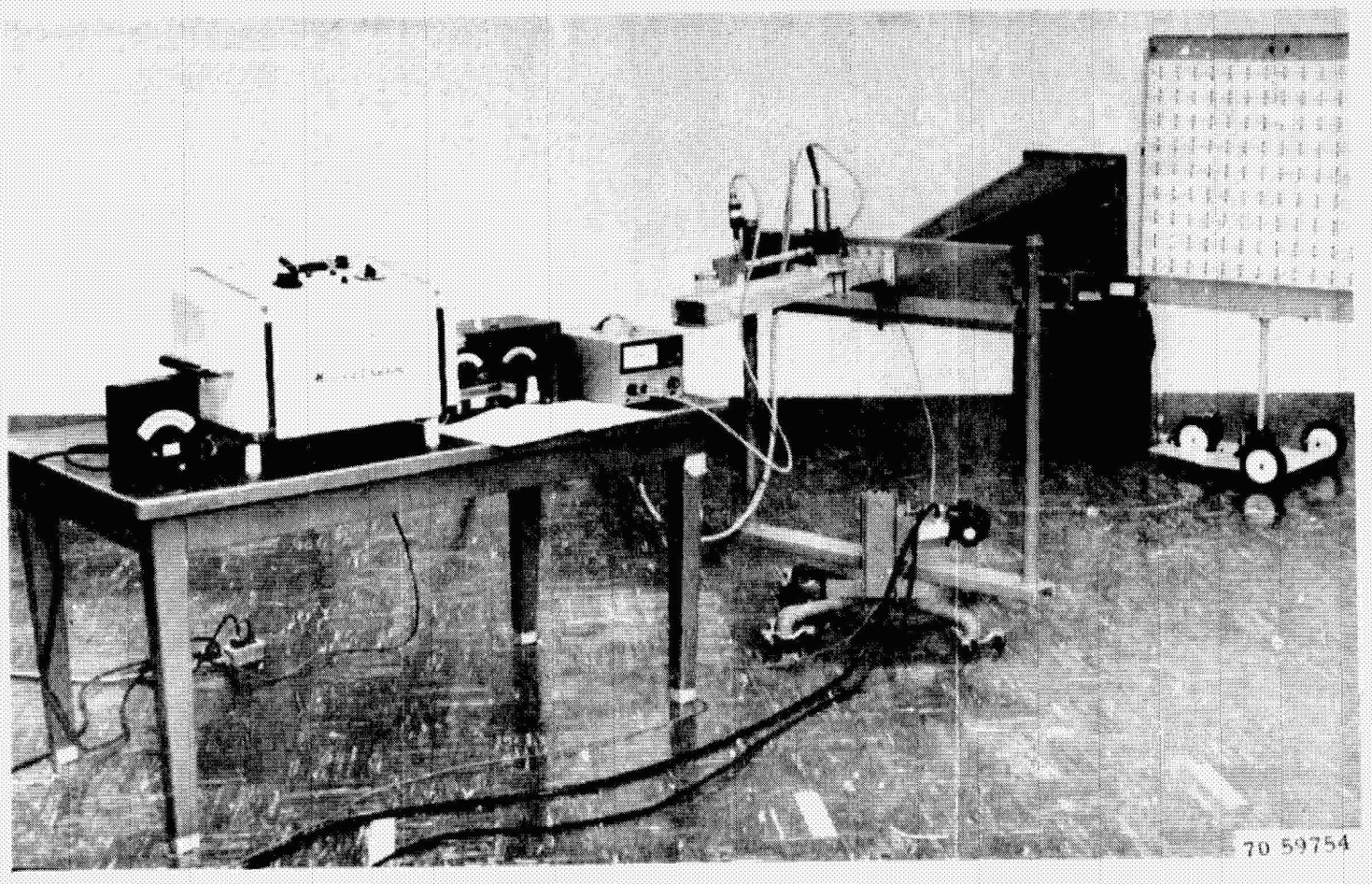

Figure 4. Demonstration of overall dc-to-dc efficiency in a microwave power transmission system at Marshall Space Flight Center in September 1970. Ratio of dc power out of rectenna to dc power going into magnetron was 26.5%. Ratio of dc power out of rectenna to rf power out of magnetron was 40.5%.

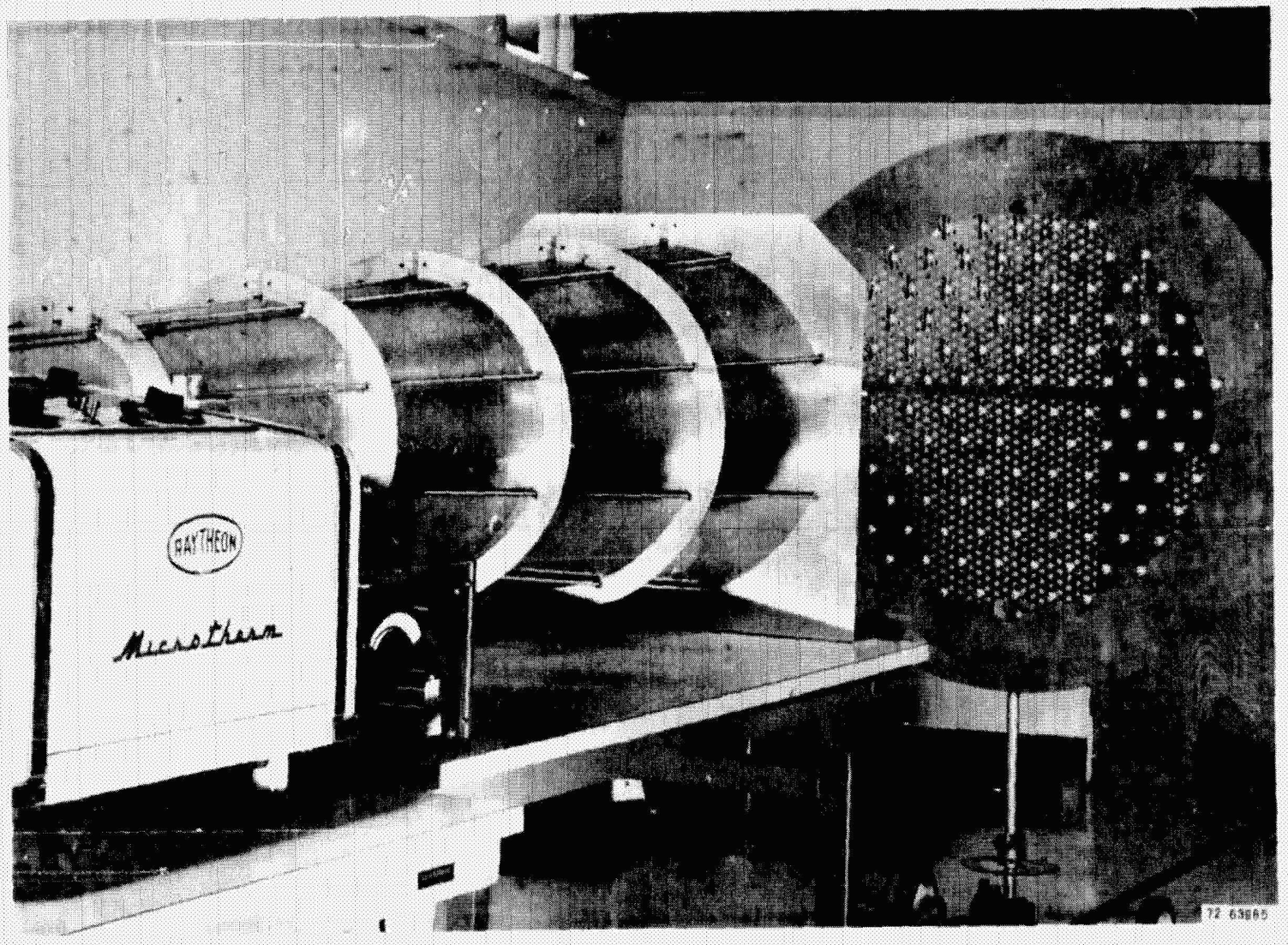

Figure 5. Experimental set-up comprised of dual-mode horn and improved rectenna. The efficiency ratio of the dc power from the rectenna to the microwave power at the input to the dual-mode horn was measured and found to be 60.2%.

The next major step forward was the construction of a greatly-improved rectenna which made use of GaAs Schottky barrier diodes. These GaAs diodes, normally used for Impatt applications, were found to have much higher power handling capability and to be considerably more efficient than the silicon Schottky-barrier diodes. These diodes were used in a greatly improved rectenna element. The element contained wave filters for the suppression of harmonic radiation and for energy storage. A single diode was used in a half-wave rectifier mode which greatly simplified the circuit topology and greatly reduced the diode cost which would have been encountered with the 4-diode full wave bridge rectifier previously used. Each rectenna element was identified with a location within the rectenna and then matched out to give minimum reflection at the power level projected for it in the array.

The much higher power handling capability of the Schottky barrier diode and the expanded size of the rectenna from 3 feet to 4 feet diameter made it possible to utilize a microwave-oven magnetron as the transmitting tube. This tube, after suitable rematching, was more efficient than the previous lower powered magnetron that had been used.

The system reflecting these additional improvements is shown in Figure 6. An overall efficiency of 48%, believed to be at the lower limit of the probable measurement error, was obtained in May 1974. With a slight change in some of the test conditions and a better method of data collection which decreased the uncertainty, a value of dc to dc efficiency of 51.2% was achieved in the following July, 1974.

This measurement concluded the effort under the MSFC contract. However, the system shown in Figure 6 became the basis of certified measurements that were made during March, 1975. The rectenna was outfitted with improved rectenna elements* which had on the average about 1.5% more efficiency. As a result of this and some minor equipment changes, a certified efficiency of 54.18 ± 0.94% was made in March, 1975.[15]

A summary of the various system efficiency tests and the efficiencies that have been obtained from them is given in Figure 7.

---

* These elements, based upon the MSFC design, were designed for a 26 square meter rectenna constructed for the transmission of 30 kW of dc power over a distance of one mile at the Goldstone facility of the Jet Propulsion Laboratory.

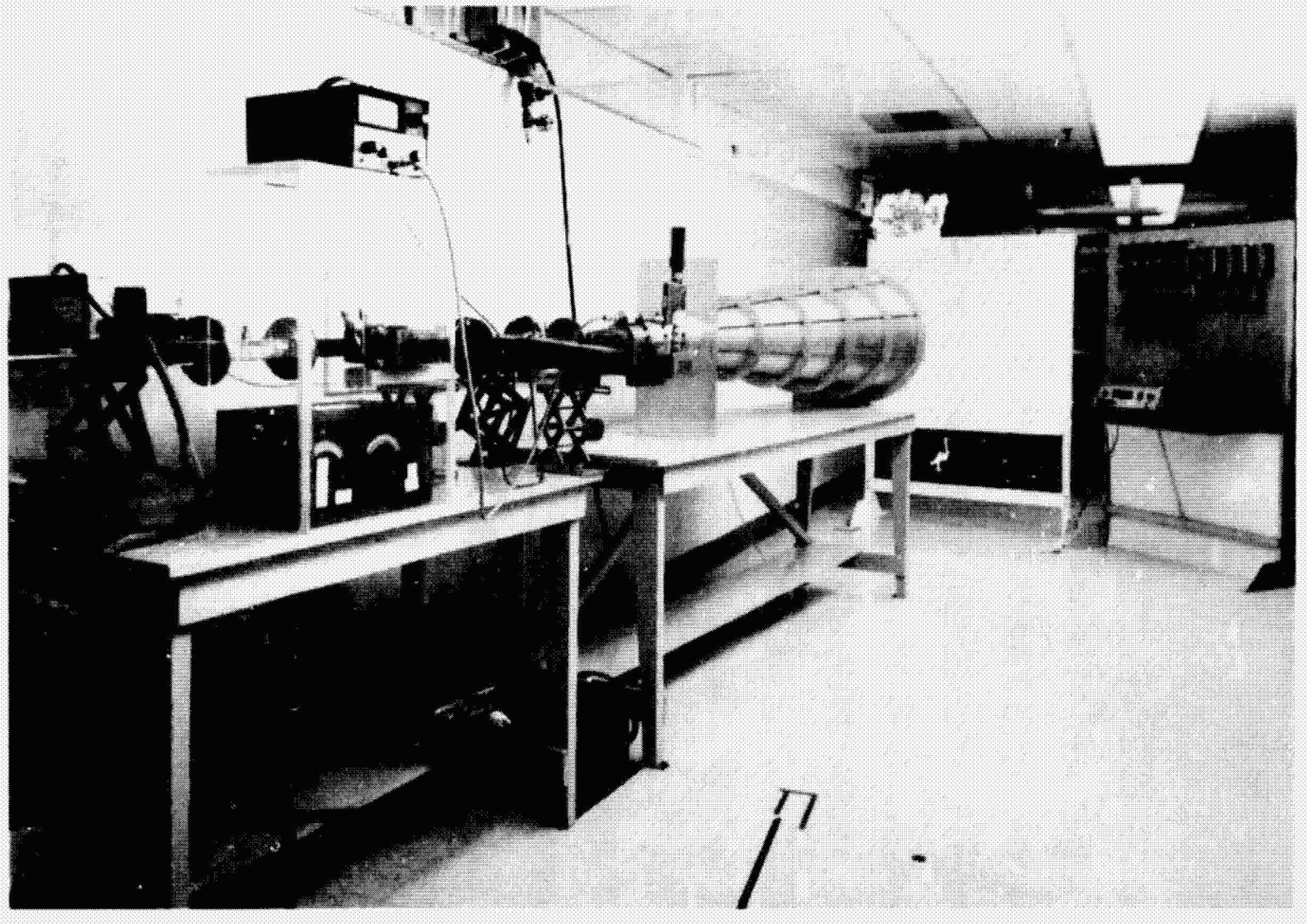

Figure 6. Photograph of the overall microwave power transmission system constructed in 1974. Magnetron at left of picture converts dc power into microwave power which is fed into the throat of the dual-mode horn. The horn illuminates the rectenna panel with a gaussian distribution of power. Rectified dc power is collected from the rectenna in circular ring paths and is dissipated in resistive loads on the test panel at the right.

EFFICIENCY TESTS		EFFICIENCIES OBTAINED			
DATE	LOCATION	η_g Generation	η_t Transmission	η_r Reception	Overall DC-DC
MAY 1963	SPENCER LAB RAYTHEON	60%	66%	38.5%	15.3%
SEPT 1970	MSFC, NASA	65	80	51.0	26.6
DEC 1971	RAYTHEON	--	94	64.0	--
MAY 1974	NEW PRODUCTS RAYTHEON	68	95	75.0	48
MARCH 1975	RAYTHEON JPL CERTIFIED	69	95	82	54

Figure 7. Summary of microwave power transmission system developments and the efficiencies that have been obtained from them.

The system efficiencies that have been obtained so far are interim efficiencies only. Considerably higher efficiencies can be expected just from taking advantage of present technology, most notably in the generator area. Additional efficiency can also be expected to result from additional development in the three major component areas. Laboratory microwave system efficiency projections are given in Figure 8. in which an efficiency of 69.0% is projected with the best use of present technology, and an efficiency of 78% is projected after a vigorous program of research and development.

1.3 Basic Improvements in Rectenna Design and Measurements of Rectenna Performance

The early system study of the design requirements imposed upon the receiving array and the subsequent efforts to improve the capture and rectification efficiency of the receiving portion of the system have provided many concepts and a great deal of design information. Much of the philosophy of rectenna design, a considerable amount of analysis, and many of the improvements in the rectenna were discussed in the Phase II final report. Work under Phase II introduced the concept of the rectenna element utilizing a half-wave rectifier circuit, a new GaAs Schottky barrier diode, and a wave-filter input for energy storage and suppression of harmonic radiation. There was also

	EFFICIENCY PRESENTLY DEMONSTRATED	*EFFICIENCY EXPECTED WITH PRESENT TECHNOLOGY	*EFFICIENCY EXPECTED WITH ADDED DEVELOPMENT
MICROWAVE POWER GENERATION	76%	85.0%	90.0%
TRANSMISSION EFFICIENCY FROM OUTPUT OF GENERATOR TO COLLECTOR APERTURE	95%	96.0%	96.0%
COLLECTION AND RECTIFICATION EFFICIENCY (RECTENNA)	82%	85.0%	90.0%
OVERALL EFFICIENCY, DC OUTPUT/DC INPUT COMPUTED	59%	69.0%	78.0%
OVERALL EFFICIENCY, DC OUTPUT/DC INPUT MEASURED	54%		

*FREQUENCY OF 2450 MHz (12.2CM WAVELENGTH)

879880

Figure 8. Microwave system efficiency projections.

a considerable amount of analysis, and the first efforts at a computer program which would accurately take the nonlinearities and the fine structure of the rectenna element into account. Work under Phase II did not result in a new rectenna but it laid the foundation for a greatly improved rectenna in Phase III. Because of the importance of this work under Phase II, we have included it as Appendix I of this report.

We will include here a brief summary of the rectenna work done under the final phase of the contract and not reported upon previously. It was apparent from an analysis effort started in Phase II and completed in Phase III of the losses in the diode, backed up by measurements of diode parameters and microwave rectification efficiency, that it should be possible to design diodes that would operate at considerably higher efficiency than those tested in Phase II and which were GaAs Schottky barrier diodes designed for Impatt Applications. This work is covered in Section 4.0 of this report. As a result of this effort and a close working relationship with the Raytheon operation which designs GaAs Schottky barrier diodes, we were able to work out a procurement program for diodes in Phase III that not only resulted in diode lots whose average efficiency was much greater but whose efficiency variation was remarkably small.

In addition, the procurement became an exercise in how to specify diodes that would provide consistently high microwave rectification efficiency without the diode manufacturer having to concern himself with any microwave testing. This became a procurement model for the diodes in the JPL RXCV program.

The distribution curve of efficiency is given as Figure 9. The critical efficiency parameter in specifying diode procurement is the forward voltage required for 200 milliamperes of forward current, as this parameter is closely related to the series resistance in the diode which is the principal source of diode loss. The distribution curve with this parameter is shown in Figure 10. The diodes having high voltage are seen to lie beyond the normal distribution curve and were invariably associated with low microwave rectification efficiency.

A decision was made in Phase III to construct the test rectenna in such a way as to obtain the maximum amount of test information from it, including some reliable measurement of the amount of reflected power. This latter measurement is desirable from a fundamental point of view, because while it has been assumed that the collection efficiency of the rectenna can, like a conventional phased array, approach 100%, an experimental confirmation is needed. The gaussian illumination pattern on the test rectenna made it necessary to operate the rectenna elements over a power range of fifty to one, and over this range an element without retuning can have a considerable percentage of the incident power reflected. It was, therefore, necessary to assign each element to a position in the array and then tune it for minimum reflected power at the power level anticipated for its operation. The circular gaussian illumination pattern made it convenient to parallel the outputs of the elements sharing a common radius and form a set which used a common load resistor. In an array of 199 elements, it was found that there were 22 common radii including the center element, and that there were either 6, 12, or 18 elements in a set, excluding the center element. It was also possible to instrument the individual power output of each element by means of an individual socket with a current jack.

The rectenna resulting from Phase III is shown in Figures 11, 12, 13, 14, and 15. These figures show in the following order: a front view of the rectenna with 199 rectenna elements in place; a rear view of the rectenna showing the individual sockets

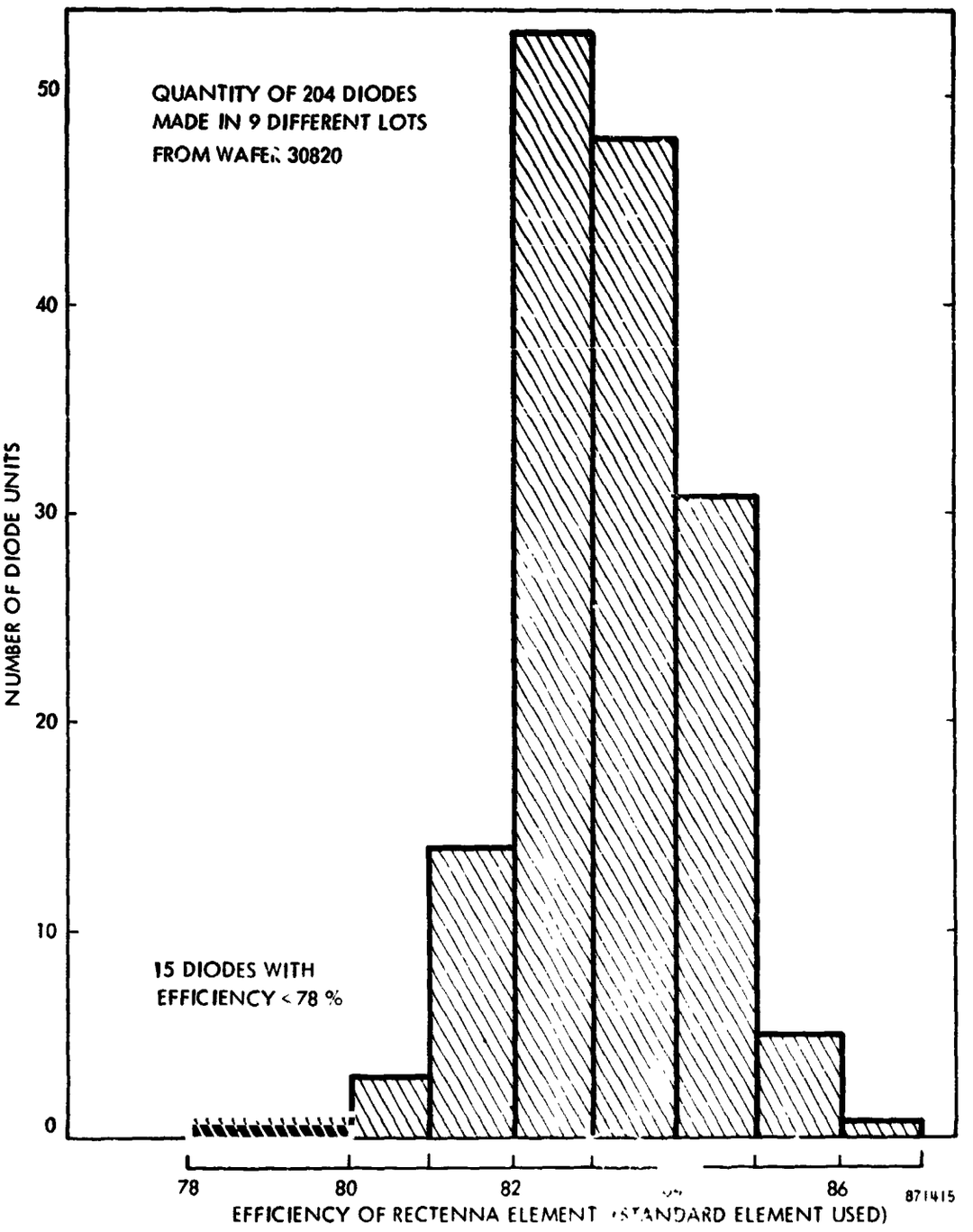

Figure 9. Distribution curve for the efficiency of a quantity of 204 Type No. MS50336 GaAs Schottky Barrier Diodes as measured in a standard rectenna element with a two-section, low-pass input filter. The rectenna elements were measured in the expanded waveguide fixture.

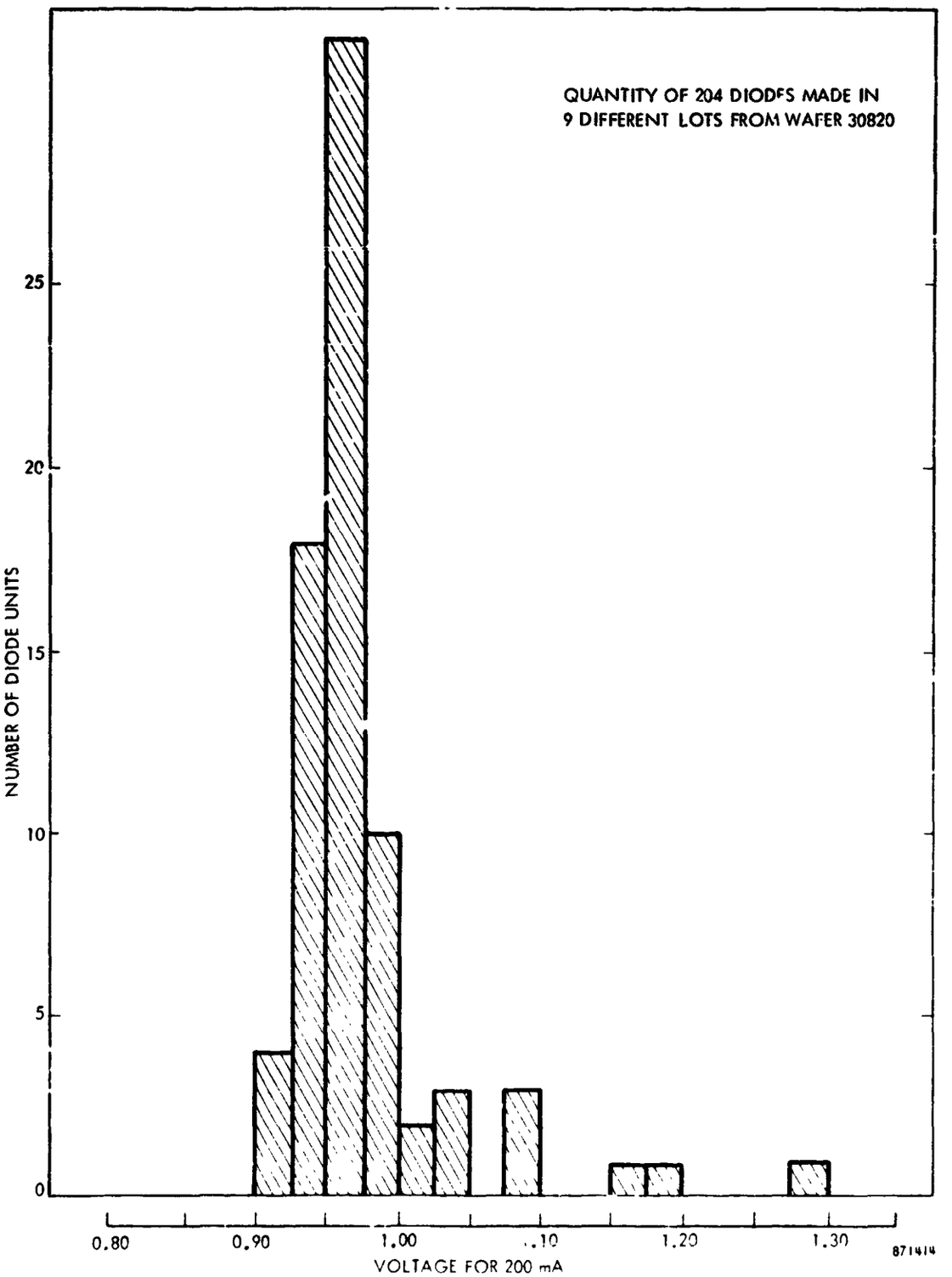

Figure 10. Distribution of a measurement parameter (forward bias voltage for 200 mA of forward current) which is closely related to the series resistance of the diode of a quantity of 204 Type No. MS50336 GaAs Schottky Barrier Diode

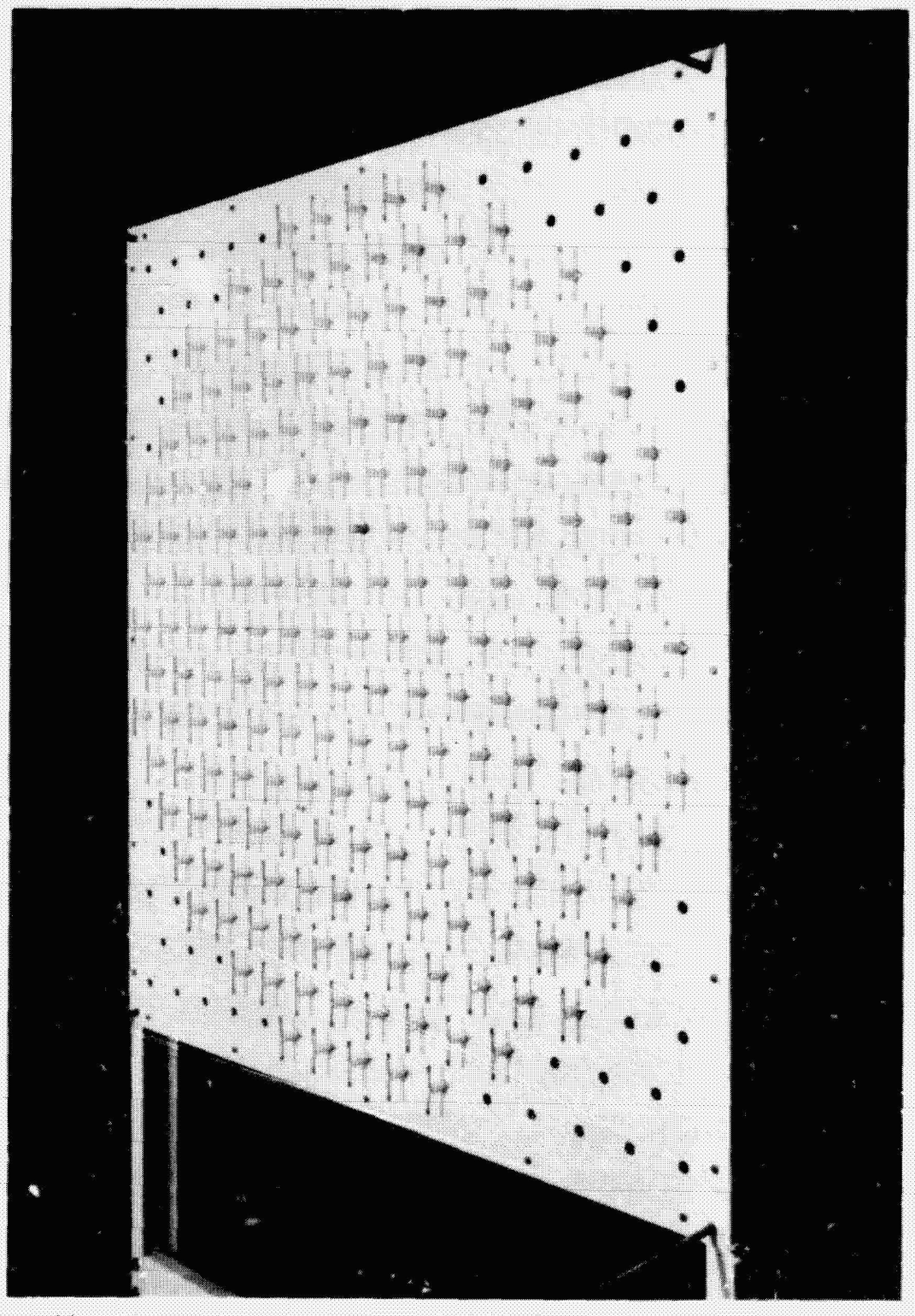

Figure 11. Front view of th Phase III 199 element rectenna. The elements are arranged in an essentially circular format. Width and height of panel are 4 feet (1.22 meters).

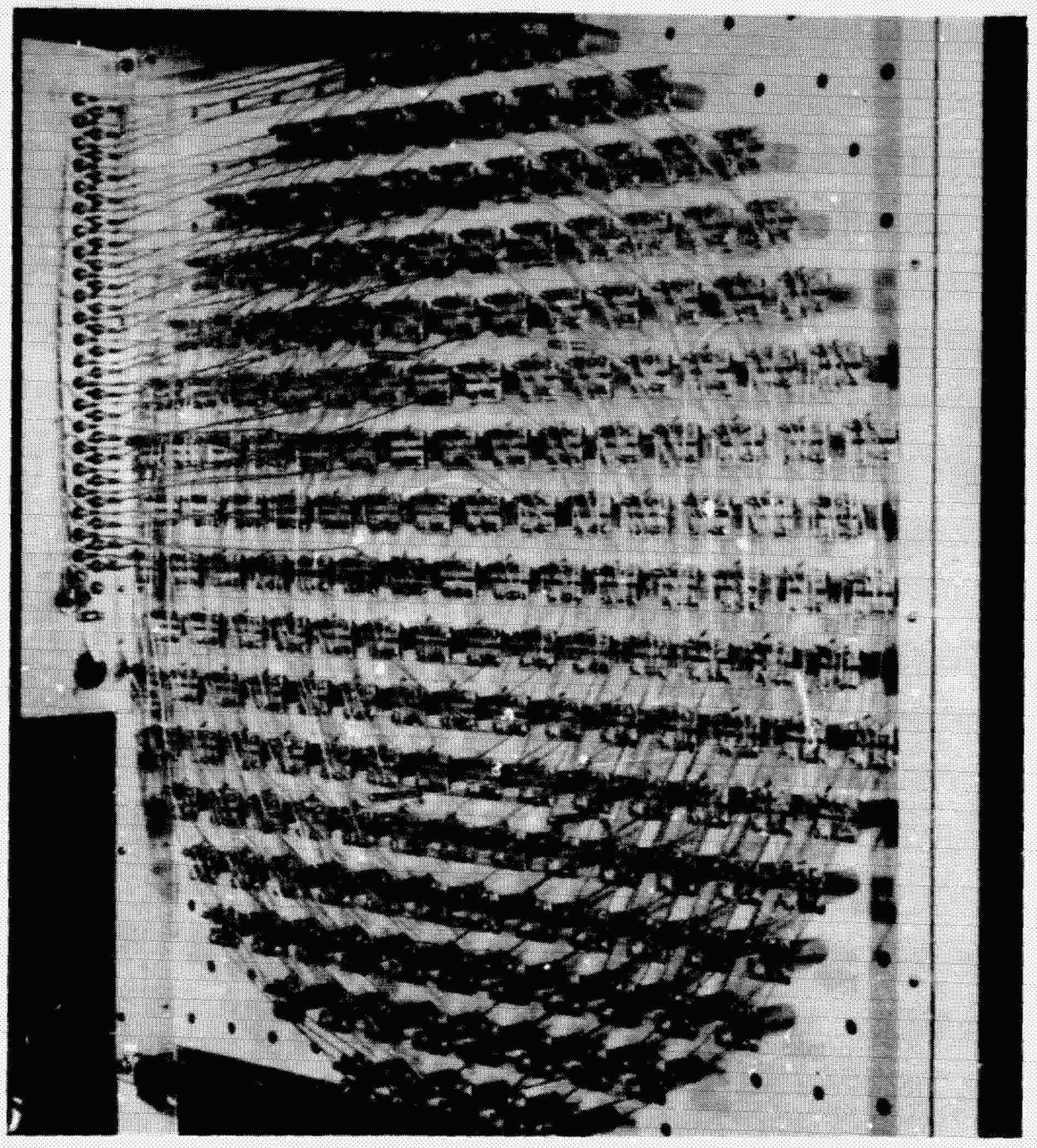

Figure 12. Back view of the Phase III 199 element rectenna, showing the circular format of the wiring and the output connections for the 22 sets of rectenna elements.

Figure 13. Close-up view of the back of the Phase III rectenna, showing the individual sockets for each element and the current jacks for measuring the current output of the element. The element makes a sliding spring contact with the socket so that the spacing of the element dipole to the reflecting plane may be easily varied.

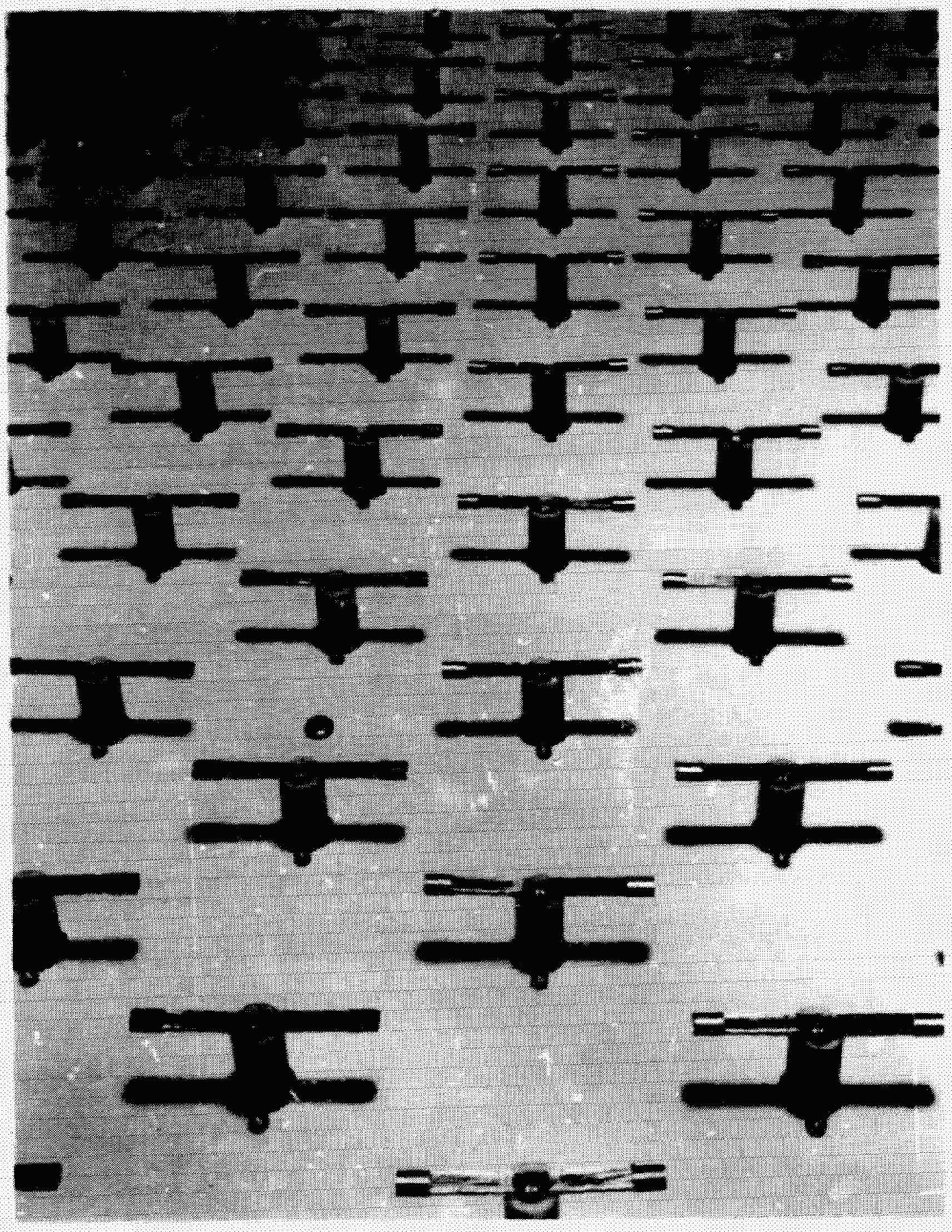

Figire 14. Close-up view of the front side of the Phase III 199 element rectenna.

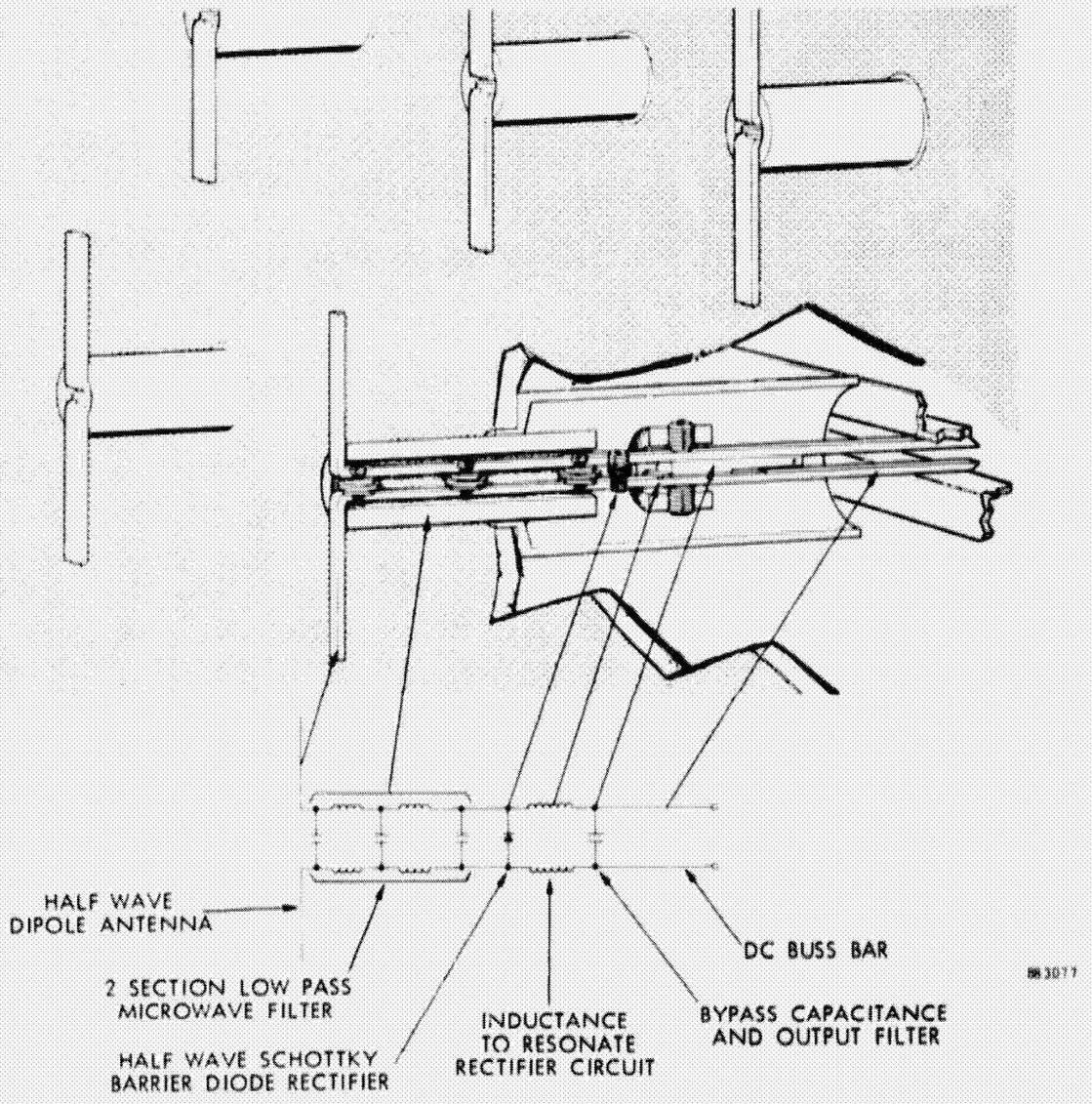

Figure 15. Cutaway section of the rectenna element showing the mechanical and electrical construction of the element, and how it plugs into its socket

and the parallel wiring which brings the dc output into 22 separate terminal pairs; a closeup view of the back of the rectenna; a closeup view of the front end of the individual rectenna elements; and a line drawing showing a cutaway view of the rectenna element and how it is connected to the socket. More views of the rectenna and its test panel are shown in Figures 6 and 30.

In sharp contrast to the work just discussed and to illustrate the wide scope of the investigations under this study, Figure 16 is included. This figure shows work that was done in Phase I of the program on printed circuit format for a flexible rectenna that would have minimal weight and could be deployed in space. A summary of this activity copied from the Phase I report is included as Appendix II.

1.4 Improved Method of Launching the Microwave Beam

A high value of overall microwave transmission efficiency is dependent upon how much of the power coming from the generator is contained in the main lobe of the microwave beam pattern. As noted in section 1.2, a simple pyramidal horn has a great deal of energy in the sidelobes. Fortunately, the development of the dual mode horn by P. D. Potter[19] of JPL. has made it possible to get almost all of the energy into the main lobe. Based upon his work, we designed a dual mode horn to operate at 2450 MHz. The design of this horn is shown in Figure 17. The completed dual-mode horn with rings in place to control concentricity is shown in Figure 18.

The dual mode horn has the very desirable characteristic that the distribution of energy in the antenna pattern is essentially gaussian for distances from the horn greater than one or two horn-mouth diameters. The shape of the pattern is shown in Figure 19.

1.5 The Development of a Design Procedure for a Microwave Beam Transmission System of Arbitrary Efficiency and Transmission Distance in Which a Point-Source of Microwave Power is Used to Excite the System.

G. Goubau[20] has shown that very high efficiency, approaching 100%, is possible for transmission of microwave power from one aperture to another, providing the distribution of illumination on the transmitting aperture is properly set. For high transmission efficiency, the distribution is sufficiently close to a gaussian, slightly truncated at the edges, to be efficiently illuminated with a beam emitted by the dual mode horn which

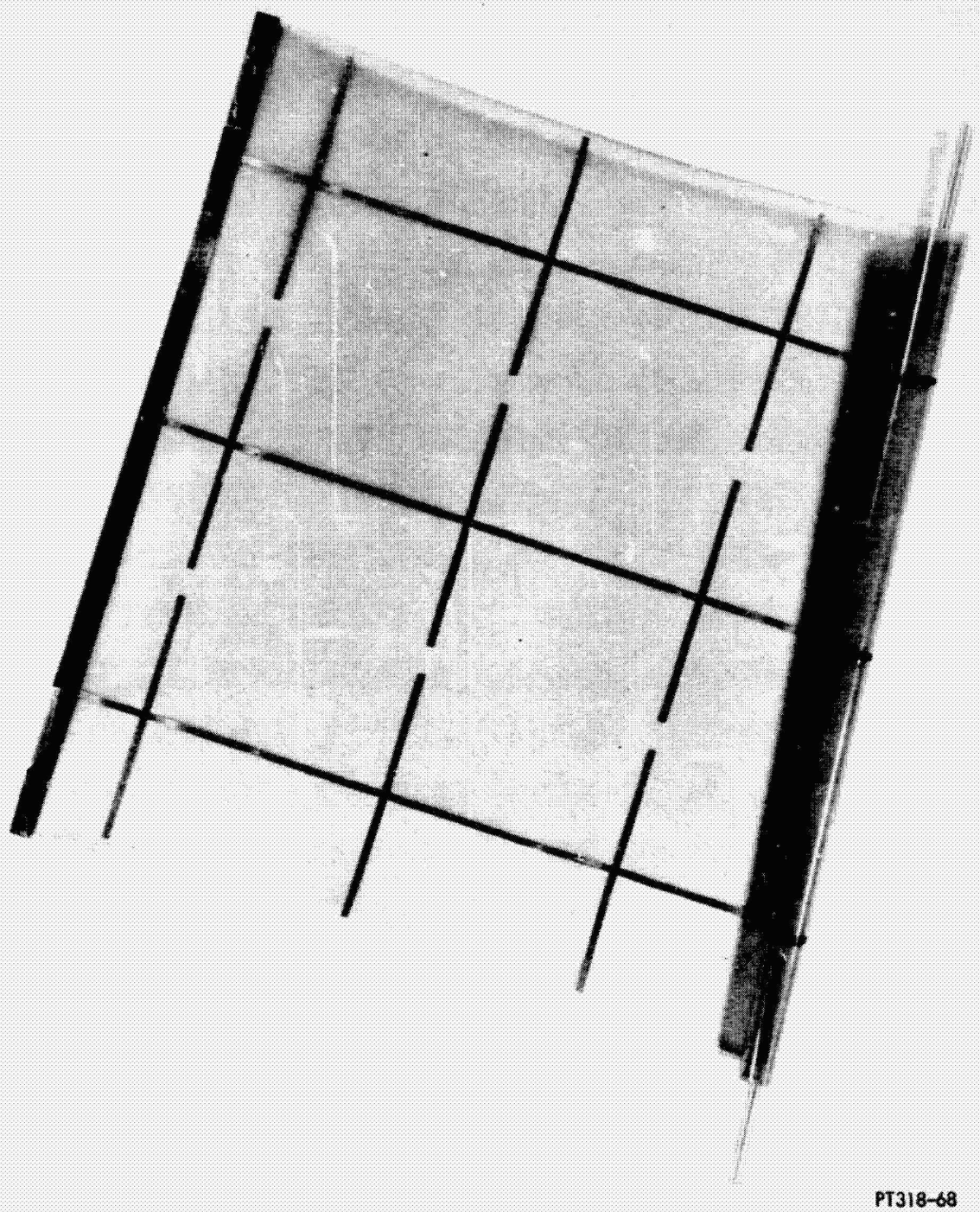

PT318-68

Figure 16. A possible physical configuration which future rectennas may assume. The rectenna is made in flexible form by employing printed circuit techniques on dielectric film material such as Kapton. Rectifiers, perhaps made by integrated circuit techniques, are bonded to the flexible printed circuit at appropriate points.

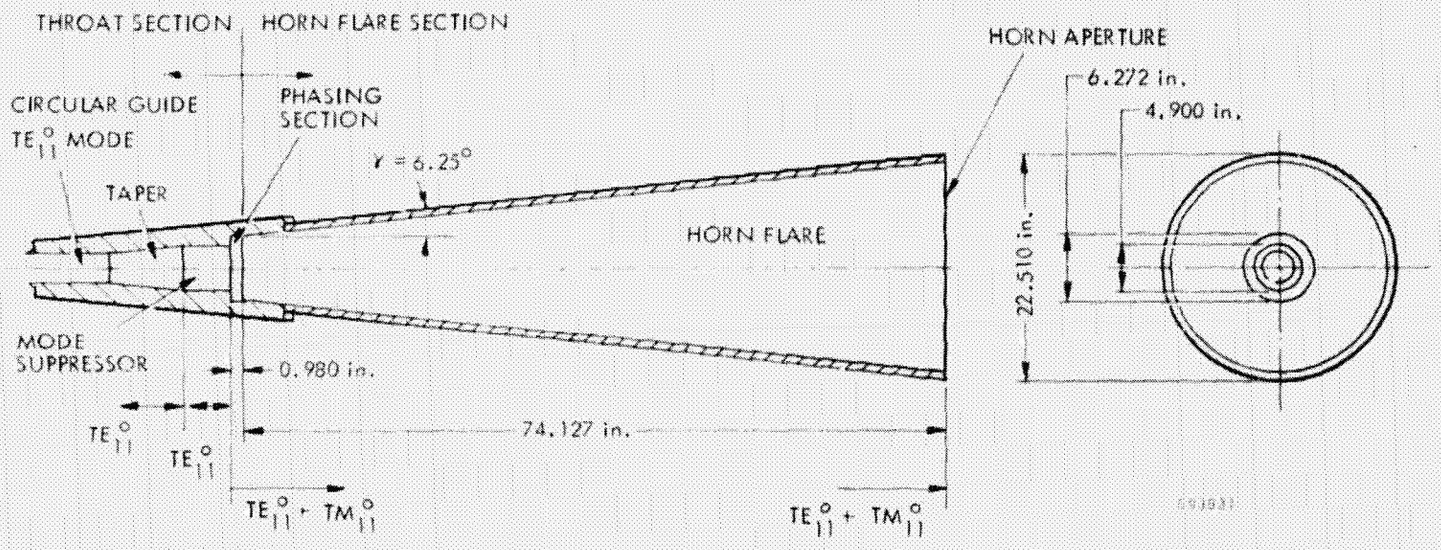

Figure 17. Dual-Mode Horn Design for the MSFC microwave power transmission system at 2450 MHz

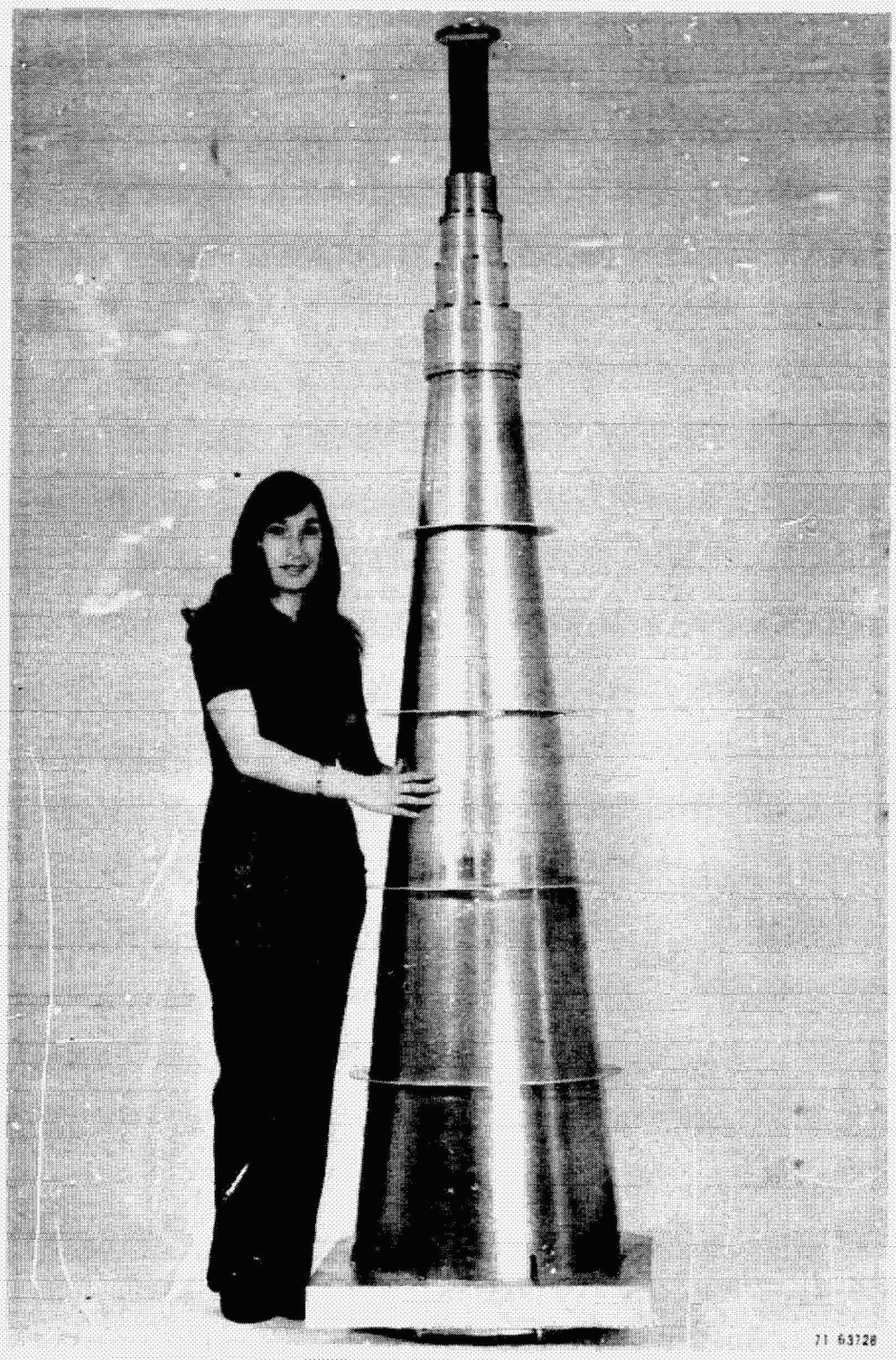

Figure 18. Completed dual-mode horn with rings in place to control concentricity.

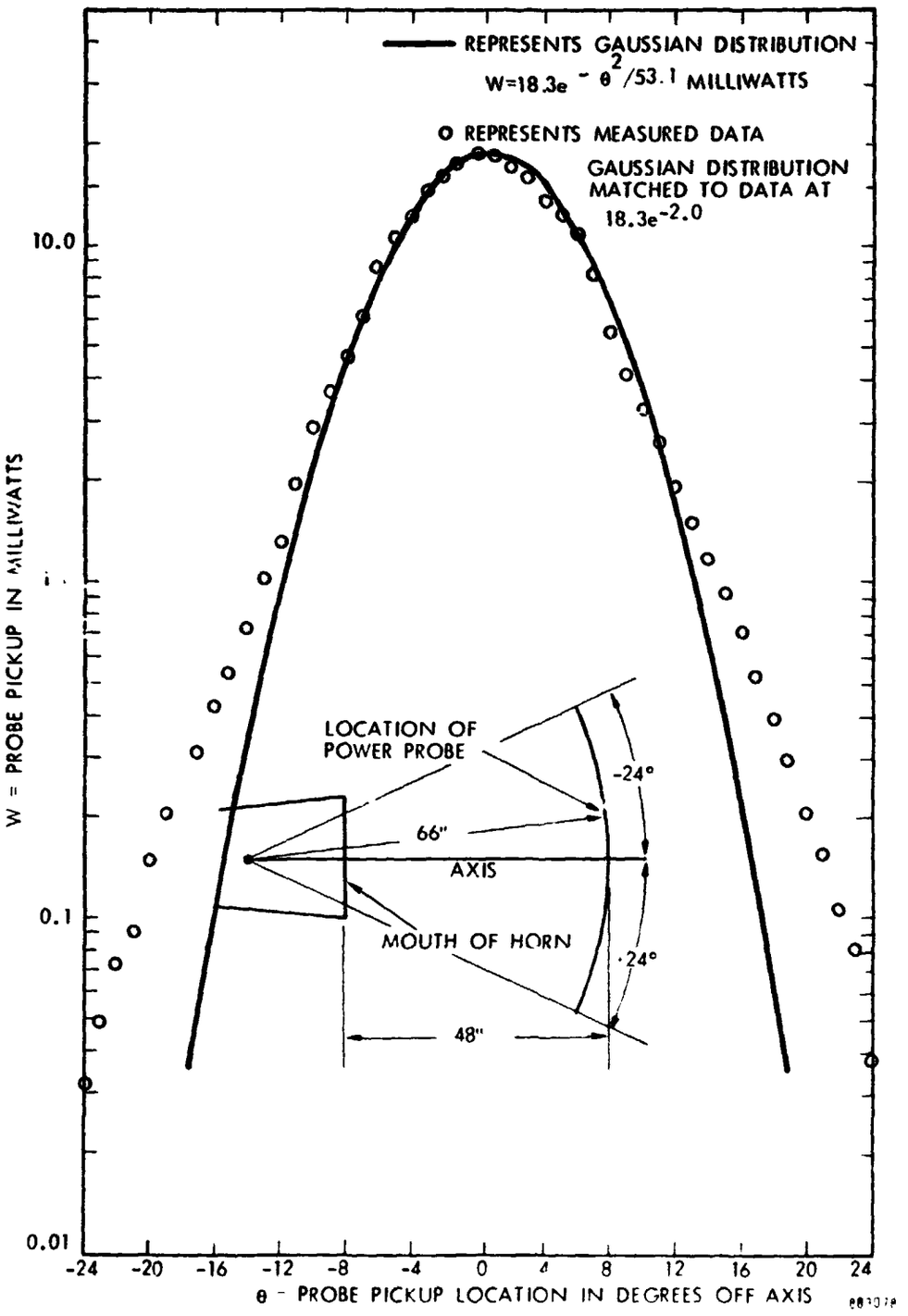

Figure 19. E-Field Pattern in the H-Plane for the Dual-Mode Horn taken at a distance corresponding closely to that of the rectenna for majority of efficiency tests.

is also close to a gaussian illumination. The phase front of the beam at the transmitting aperture must be spherically concave to fit the Goubau relationship. The use of an ellipsoidal reflector converts the convex phase front of the beam from the dual mode horn to the desired concave shape. The general approach for the whole system is shown in Figure 20.

One of the exercises in this study was to develop the equations for the design of such a system. It is believed that this is the first time it has been done. The results of this study were published in Reference 11.

A complete system as shown in Figure 21 was also constructed and experimental data obtained. The system and the microwave beam patterns obtained from it are discussed in the Phase II report. During Phase III there was an opportunity to perform dc to dc tests using this system. It performed well, yielding an overall efficiency of 45.6% compared with an efficiency of 51.2% without the ellipsoidal reflector. The results would have compared more favorably if there had not been some aperture blockage of the rectenna caused by the dual mode horn itself.

1.6 A New Design Procedure for a Low-Cost Ellipsoidal Reflector

The need to develop a new cost-effective procedure for the design and construction of ellipsoidal reflectors became evident in the desire to check out the design procedure as outlined in Section 1.5.

It is believed that a novel solution was worked out for this need. Figure 22 illustrates the construction technique. In essence the spatial coordinates for points on a plane passing through the ellipse are generated and transferred from a computer program to a tape controlled machine which punches holes corresponding to these coordinates in a sheet of metal. This sheet of metal is then bolted at the construction site if desired, to vertical columns in a plane surface. Other sheets corresponding to other planes passing through the ellipse are punched in a similar fashion. When all the sheets are bolted into position, thin metal rods are pushed down through the holes, and it is the total surface generated by these rods which defines the ellipsoid surface. The tolerance that can be held by this technique is plus or minus 0.010 of an inch exclusive of the flatness of the plane surface to which the members are bolted.

The finished reflector is shown in Figure 23.

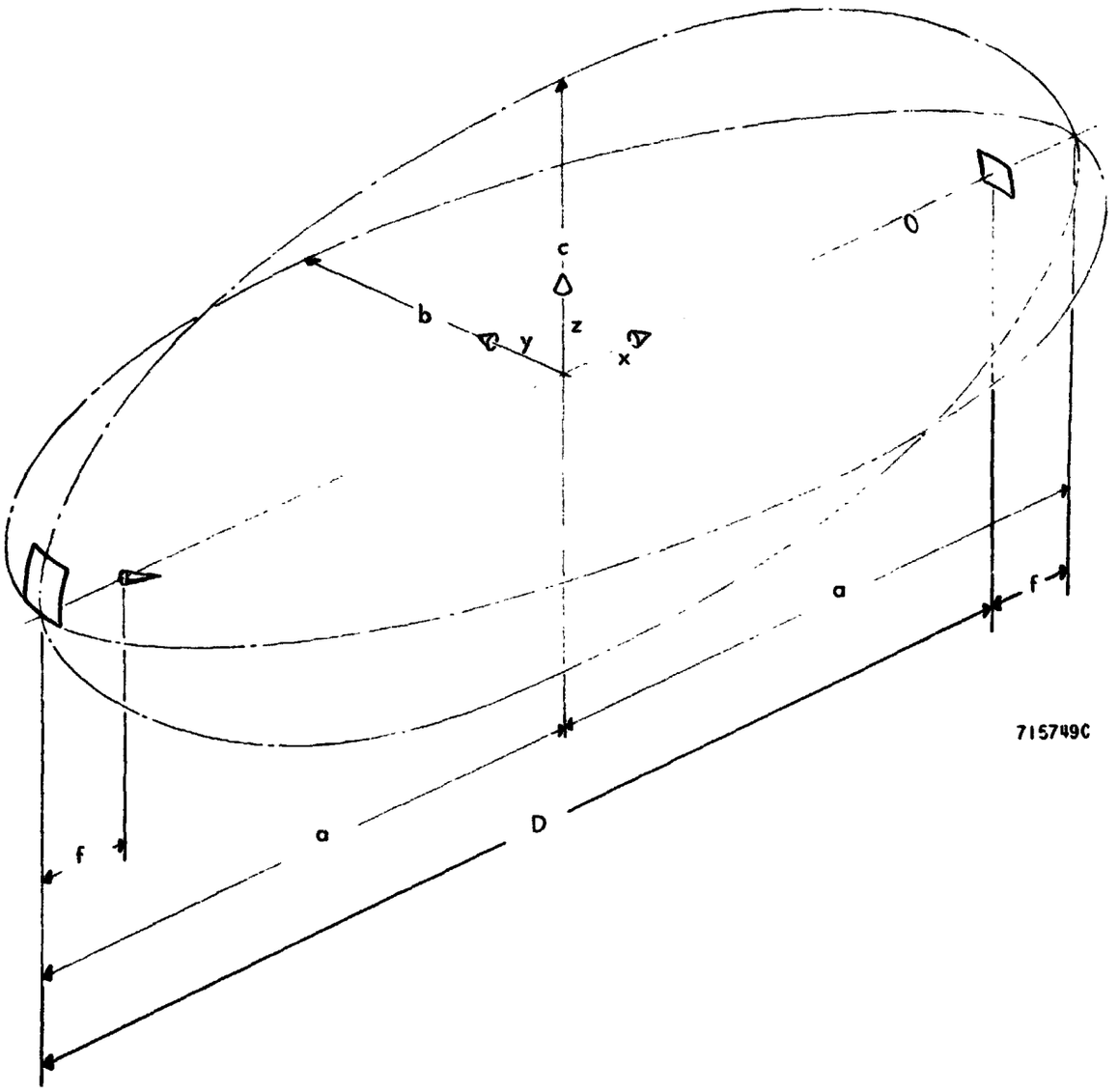

Figure 20. The design approach to a microwave power transmission system of arbitrary distance and efficiency makes proper use of an elliptical geometry and the focal points of an ellipse. The feed horn placed at one focal point illuminates an appropriately sized area of the ellipse which efficiently focuses the microwave power upon a collection or reflector area at the second focal point.

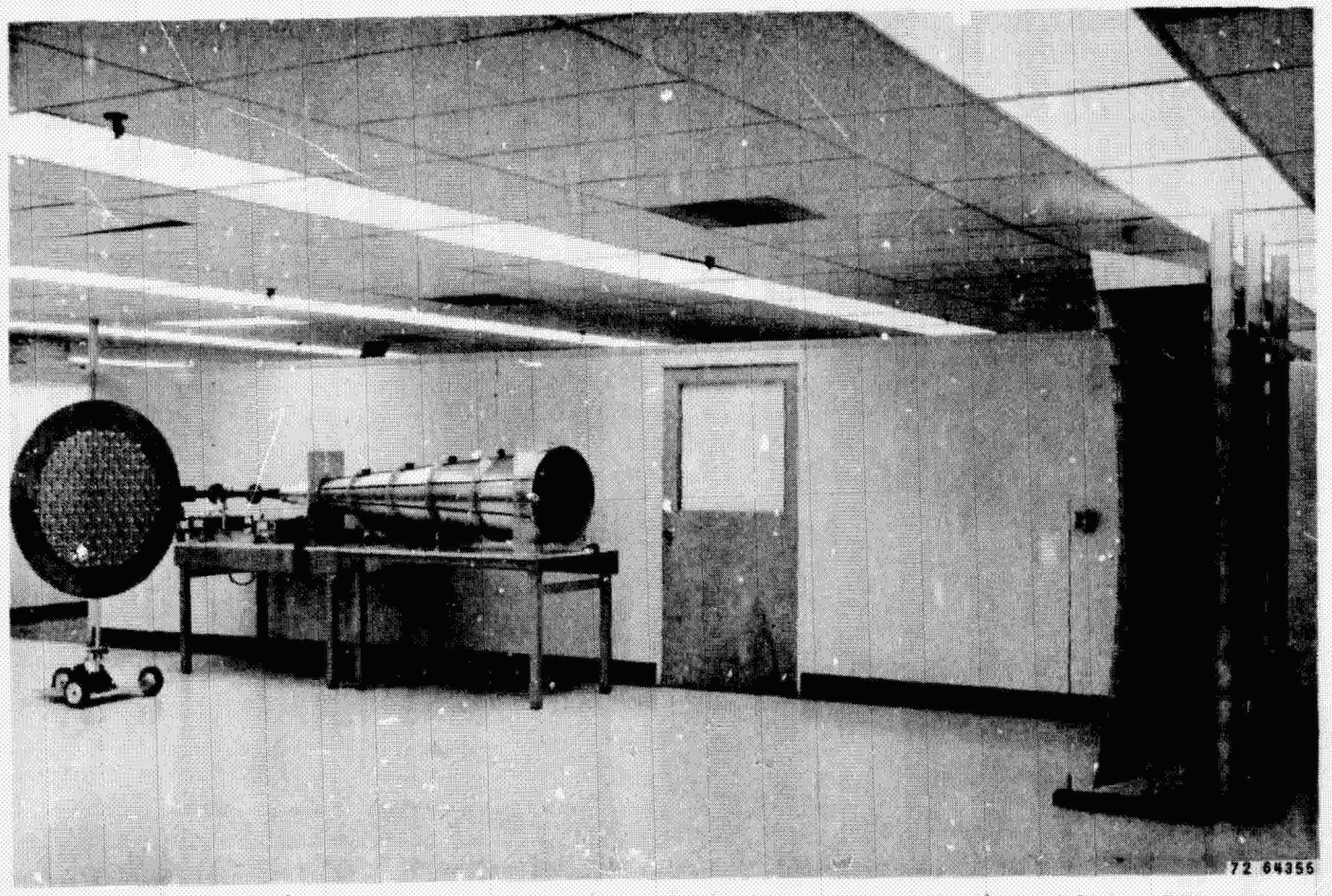

Figure 21. Complete microwave power transmission system starting with a point source of microwave energy. The microwave power is formed into a Gaussian beam by the dual-mode horn. The ellipsoidal reflector then transforms the divergent beam into a slightly convergent beam with a spherical phase front. The beam then converges upon the rectenna which is 20 feet from the reflector.

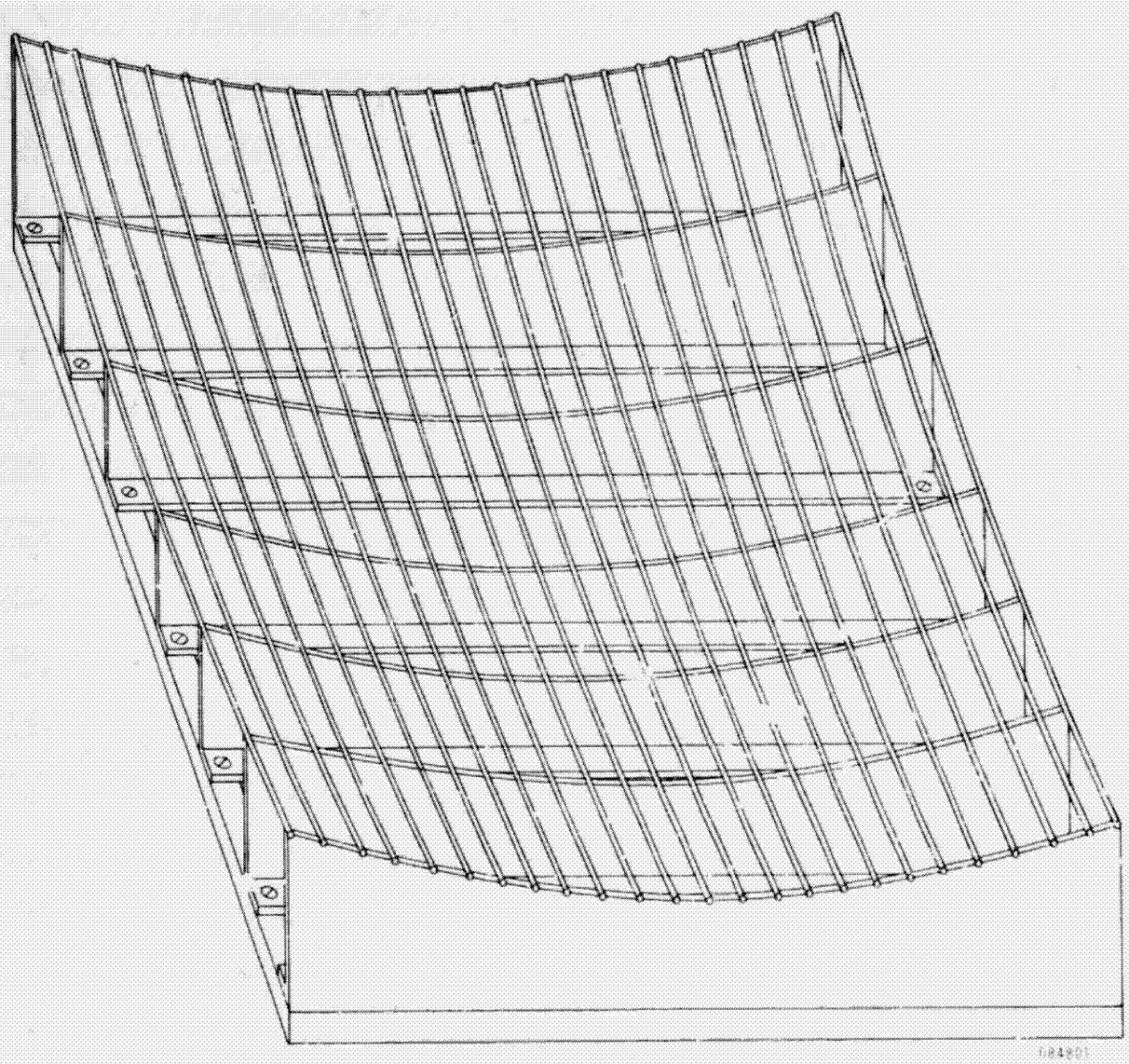

Figure 22. General mechanical design approach to the construction of an ellipsoidal reflector. Surface of ellipse is developed from closely spaced parallel rods which are positioned by threading through holes accurately located spacially in flat sheets which are in turn attached to a rigid flat refe.ence plane.

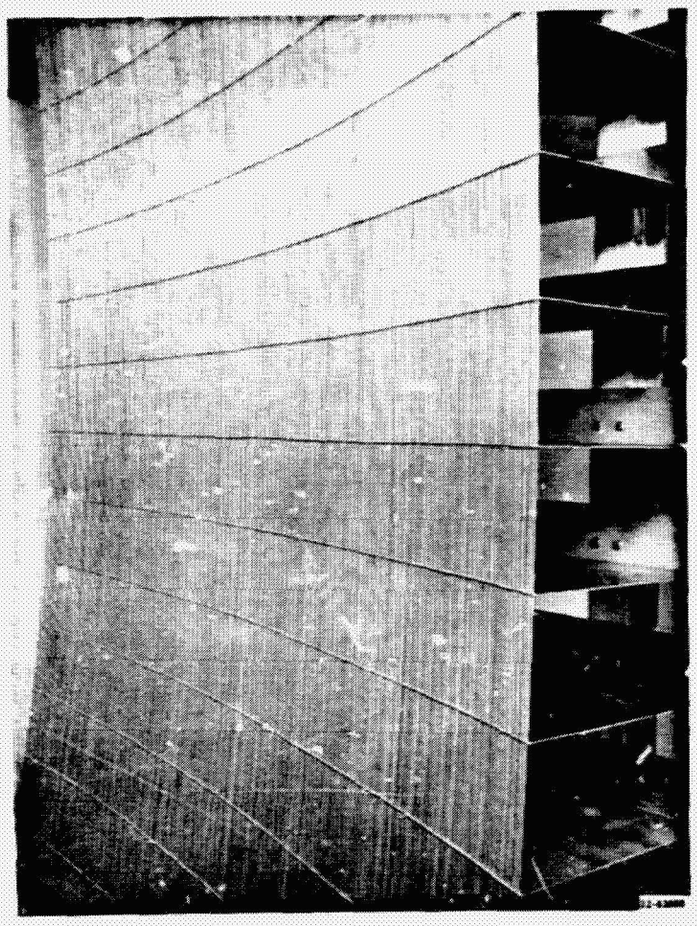

Figure 23. Finished ellipsoidal reflector mechanically designed according to the principle shown in Figure 21.

2.0 OVERALL DC TO DC EFFICIENCY MEASUREMENTS

Measurements were made on two different laboratory systems for the measurement of high overall dc to dc efficiency. In the first system, the rectenna was directly radiated by the dual horn. In the second system an ellipsoidal reflector was used to increase the distance of power transfer but still maintain high efficiency as explained in Section 1.5. A photograph of the first system is shown in Figure 6. A photograph was not taken when the measurements on the second system were made but the arrangement of the dual mode horn and the reflector is identical to that shown in Figure 21. The improved rectenna also occupied the same position as the earlier model rectenna occupied in Figure 21.

Both experimental systems were identical from the power input to the power supply for the magnetron to the output of the dual-mode horn. The schematic for this part of the system is shown in Figure 24. The complete system for the direct radiation of the rectenna is shown in Figure 25. As shown in Figure 24 a microwave-oven magnetron was used as the dc to microwave converter. Its output was connected through a ferrite circulator to the input of a dual mode horn. The gaussian- shaped radiation pattern from the dual mode horn was directed upon the rectenna array which contained 199 rectenna elements. The dc output connections from the rectenna elements were wired together in sets as shown in the format of Figure 26. All rectenna elements in a given set had approximately the same incident power level upon them and they were individually matched for minimum reflected power at a particular incident power level. The matching was done in the expanded waveguide test fixture shown in Figure 27. As shown in Figure 26, the dc output of each set of elements was fed into a separate load resistor. There were 22 load resistors in all. The total dc power output was the sum of the powers in the separate load resistors.

A typical set of data is shown in Figure 28. The dc input power into the magnetron is measured carefully, and the dc power output from all of the load resistors is added together to give the total power output. The efficiency is the dc power output divided by the dc power input. The data in Figure 28 indicates an overall efficiency of 50.0%. The estimated probable error is 2% giving a possible range of 48% to 52% for the efficiency.

In addition to computing the overall efficiency, the ratio of the dc power output to the rf power input to the throat of the dual mode horn was measured. In this particular

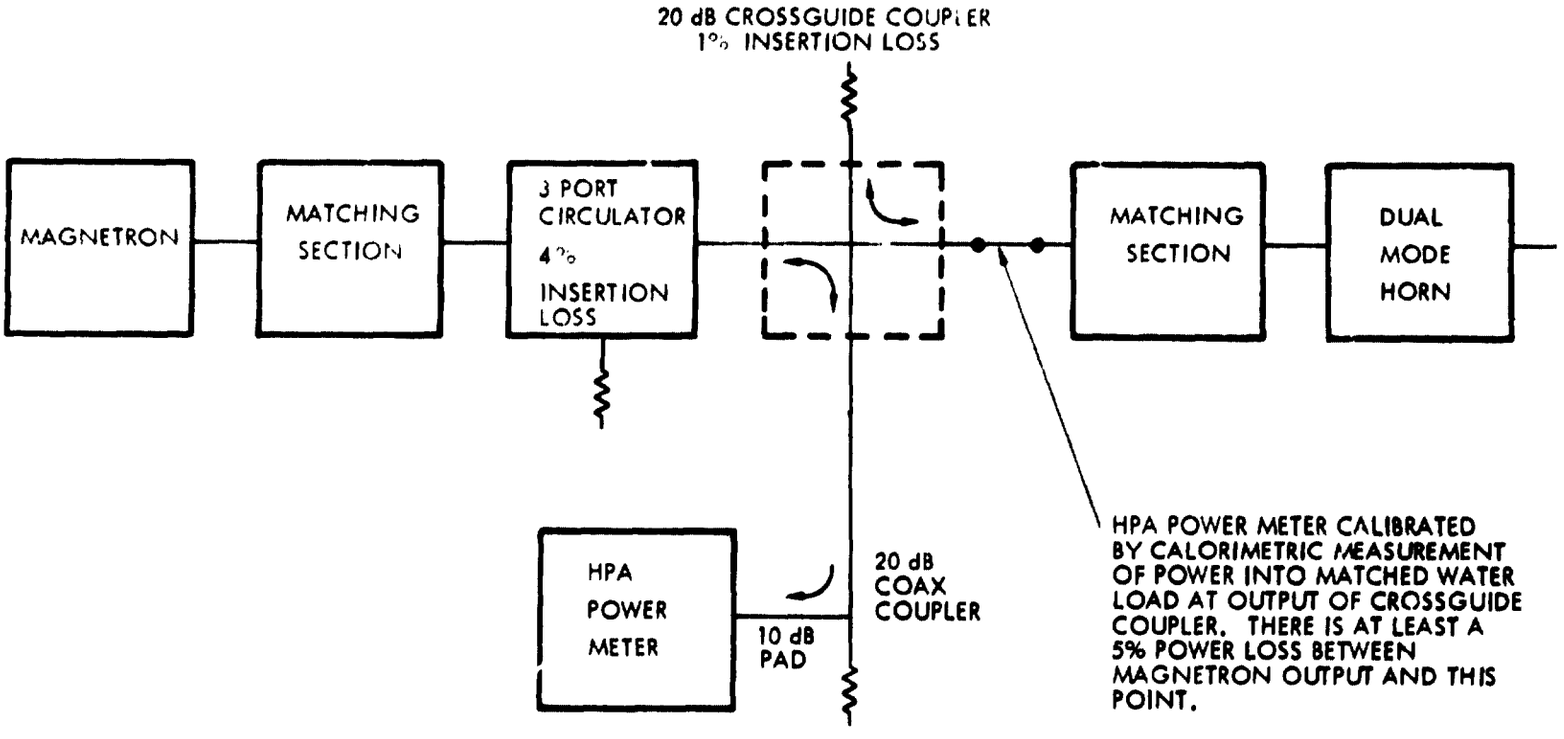

Figure 24. Schematic showing electrical details of the laboratory high efficiency microwave power transmission system

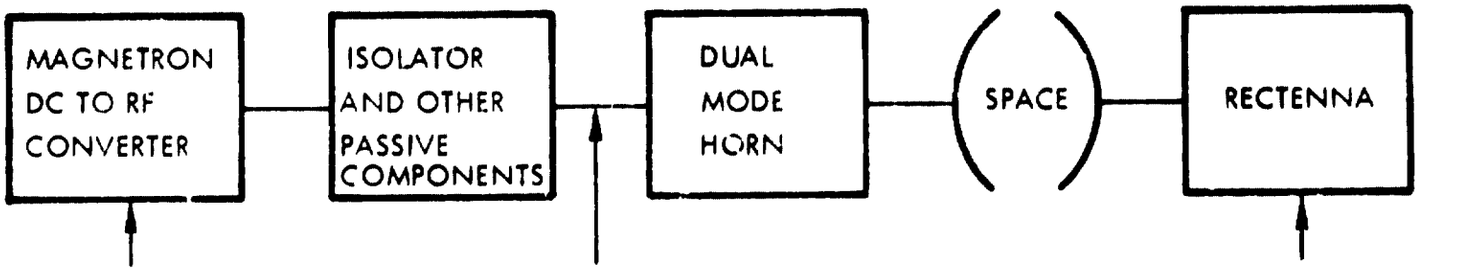

$$\text{OVERALL DC EFFICIENCY } \eta = \frac{4 \times 5}{1 \times 2}$$

$$\text{RF TO DC EFFICIENCY } \eta_t \eta_r = \frac{4 \times 5}{3}$$

Figure 25. Schematic outline for the complete laboratory microwave power transmission system in which direct radiation of the rectenna is used

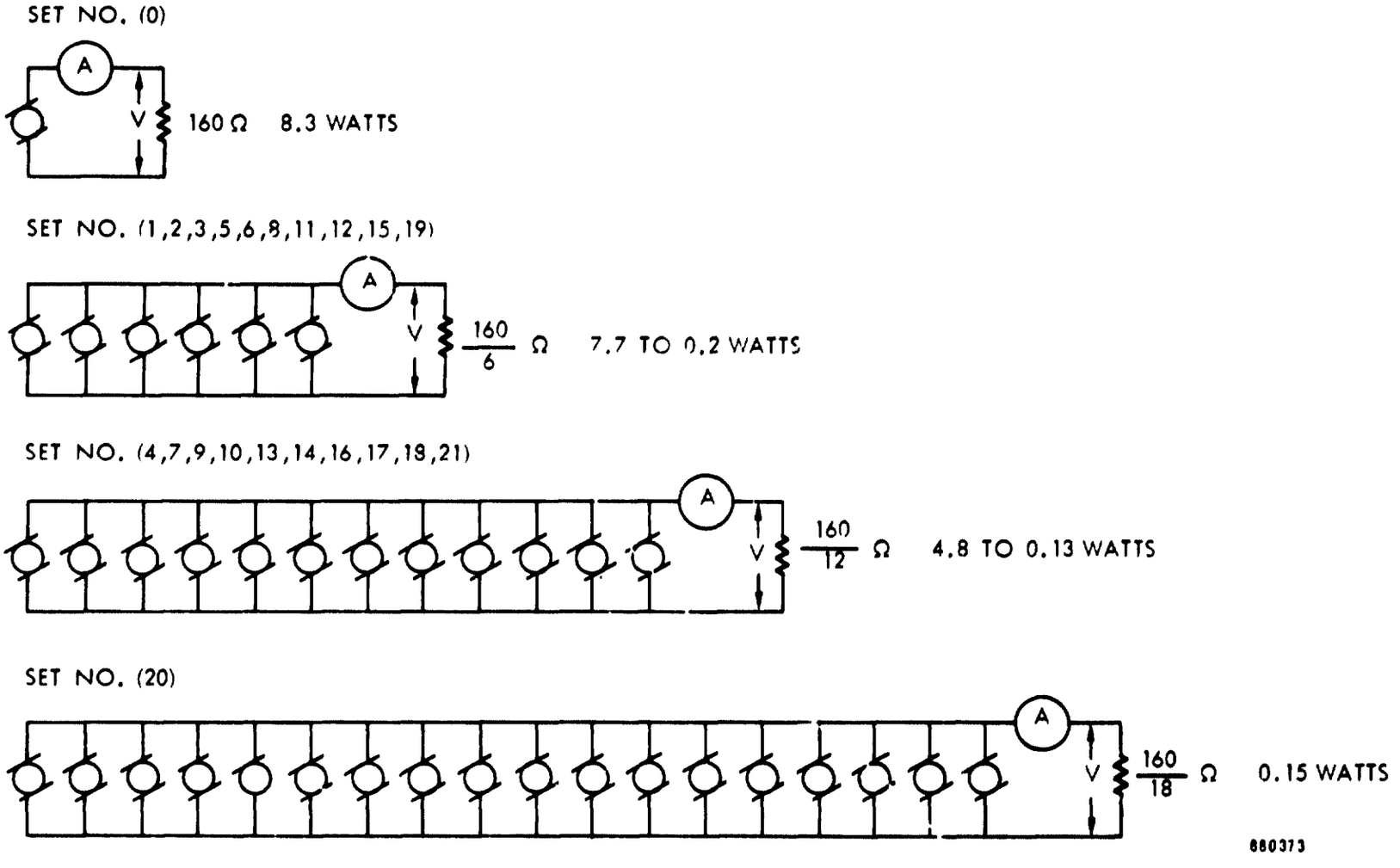

Figure 26. Wiring format for Phase III rectenna

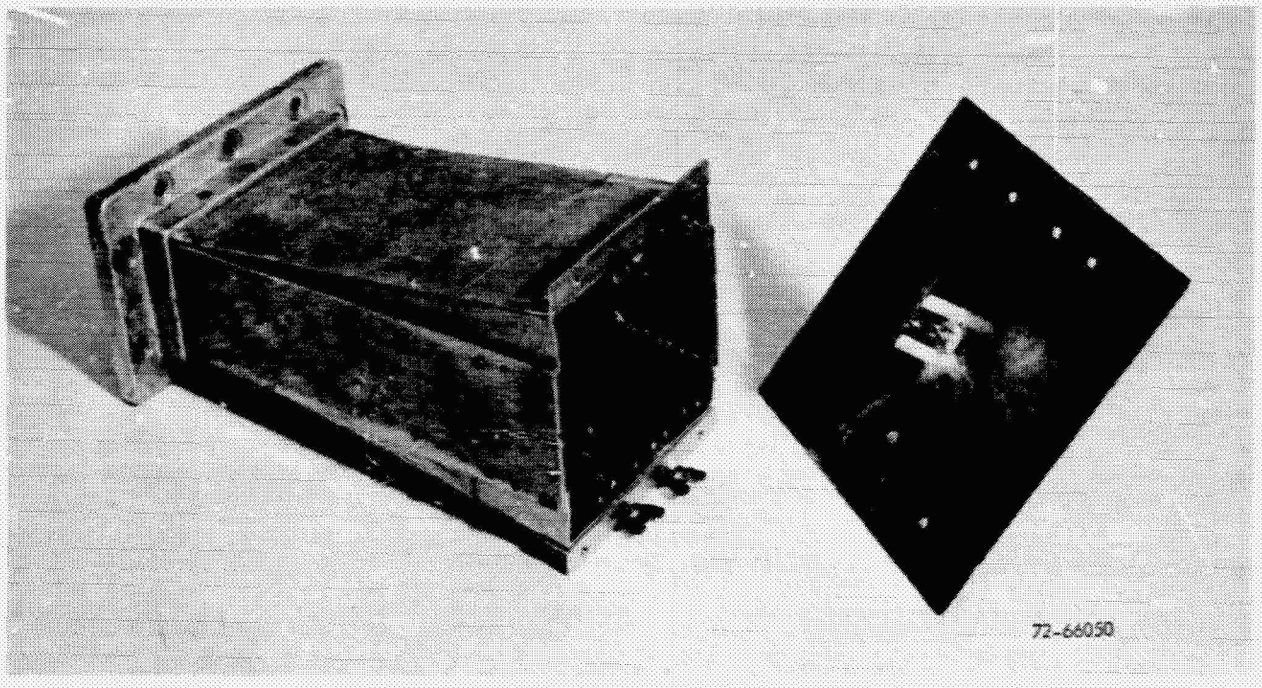

Figure 27. Expanded waveguide test fixture for evaluating efficiency of rectenna element. The test fixture is a closed system, in which the incident microwave power is either absorbed in the rectenna element and converted into DC power or heat losses, or is reflected.

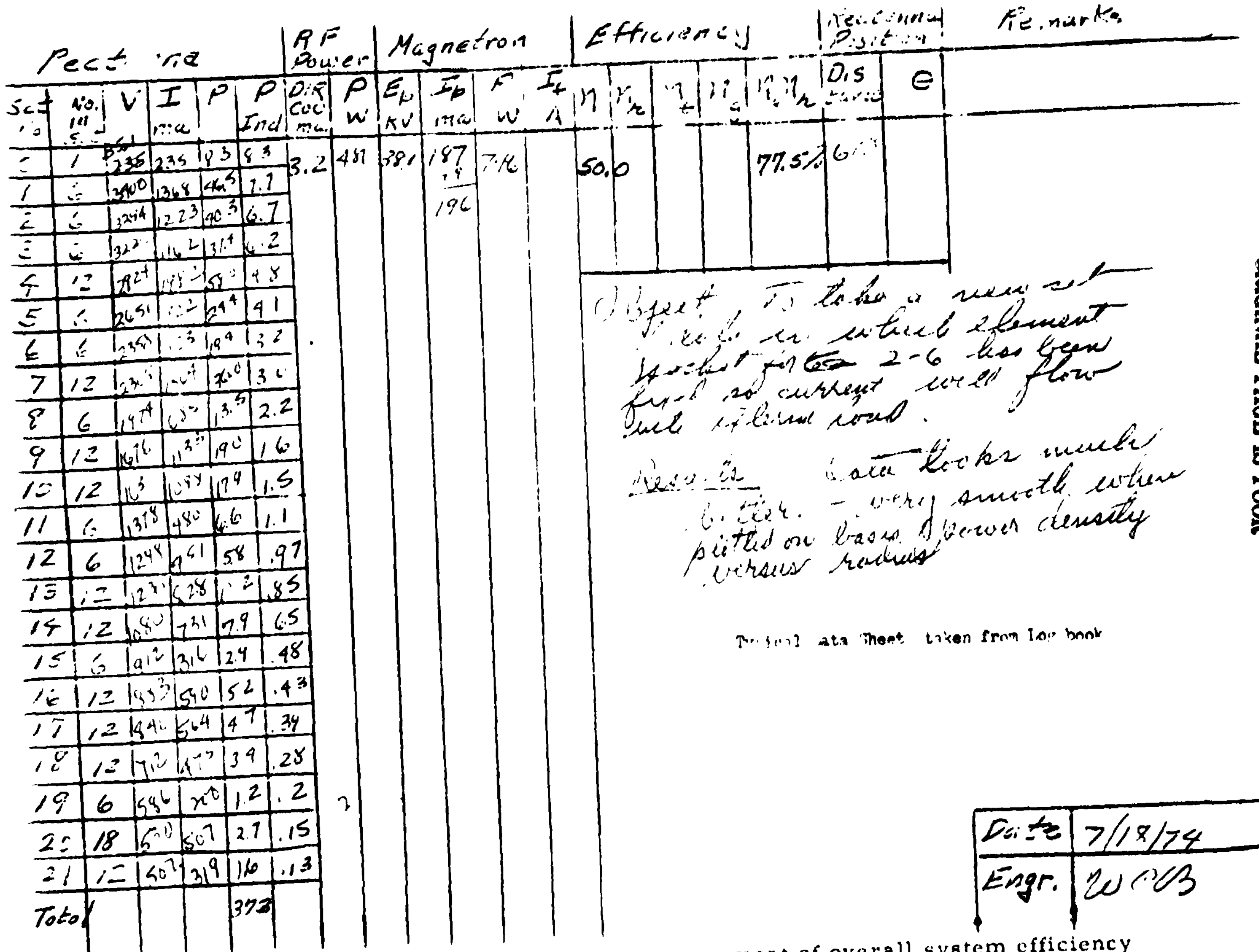

Set No.	No. of S.	V	I ma	P	P Ind
0	1	235	235	93	93
1	6	3400	1368	46.5	7.7
2	6	3294	1223	40.3	6.7
3	6	322[illegible]	1162	37.4	6.2
4	12	[illegible]	[illegible]	[illegible]	4.8
5	6	2651	[illegible]	29.4	4.1
6	6	2358	[illegible]	19.4	3.2
7	12	[illegible]	[illegible]	20.0	3.0
8	6	1974	[illegible]	13.5	2.2
9	12	1676	1135	19.0	1.6
10	12	163	1094	17.4	1.5
11	6	1378	480	6.6	1.1
12	6	1248	461	5.8	.97
13	12	1231	628	[illegible]	.85
14	12	1080	731	7.9	.65
15	6	912	316	2.4	.48
16	12	933	590	5.2	.43
17	12	840	564	4.7	.34
18	12	712	477	3.9	.28
19	6	586	[illegible]	1.2	.2
20	18	530	507	2.7	.15
21	12	507	319	1.6	.13
Total				373	

RF Power: Dir Coc ma	RF Power: P W	Magnetron: E_p KV	Magnetron: I_p ma	Magnetron: F W	Magnetron: I_f A	Efficiency: η	η_r	η_t	η_a	$\eta_t \eta_r$	Rectenna Position: Distance	θ
3.2	481	381	187 + 9 = 196	7.16		50.0				77.5%	6[illegible]	

Object: To take a new set [illegible] in which element [illegible] 2-6 has been [illegible] so current will flow [illegible].

Results: Data looks much better. — very smooth when plotted on basis of power density versus radius

Typical Data Sheet taken from Log book

Date: 7/18/74
Engr. W C B

Figure 28. Typical data sheet for measurement of overall system efficiency taken from log book

case an efficiency of 77.5% was computed.

The value of 51.2% for dc to dc efficiency was obtained on July 19th, 1974. This measurement compares with the certified 54.2% that was made in March, 1975, after an efficiency improvement in the rectenna elements of 1.5% and efficiency improvements in magnetron and waveguide.

Figure 29 shows the power outputs of the elements in an array as a function of their distance from the center of the array. A gaussian curve can be fitted to this data quite accurately, indicating that the distribution of rectified power output in the rectenna closely follows the distribution of incident microwave power.

During the development of this array, it was difficult to predict in advance the amount of the incident power that would be reflected from the array. However, a number of things can be varied after the rectenna is constructed to give some adjustment. The power input, the separation of the dipole from the reflecting plane, and the load resistance can be varied.

The amount of reflected power can be measured by examining the standing wave ratio in front of the rectenna. The results are not generally valid for arbitrary illumination, but if the incident beam is gaussian and the reflected beam is also gaussian, the measurement is considered to be valid. The VSWR measurement is made by means of a motorized probe as shown in Figure 30. For accurate data the probe is positioned at one centimeter intervals and the readings of probe power are made with the probe stationary.

Using the VSWR measurements as a criteria, it was found that the amount of reflected power was quite small. Although the value varied with the separation of the dipole from the reflecting plane, the maximum amount of reflected power was still small. The data below indicates how reflected power varied with the dipole to reflecting plane separation.

Separation distance between dipole and reflecting plane	VSWR ratio db	Corresponding value of reflected power
2.1 cm	3.3	3.5%
2.3 cm	2.0	1.2%
2.5 cm	1.8	1.06%
2.7 cm	1.0	0.3%
2.9 cm	less than 1.0	less than 0.3%

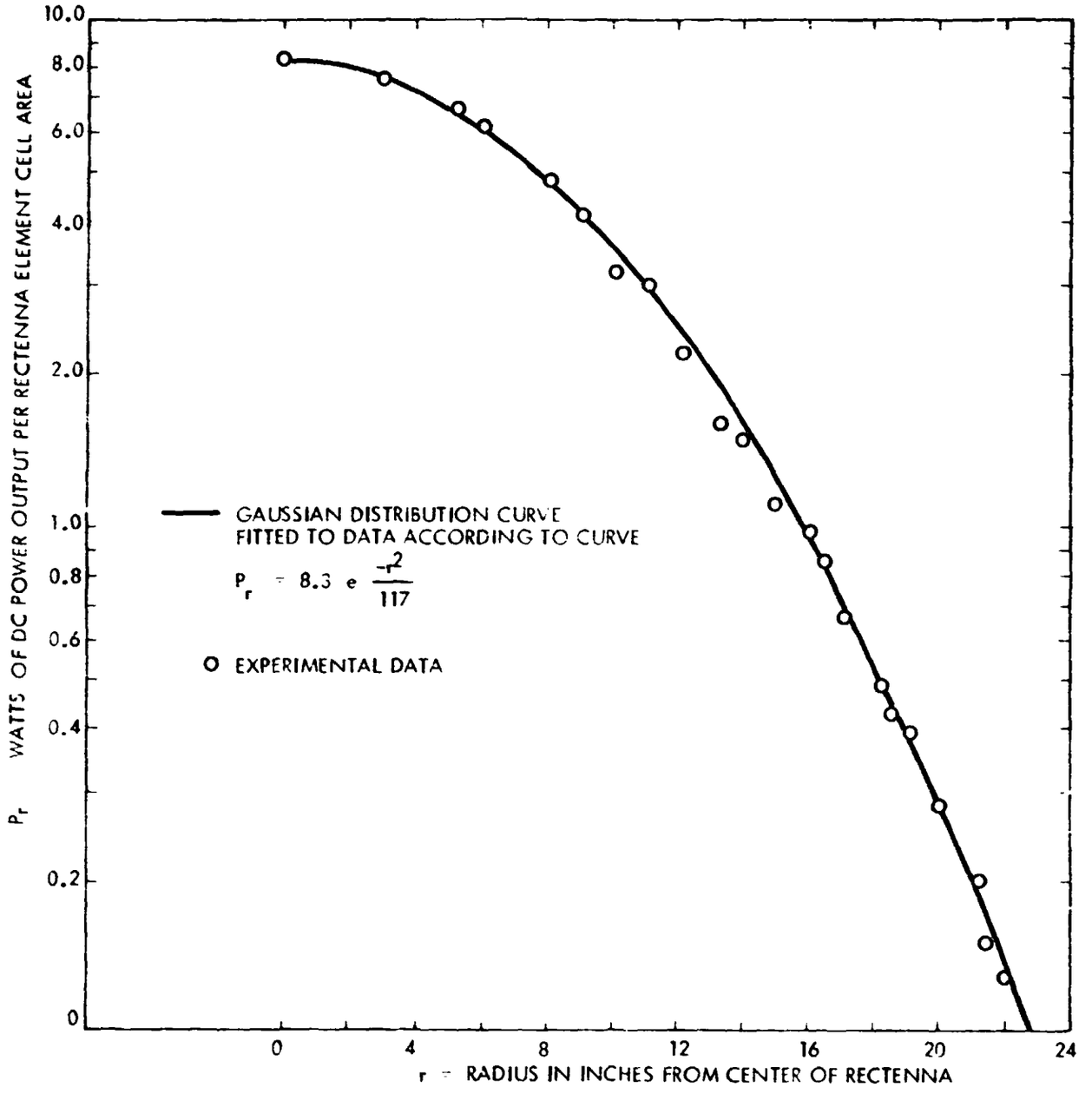

Figure 29. The average DC power output per element in a set of elements is plotted as a function of the radial distance of the set. The resulting points of data may be easily fitted to a Gaussian curve which is the approximate power density distribution in the beam.

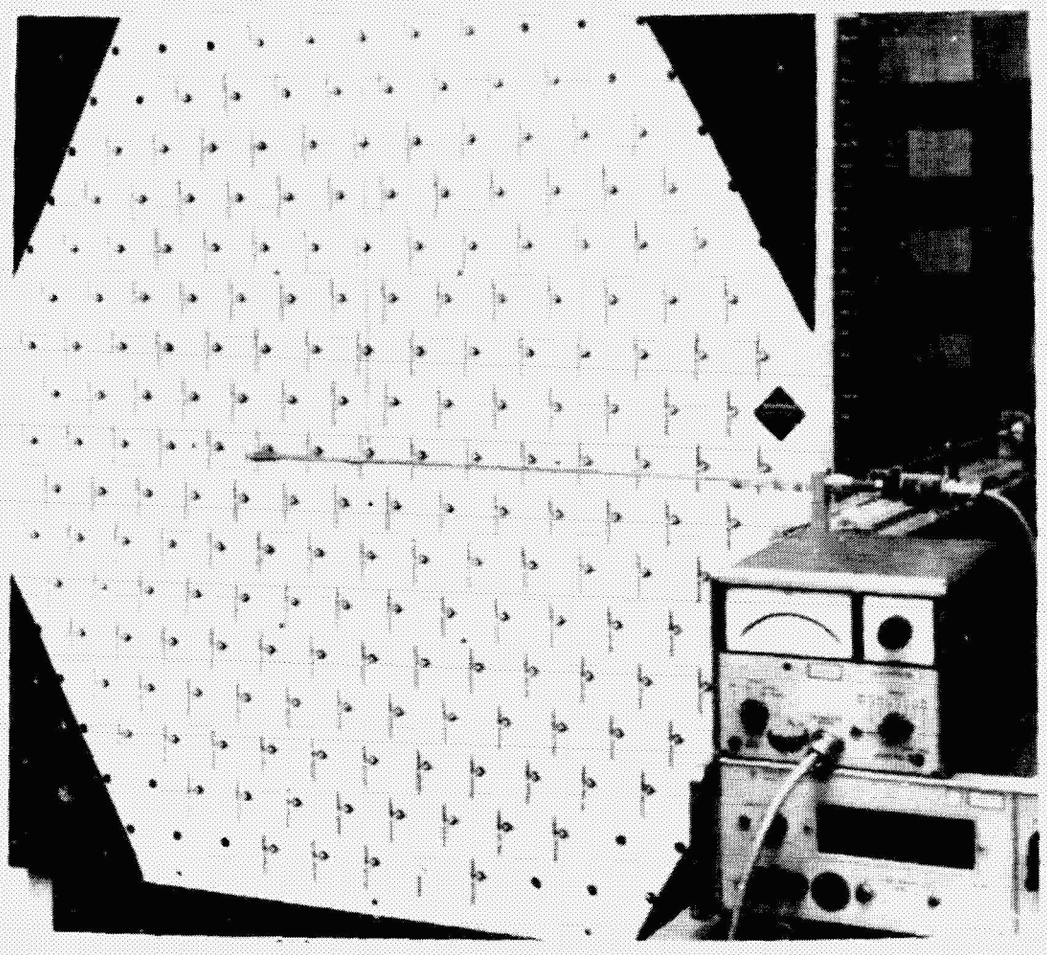

Figure 30. Motorized probe for making standing wave measurements in front of the rectenna

The above data was taken with an rf power output level of 478 watts.

The value of efficiency obtained when the ellipsoidal reflector was used and the rectenna moved to a point 20 ft from the reflector was 45.6%. This value agrees well with the expected degradation from 51.2% caused by spillover losses around the ellipsoidal reflector and blockage of some of the reflected power by the dual mode horn.

In conclusion, it is noted that the various procedures and instrumentation for obtaining accurate data were not discussed in detail in view of the fact that the certified tests made later are the important ones in establishing the credibility of the measurements.[15] However, measurements were made with care for accuracy and validity and all meters were properly calibrated.

3.0 PERFORMANCE CHARACTERISTICS OF THE RECTENNA ELEMENT

By using a testing arrangement such as shown in Figure 27, it is possible to approximate the incident free-space radiation that the element would be exposed to in its position in the rectenna while still having a closed system in which the incident and reflected powers can be measured very accurately. As a result of this testing arrangement, it is possible to conveniently investigate a wide range of performance parameters, and relate the microwave behavior at the set of input terminals with the dc behavior at the set of output terminals, or vice-versa as shown in Figure 31. These relationships are most important in predicting the behavior of the rectenna.

3.1 Overall Efficiency and Conversion Efficiency as a Function of DC Load Resistance

This relationship, experimentally measured, is shown in Figure 32. For a given rectenna element circuit design, it is found that for every input power level there is a combination of dc load resistance and position of the trimmer which will reduce the reflected power to zero. Then if the dc load resistance is varied, the overall efficiency and conversion efficiency will vary as shown in Figure 32. It is seen that the dc load resistance can vary considerably from its optimum value without a drastic impact upon the efficiency. The data of Figure 32 indicates, however, that if the reflected power is subtracted from the incident power to compute the conversion efficiency, there is still an efficiency drop which varies with load in a symmetrical w about the matched load resistance. Hence there are other contributions to the drop in overall efficiency beyond that of the reflected power loss. The data shown in Figure 32 was taken for one value of microwave input power, 3 watts.

3.2 Reflected Power as a Function of DC Load Resistance for Two Values of Microwave Power Input

This relationship is shown in Figure 33. The reflected power as a function of the dc load resistance can be roughly predicted on the basis of reflection loss from an unmatched transmission line, that is, a change in the dc load resistance appears as an equivalent change in the microwave load. However, the reflection factor does not go to unity with short circuit or open circuit loads. For the 10 ohm load and 1000 ohm load conditions shown in Figure 33, the element absorbs about 30 % of the power falling on it.

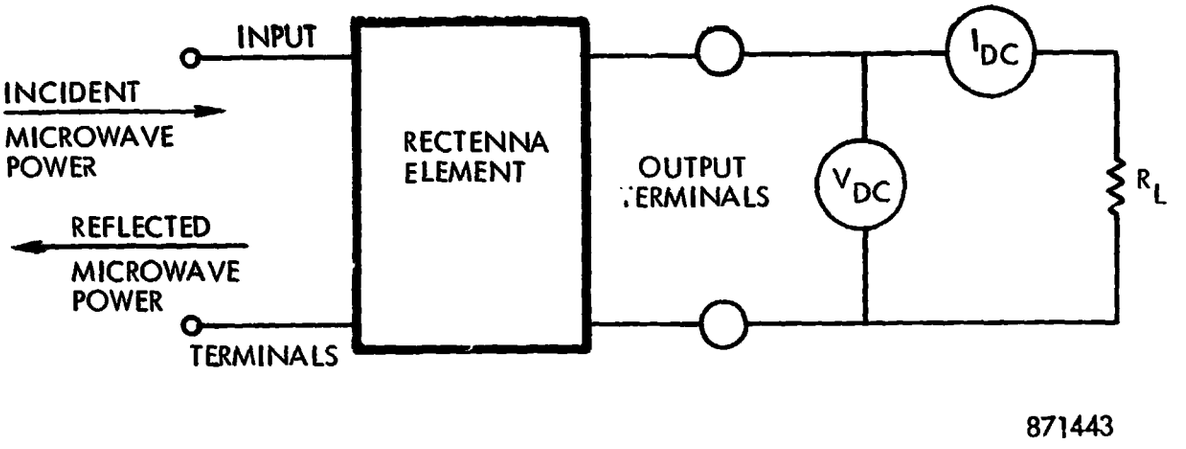

Figure 31. Input-output characterization of the rectenna element

RECTENNA ELEMENT EFFICIENCY AS A FUNCTION OF LOAD

$$1 - \text{OVERALL EFFICIENCY} = \frac{\text{DC POWER OUT}}{\text{INCIDENT RF POWER}}$$

$$2 - \text{RECTIFICATION EFFICIENCY} = \frac{\text{DC POWER OUTPUT}}{\text{INCIDENT RF POWER - REFLECTED RF POWER}}$$

INPUT POWER LEVEL - 3.0 WATTS

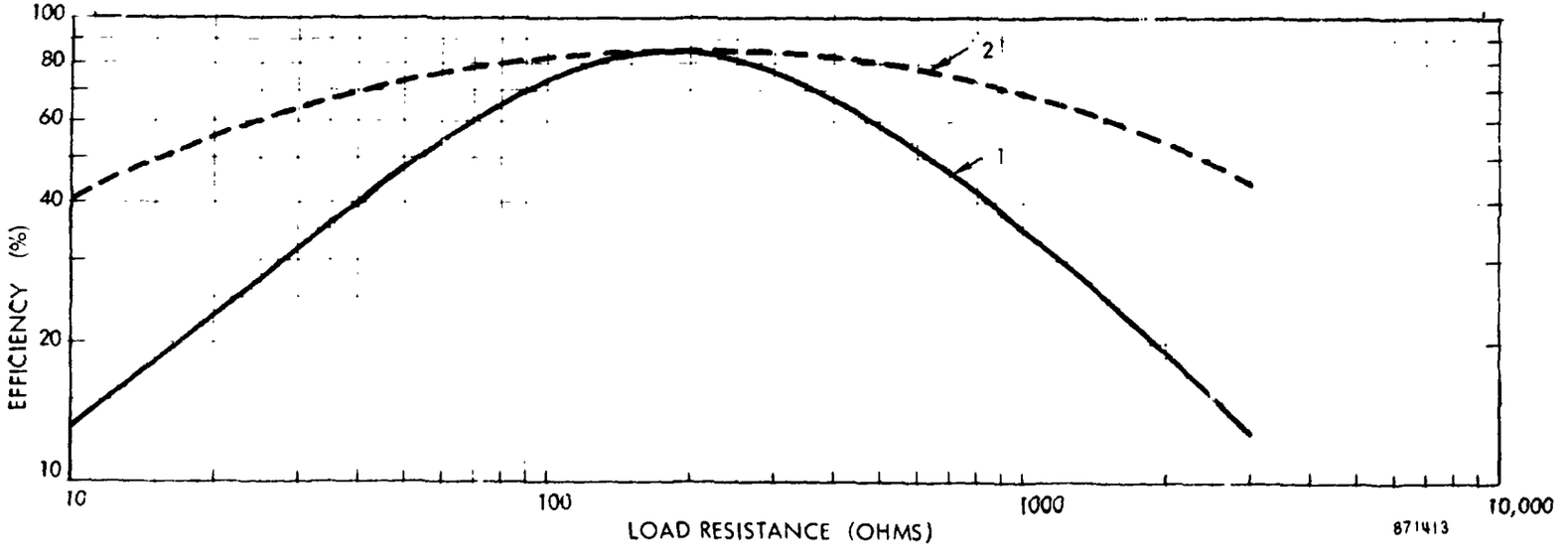

Figure 32. Rectenna element efficiency as a function of load resistance

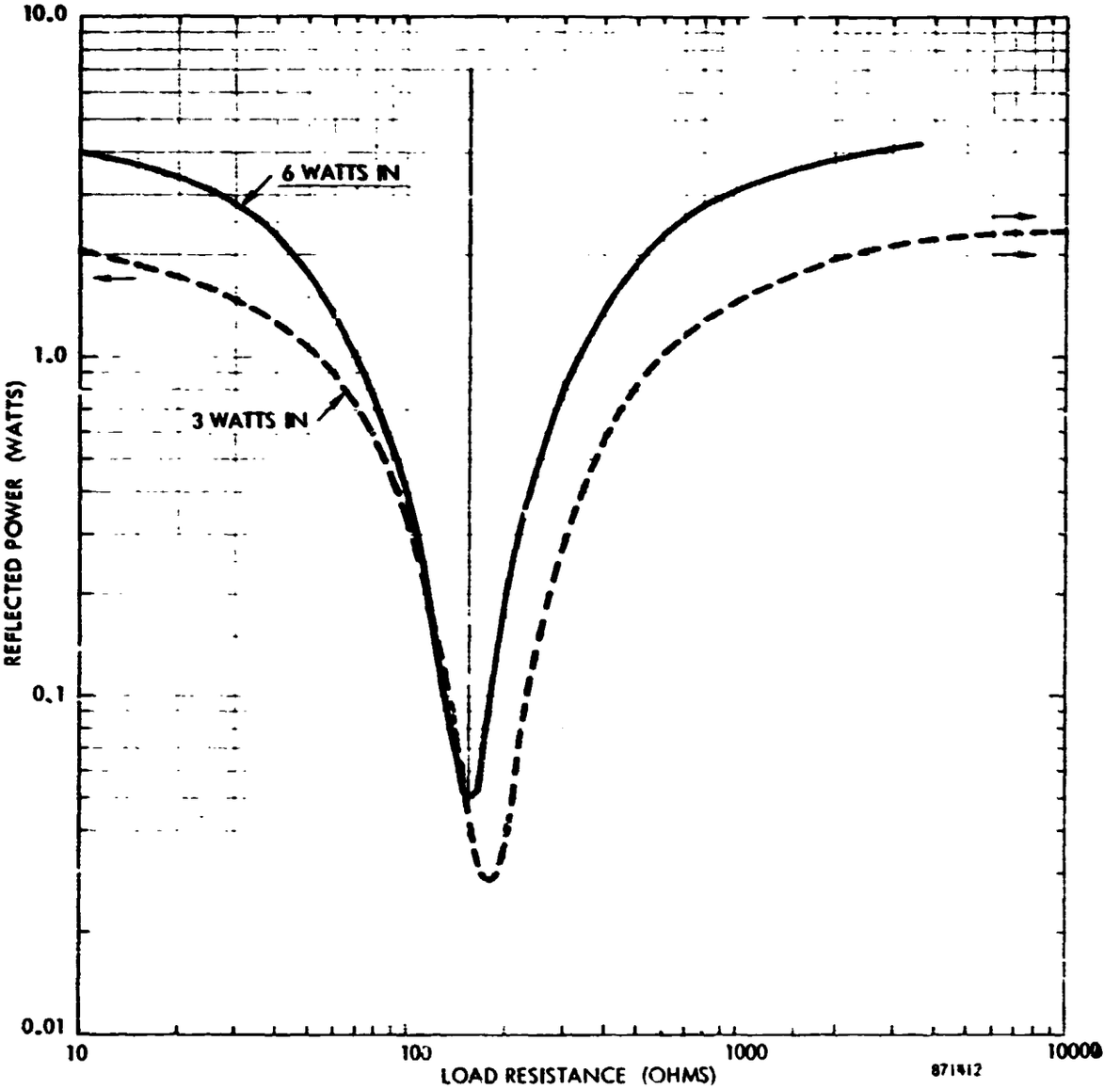

Figure 33. Reflected power from the MSFC rectenna element as a function of load resistance and microwave power input.

The power absorbed in the diode and the rest of the rectifying circuit under these conditions must be dissipated in the rectenna element itself. The data of Figure 33 is, therefore, important in determining the amount of power absorbed. Even if all the absorbed power shown in Figure 33 at the short and open circuited conditions were dissipated in the diode, the values are quite low for the three watt and six watt input conditions and should not be a source of failure. However, for open-circuit conditions and higher power levels, the dissipation in the diode may be considerably higher than for the same power under short circuited conditions.

3.3 Overall Efficiency and Reflected Power as a Function of Frequency with the Rectenna Elements Optimized at 2445 MHz

As shown in Figure 34, the rectenna element is a broadband device whose efficiencies remain high over a quite broad range of frequencies. The rectenna element used in the test was tuned for optimum response at 2445 MHz. The measured efficiency over the band 2365 MHz to 2470 MHz is 83 ± 1%. The increase in efficiency shown below 2350 MHz is probably not real. The measuring system was not calibrated in this region. The cause of the small cyclic variation in efficiency evident in the data has not yet been identified but is apparently related to the configuration of the test setup used.

3.4 Overall Efficiency and Reflected Power as a Function of Input Power Level for an Element Matched for an Incident Power Level of 3 Watts

This data is shown in Figure 35.

The variation of reflected power as a function of overall efficiency and input power level for a given setting of the trimmer is of practical importance. This variation is shown for one of the MSFC elements whose trimmer is set for minimum reflection at an input power level of three watts. It is noted that the efficiency remains high for a high range of microwave power input.

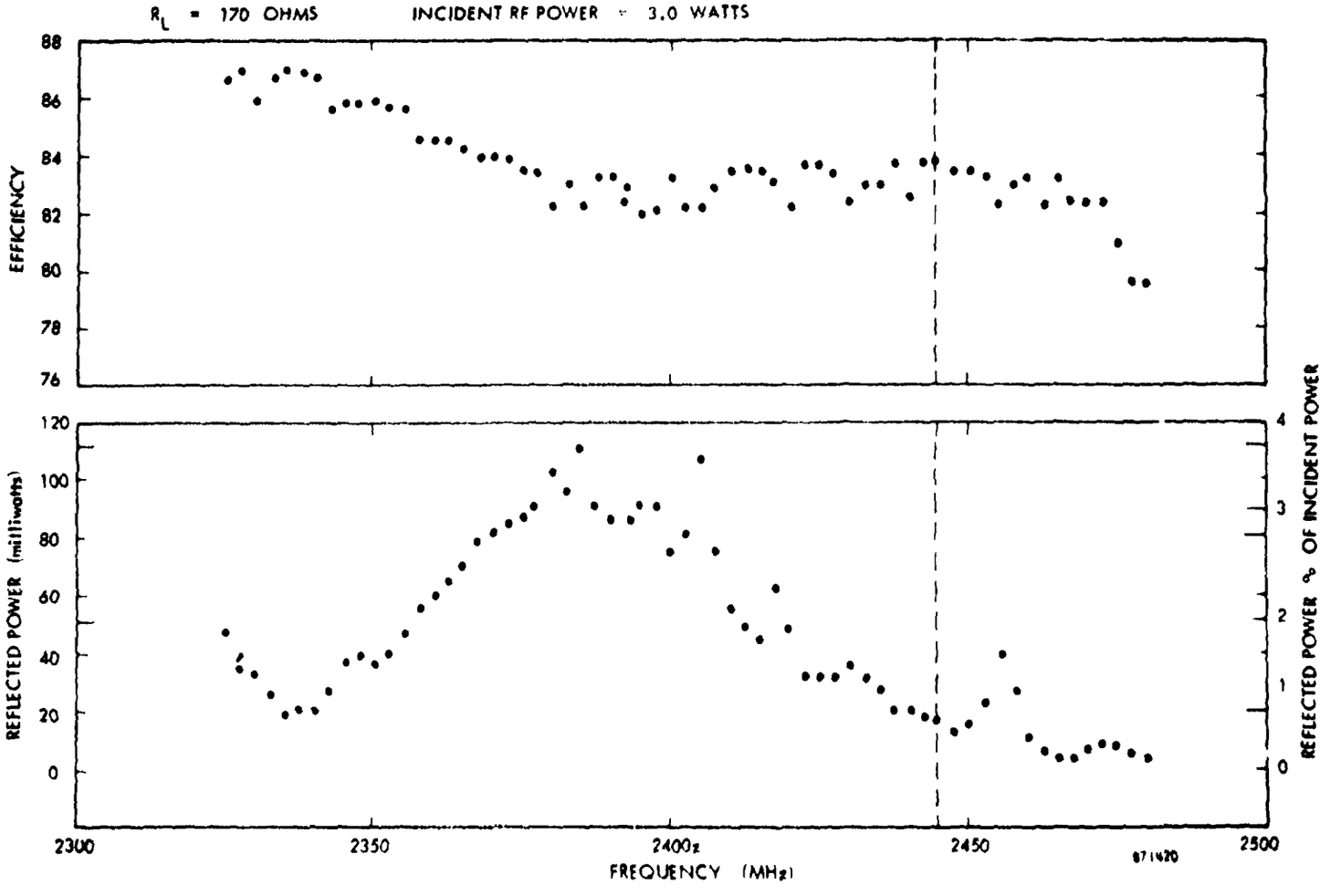

Figure 34. Overall efficiency and reflected power as a function of frequency with the rectenna element optimized at 2445 MHz.

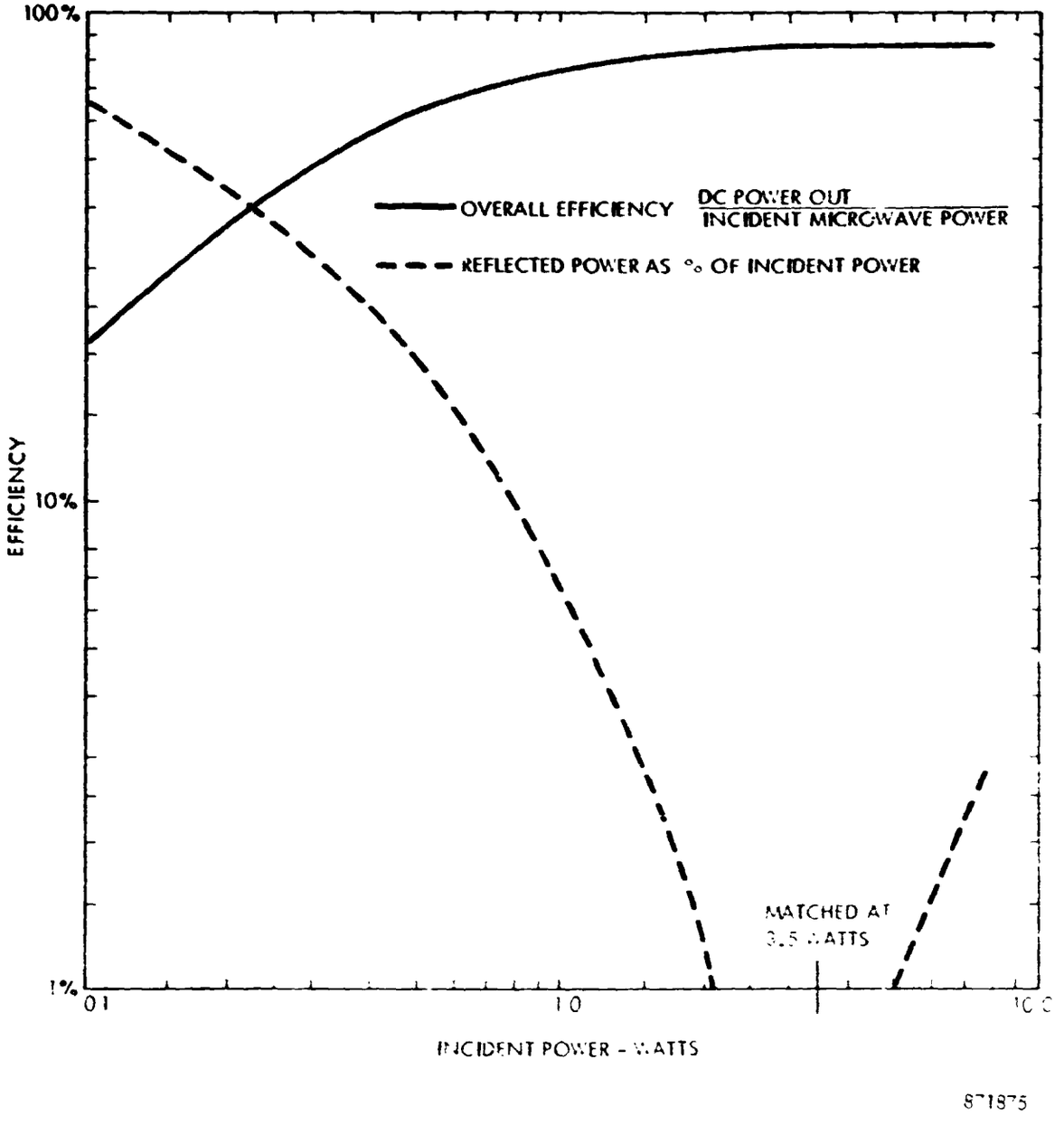

Figure 35. Overall efficiency and reflected power as a function of input power level for an element matched for an incident power level of 3.5 watts at 2388 GHz.

3.5 DC Output Current and Reflected Power as a Function of Microwave Power Input for a Low Pass Short

The relationship is shown in Figure 36. It is an important relationship in ascertaining the amount of current which is drawn through the diode when it is operating into a short circuit. The amount of current, in turn, is important in clearing a fault caused by one of many diodes operating in parallel developing a short circuit within itself.

Another important but simple relationship in the rectenna element is the highest temperature reached by the diode as a function of heat dissipation within the diode. This relationship may be shown schematically as in Figure 37. For practical purposes, in the rectenna element there are two heat resistances connected in series. One of these is the resistance to heat flow within the diode itself, and the other is the resistance to heat flow from the point of thermal connection to the diode to the point where the rectenna element is heat-sinked. The latter point is where the rectenna element is connected to the dc current collecting bus which usually has a large radiating area and which will run at a temperature of at most $20C^{O}$ above ambient. The heat resistance of the diode is 16 to $20C^{O}$ per watt and the heat resistance of that portion of the rectenna element which transports heat to the heat sink area is $15C^{O}$ per watt. Therefore, if the diode is dissipating one watt within itself, there will be a maximum temperature drop of $35C^{O}$ to the heat sink point.

3.6 Characteristics of the Low Pass Wave Filter

Another important property of the rectenna element is its harmonic filtering capability. This is essential not only to prevent excessive harmonic radiation from the rectenna but is also essential for the highly efficient operation of the rectenna element. The two section low pass filter, shown in Figure 15, as the section nearest to the dipole, was designed using conventional wave-filter theory and taking fully into account the two terminal-pair characteristics of the transmission line sections which comprise the "inductive" sections of the filter. The computed phase shift and mid-shunt characteristic impedance of a network section as a function of frequency are shown in Figure 38. The attenuation characteristic of the network as a function of frequency is shown in Figure 39. It will be noted that the characteristics are somewhat different from a lumped-circuit

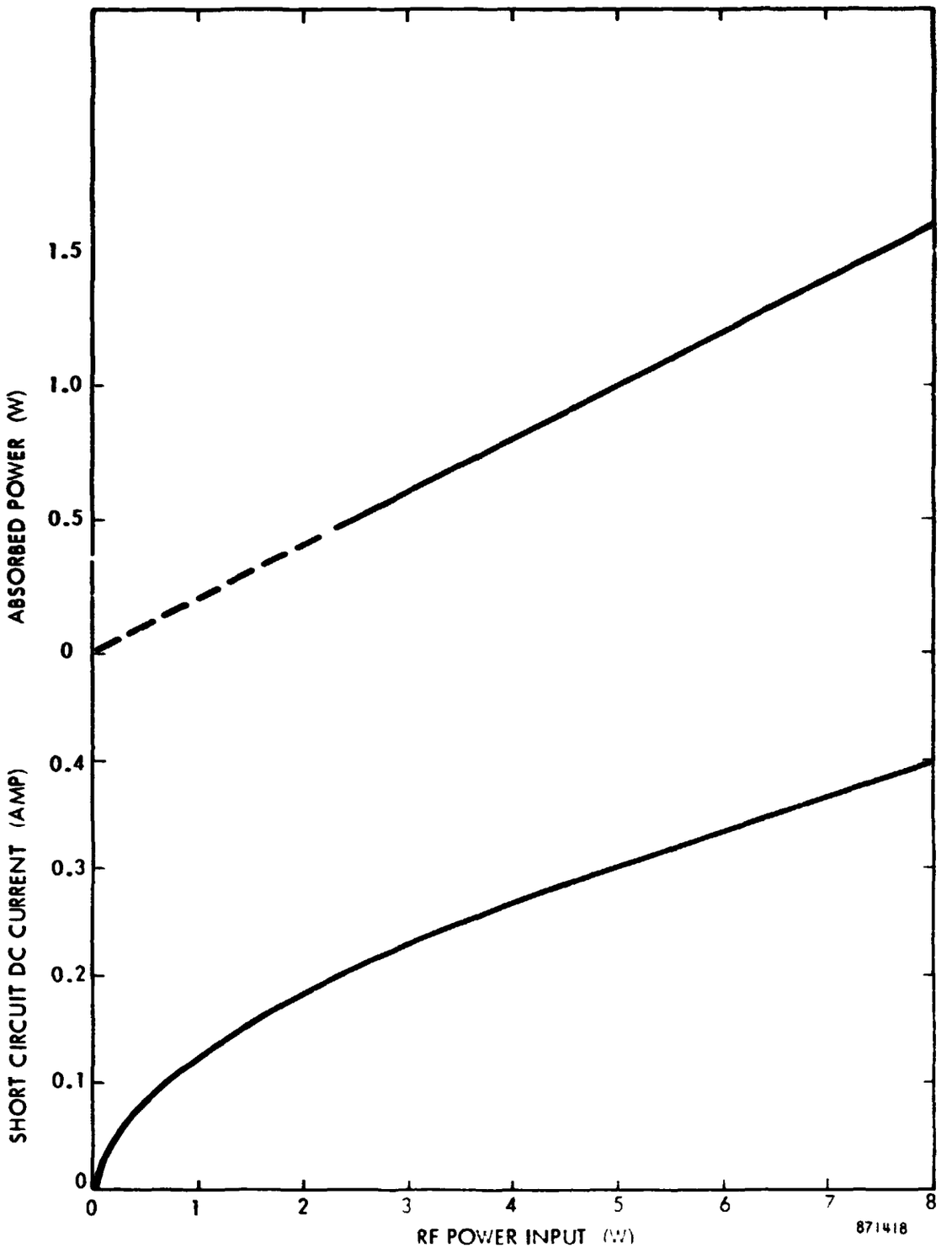

Figure 36. DC output current and absorbed power as a function of microwave power input for a DC load short in the rectenna element.

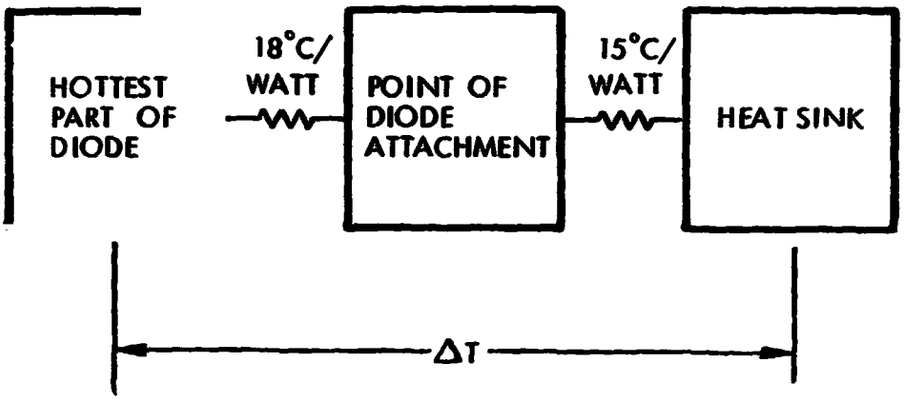

Figure 37. Equivalent circuit of heat flow from the hottest part of the diode to the heat sink in the MSFC rectenna element.

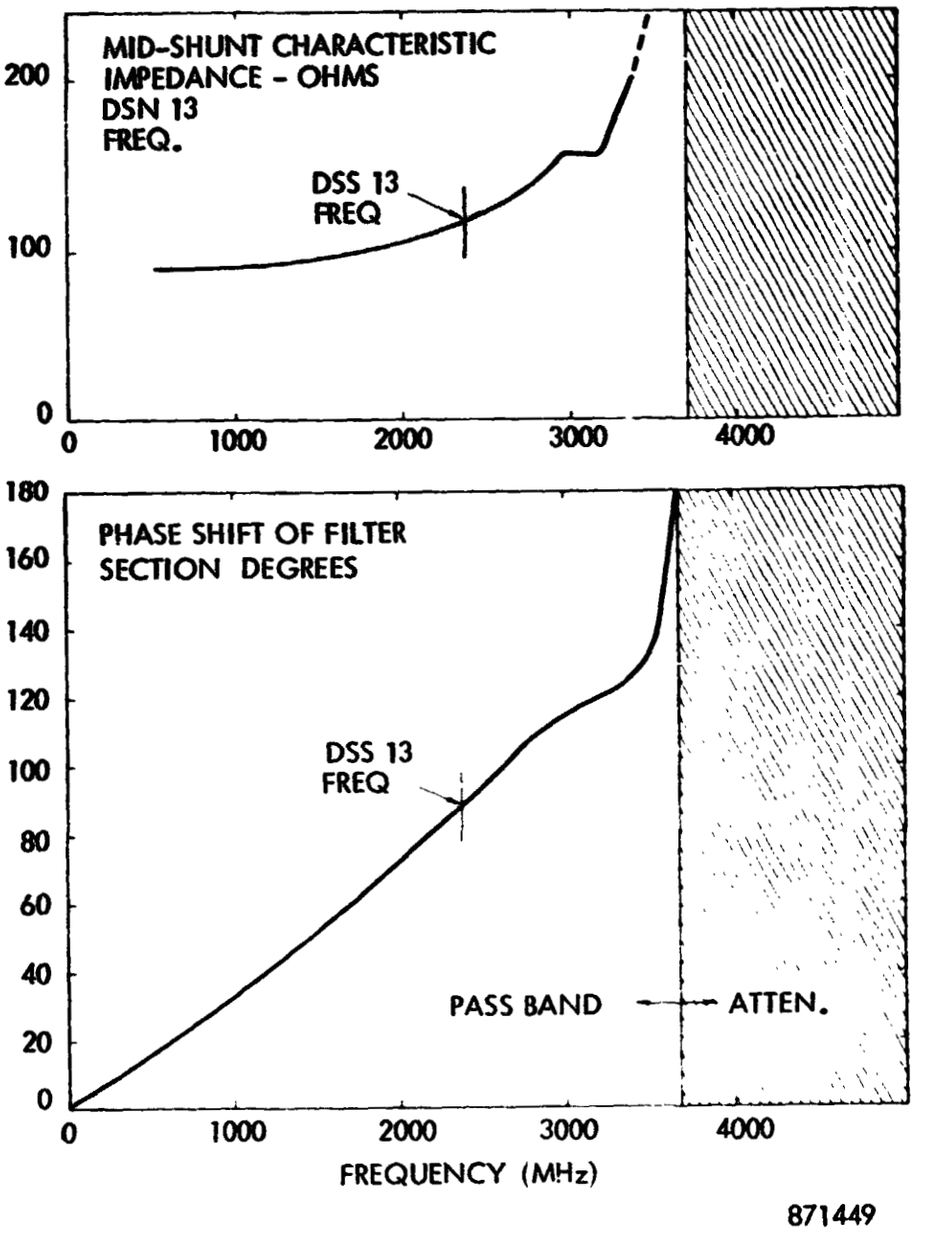

Figure 38. Mid-shunt characteristic impedance and single-section phase shift as a function of frequency for the filter in the MSFC rectenna element.

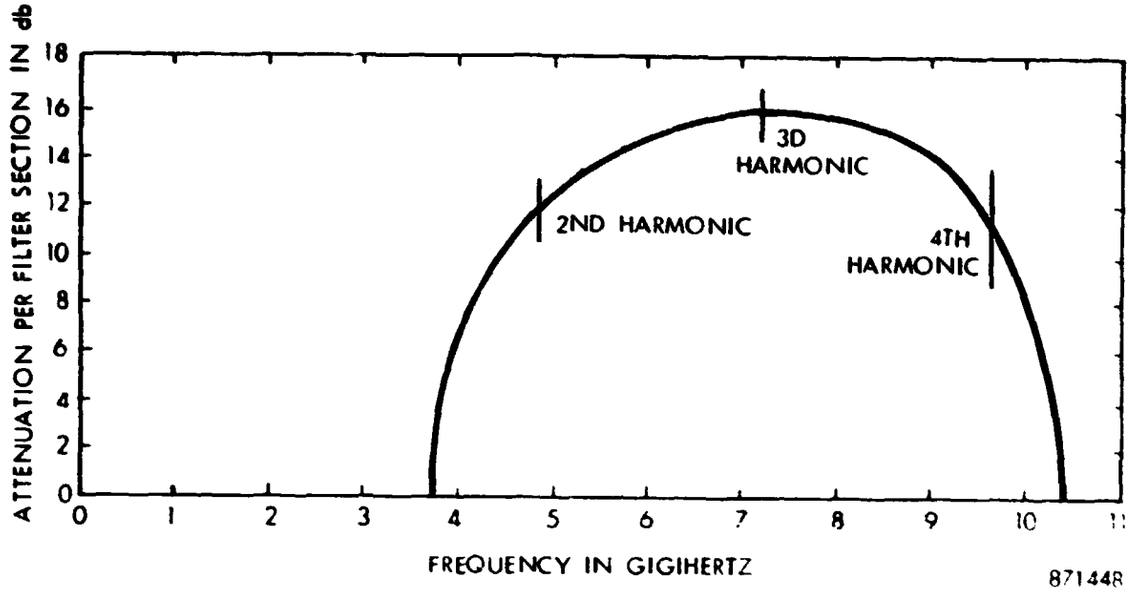

Figure 39. Attenuation characteristic for a single section of the low pass filter in the MSFC rectenna element.

filter design as would be expected. The filter characteristics were not generally experimentally evaluated. However a check was made at the fundamental frequency by means of "S-curves" to determine how well the characteristic impedance of the network matched the input impedance to the antenna. The impedance match was well within 25% and may have been better. The match is certainly good enough to reduce standing wave losses in the filter sections to a negligible amount compared with other losses in the rectenna element.

4.0 DESIGN OF A DIODE FOR THE NEW MSFC RECTENNA

Initial experimental and analytical work on the characterization of critical diode parameters in Phase II made it possible to specify a diode design for the improved Phase III rectenna. While we had a substantial number and variety of Schottky barrier diodes to test in Phase II, there were few instances in which the rectenna element efficiency exceeded 80%. Clearly, an improved diode design was needed.

Appendix I indicates the nature of the losses in a diode. They consist of (1) the Schottky barrier voltage drop, (2) the loss in the series resistance of the diode during the conduction period, and (3) the loss in the series resistance of the diode during the non-conduction period caused by the charging currents flowing to the capacitance of the diode. Appendix I also provides an approach to estimating these losses individually.

During Phase III some simplifying assumptions were made concerning the operation of the diode which permitted estimating the losses in the diode as a function of the voltage breakdown, V_{br}, in the reverse direction, and the area of the junction. With these simplifying assumptions and the use of Figure 5-10 in Appendix I, it was possible to find an optimum design for the diode.

The model of the simplified rectification cycle is shown in Figure 40. In using this model it is assumed that:

1. The conduction current in the forward direction is flat topped--that is, it has a constant value throughout the conduction cycle.
2. The voltage waveform during the non-conduction period is sinusoidal and the maximum inverse voltage just swings to the V_{br} of the diode.
3. The Schottky barrier voltage is taken as the intercept of the tangent to the forward voltage current characteristic at a value of 500 ma with the zero current axis.

These assumptions in conjunction with the work in Appendix I results in the set of equations given in Appendix III.

When this set of equations is applied to both the GaAs-Pt barrier and the Si-W barrier, we obtain the curves shown in Figure 41. These curves point out how the

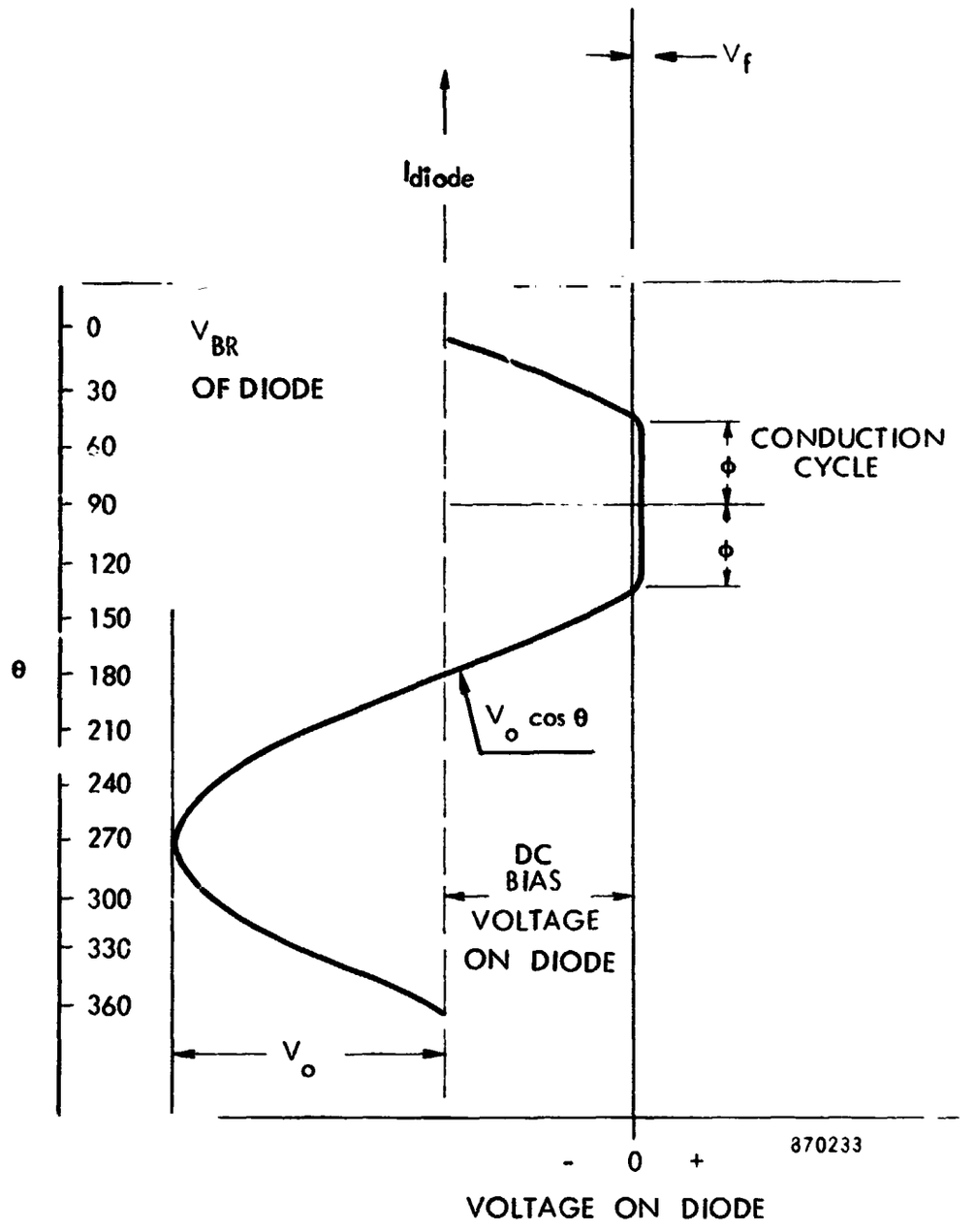

Figure 40. Idealized model of the rectification cycle in the use of a diode in a half-wave rectifier configuration.

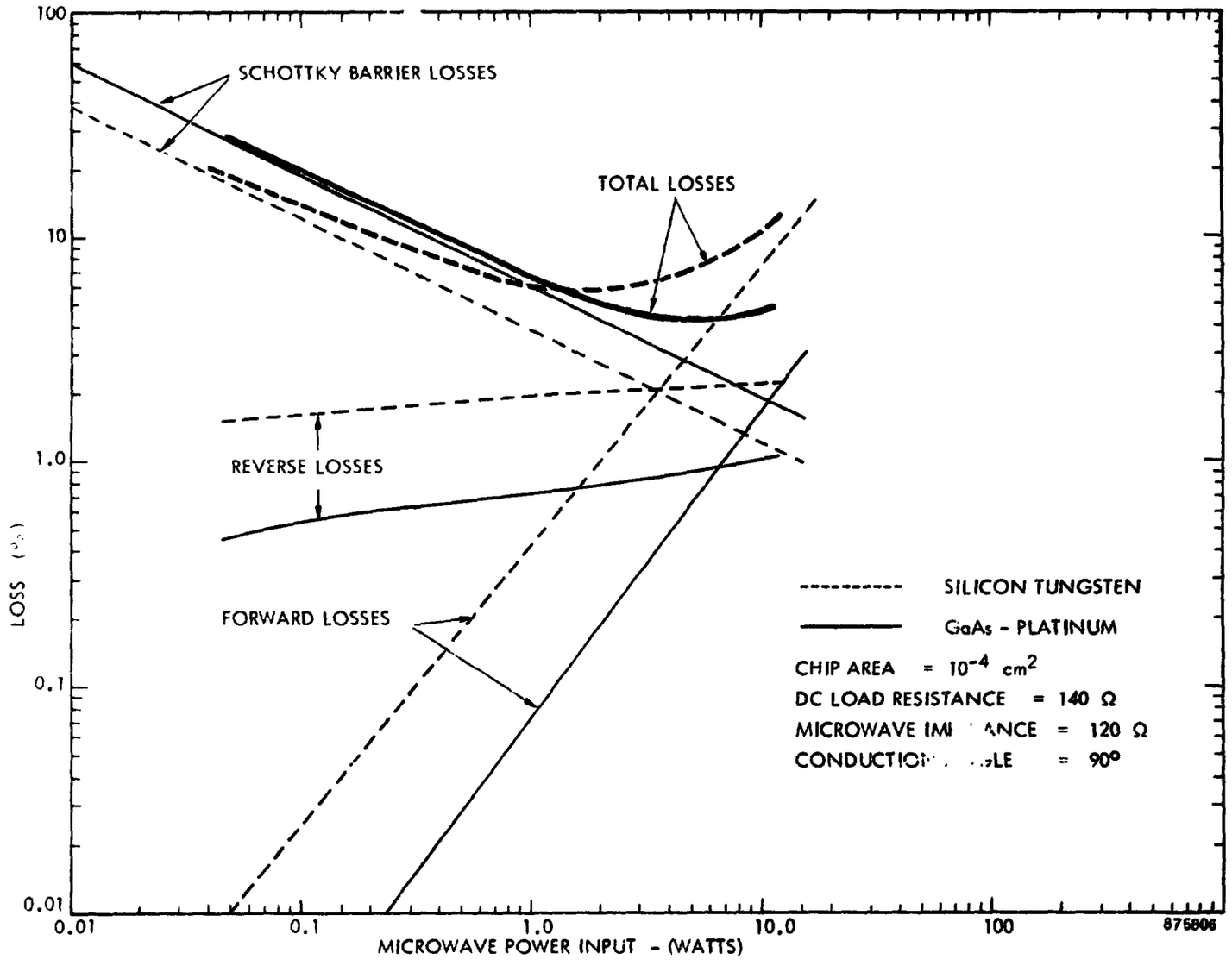

Figure 41. Microwave losses in an optimally designed diode as a function of input power level for a microwave impedance level of 120 ohms.

individual losses vary as a function of the power level. The total-loss curve shows the substantial superiority of the GaAs material at the higher power levels.

Figure 42 indicates how the area of the junction impacts the efficiency. At high power levels, a large junction area is clearly indicated.

Figure 43 indicates how the reverse breakdown voltage varies as a function of power level for an optimally designed diode. Given also on this figure are the zero-bias junction capacitances for various sized junctions and V_{br}'s.

The use of this design process has been quite effective in increasing the efficiency of diodes in rectenna element circuits. However, the simplifying assumptions must introduce substantial errors, since no account is taken of circulating harmonics which must increase the losses.

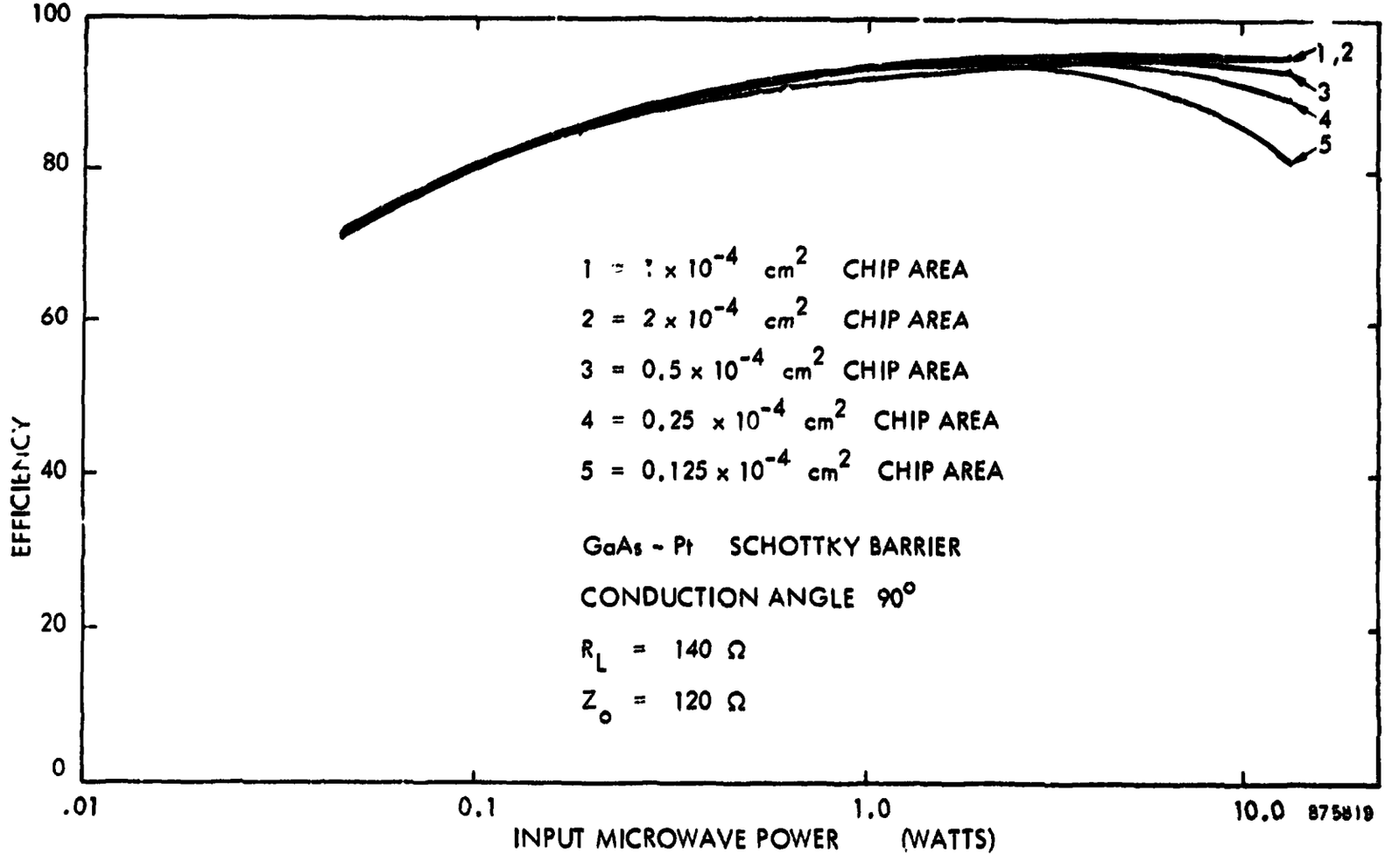

Figure 42. Computed diode efficiency as a function of chip areas and microwave power input for GaAs-Pt for a microwave impedance of 120 ohms.

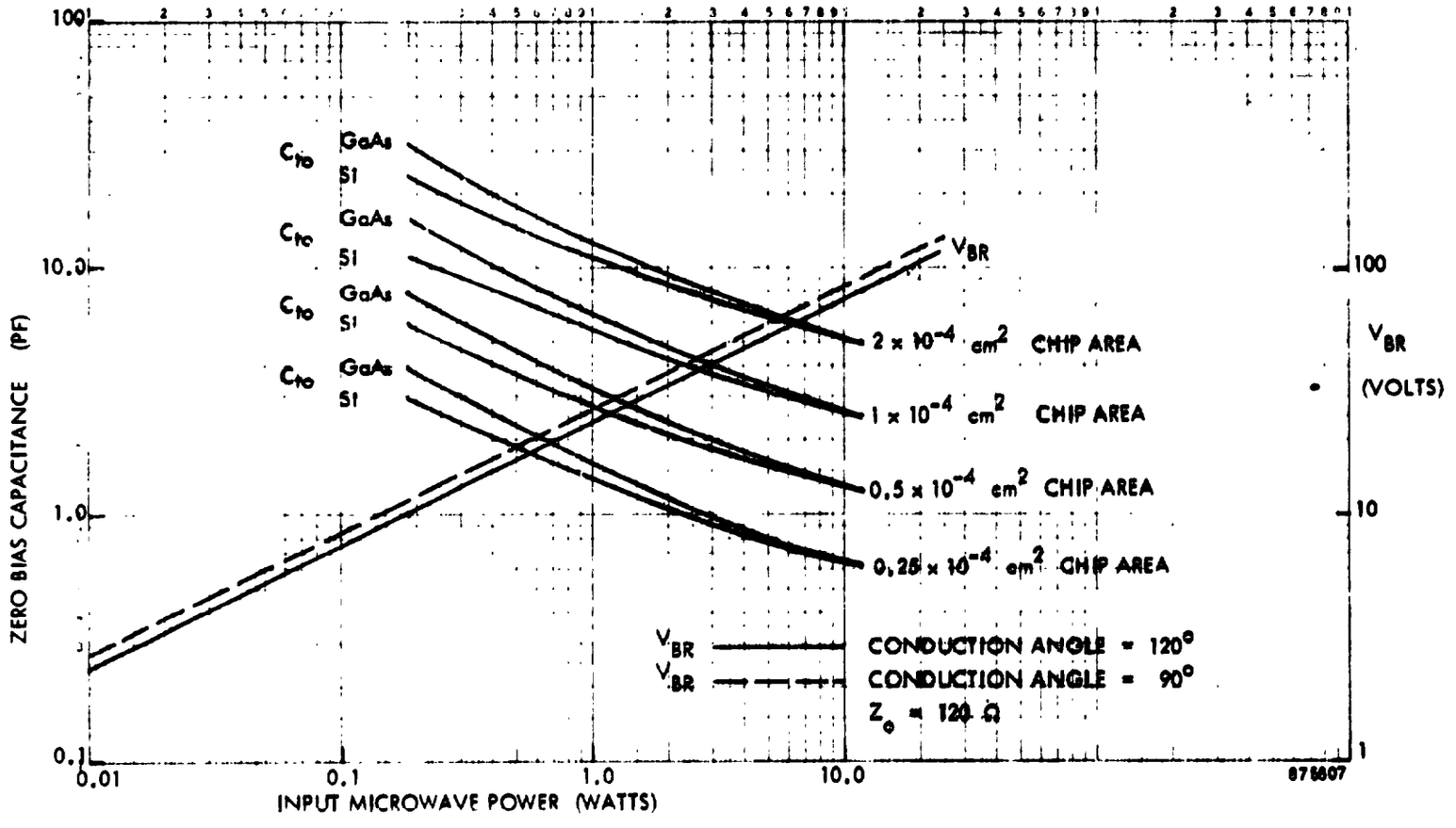

Figure 43. Junction capacitance and V_{br} as a function of input microwave power for an optimally designed diode.

5.0 RECOMMENDATIONS FOR FUTURE DEVELOPMENT EFFORT

The following recommendations are made within the context of improving the basic technology of microwave power transmission in terms of better components and in terms of better overall efficiency and distance of transmission. The influence of specialized applications such as the Satellite Solar Power Station which results in specific component hardware is minimized in favor of obtaining higher level performance in essentially laboratory demonstrations in the near-term time frame:

(1) Frequency Selection for Development Effort

The ISM Band 2450 plus and minus 50 MHz is recommended on the basis that (1) the frequency is in a region where high efficiency of the components can be obtained, (2) nearly all of the microwave power transmission experience has been accumulated at this frequency, and because (3) important applications may fall at or near this frequency.

(2) Development of a Highly Efficient Microwave Generator

The emphasis of the MSFC effort has been upon improving the rectenna device to the point where the microwave generator is now the bottleneck in improving the overall efficiency. Therefore, emphasis should now be placed on the development of an efficient microwave generator. A decision on the power level and the general format of such a tube may be dependent upon some application, assuming that the application does not compromise the goal of obtaining the highest efficiency possible. The SSPS application which requires a directional amplifier in the 5 kilowatt CW region and the use of a pure-metal platinum secondary emitter cathode for long life could set the parameters for such a tube development. The efficiency goal of such a development should not be less than 85% as defined by the ratio of microwave power added by the generator to the dc power input to the generator. Since 85% can probably be reached with present design expertise, a longer range goal of 90% should be set in order to introduce additional design approaches and refinements.

(3) Demonstration of Improved Overall DC to DC Efficiency

It is recommended that a laboratory set-up for the demonstration of improved dc to dc efficiency with an objective of an overall efficiency in the 65 to 70% region be assembled, that the highly efficient generator developed under item 2 be

used as the generator and that an improved rectenna* sufficiently large to absorb the 5 kilowatts of rf power be used as the receiving element. The standard dual mode horn would be used as the transmitting antenna.

(4) Demonstration of Improved DC to DC Efficiency Over a Longer Distance

Present demonstrations of overall dc to dc efficiency over short distances in an inside laboratory fall short of full effectiveness in demonstrating the concept of transmitting power without wires. It is recommended that the techniques that have been developed for efficiently transmitting microwave power over longer distances and described in section 1.5 be utilized for a demonstration of free-space power transmission over much longer distances.

*Improvements in the analysis of and the efficiency of rectenna elements is now in progress under NASA LeRC Contract # NAS 3-19722.

REFERENCES

1. Stuhlinger, E., and Bucher, G. C., "A Concept for an Orbiting Astronomical Station", R-SSL, MSFC, Working Paper, August 1967.

2. Orbital Astronomy Support Facility, (OASF) Study. NASA-MSFC Contract NAS8-21023. Douglas Aircraft Co., DAC-58142, June 28, 1968.

3. Robinson, W. J., "The Feasibility of Wireless Power Transmission for an Orbiting Astronomical Station" (Revised). NASA Tech Memorandum, Report No. 43806, May 27, 1969.

4. Brown, W. C., "A Survey of the Elements of Power Transmission by Microwave Beam", 1961 IRE Internat'l Record, Vol. IX, pt. 3, pp. 93-106.

5. Brown, W. C., "Experiments in the Transportation of Energy by Microwave Beam", 1964 IEEE Internat'l Conv. Record, Vol. XII, pt. 2, pp. 8-17.

6. Brown, W. C., "Experimental Airborne Microwave Supported Platform", Technical Report No. RADC-TR-65-188, Dec., 1965. Contract AF30 (602) 3481.

7. Goubau, G., Schwering, F., "On the Guided Propagation of Electromagnetic Wave Beams", IRE Trans. on Antennas and Propagation, Vol. AP-9, May 1961, pp. 248-256.

8. Okress, E. C., Brown, W. C., Moreno, T., Goubau, G., Heenan, N. I., George, R. H., "Microwave Power Engineering", IEEE Spectrum, October 1964.

9. Brown, W. C., "Free-Space Microwave Power Transmission Study", Raytheon Report No. PT-2931 covering period of Dec., 1969 to Dec. 1970. NASA contract no. NAS-8-25374.

10. Brown, W. C., "Free-Space Microwave Power Transmission Study, Phase 2", Raytheon Report No. PT-3539 covering period from April, 1971 - August, 1972. NASA contract no. NAS-8-25374.

11. Brown, W. C., "The Technology Application of Free-Space Power Transmission by Microwave Beam", Proceedings of the IEEE, Vol. 62, No. 1, Jan. 1974, pp. 11-25.

12. Brown, W.C., "High Power Microwave Generators of the Crossed-Field Type", Journal of Microwave Power, Vol. 5, No. 4, pp. 246-260, 1970.

13. Ruden, T.C., Large Signal Analysis. Twenty-second Quarterly and Final Report, Contract No. NObsr-77590, Sept. 7, 1964. Raytheon Report No. SPO-012, Section 2. 3, pp. 41-60.

14. Twisleton, J.R.G., Proc. IEE, Vol. 111, No. 1, January 1964, pp. 51-56.

15. Dickinson, R.M., Brown, W.C., "Radiated Microwave Power Transmission System Efficiency Measurements", NASA Technical Memorandum 33-727, Jet Propulsion Lab., Cal. Inst. Tech., May 15, 1975.

16. Robinson, W.J., "Wireless Power Transmission in a Space Environment", J. Microwave Power, vol. 5, Dec. 1970.

17. Brown, W.C., "Experiments Involving a Microwave Beam to Power and Position a Helicopter", IEEE Trans. on Aerospace and Electronic Systems, Vol. AES-5, No. 5, pp. 692-702, Sept., 1969.

18. Brown, W.C., "Progress in the Efficiency of Free-Space Microwave Power Transmission", J. Microwave Power, vol. 7, no. 3, pp. 223-230.

19. Potter, P.D., "A New Horn Antenna with Suppressed Sidelobes and Equal Beamwidths", Microwave J., pp. 71-78, June 1963.

20. Goubau, G., "Microwave Power Transmission from an Orbiting Solar Power Station", J. Microwave Power, vol. 5, Dec. 1970.

APPENDIX I

RECTENNA DESIGN IMPROVEMENT IN PHASE II ACTIVITY

Pages 5-15 through 5-62 reprinted from PT-3539, the Phase II Final Report.

5.3 Topology of Rectenna Circuits

One of the elements in the rectenna improvement program is the incorporation of a low-pass filter which will prevent the reradiation of power at harmonic frequencies, thereby preventing undesirable radio frequency interference (rfi) to other users of the radio frequency spectrum and maximizing the operating efficiency of the rectenna element. A second objective of the program is a design which can eventually be directly incorporated into a printed circuit or stripline configuration. Such a configuration has long been the ultimate objective of the rectenna development because of its light weight, low cost, and physical flexibility. Flexibility is desirable in a space application because of in-flight storage and in-space deployment considerations.

To further understand the new design approach in terms of the dual objectives of utilizing printed circuit or stripline technology and incorporating filters, the reader is reminded that to achieve high efficiency, a rectenna must be a two-level structure. However, the second level is merely a reflecting surface which need not be physically coupled to the front surface. The front surface plane can then be used to:

1. Absorb microwave power
2. Rectify it
3. Collect rectified power in dc collecting busses which carry the dc power to the edges of the rectenna section for collection into larger busses
4. Prevent radiation of power at harmonic frequencies

The use of the front plane for the first three of these functions is characteristic of several experimental rectennas that have been constructed and tested. However, the installation of filters which will prevent the reradiation of all power at harmonic frequencies has not been characteristic of the experimental rectennas constructed so far. To prevent harmonic radiation it is necessary to insert a low-pass filter between the antenna element, which absorbs the power from space, and the rectifying element. This is shown schematically in Figure 5-3.

A low-pass filter must be constructed with inductance and capacitance if the losses are to be minimized, and the resulting configuration is shown in Figure 5-4a. Figure 5-4b also shows how a single diode could be incorporated as a rectifier, but there are other arrangements which could incorporate several diodes in a function other than pure parallel operation. For the present discussion, however, attention will be focused on the filter.

It will be noted first that the low-pass filter allows the top and bottom of the network to be at different dc potentials. It therefore follows that the conductors which form the top and bottom of the filter can be used as dc busses to transport the rectified power to the edges of the array. A second aspect of the filter that must be taken into consideration is that a physical space is required for the construction of the filter. The space required is roughly proportional to the number of filter sections required, and there are likely to be at least two. A convenient place to put these filters is in the space between two of the half-wave dipole antennas as shown in Figure 5-4b.

The second consideration is the possible rectifier configuration that could be employed at the two-terminal A-A' connection shown in Figure 5-4a. If a full-wave rectifier is employed as in Figure 5-5a, an additional bus will be required, and if it is kept in the same plane as the other conductors without intersecting them, it must pass through the center line of

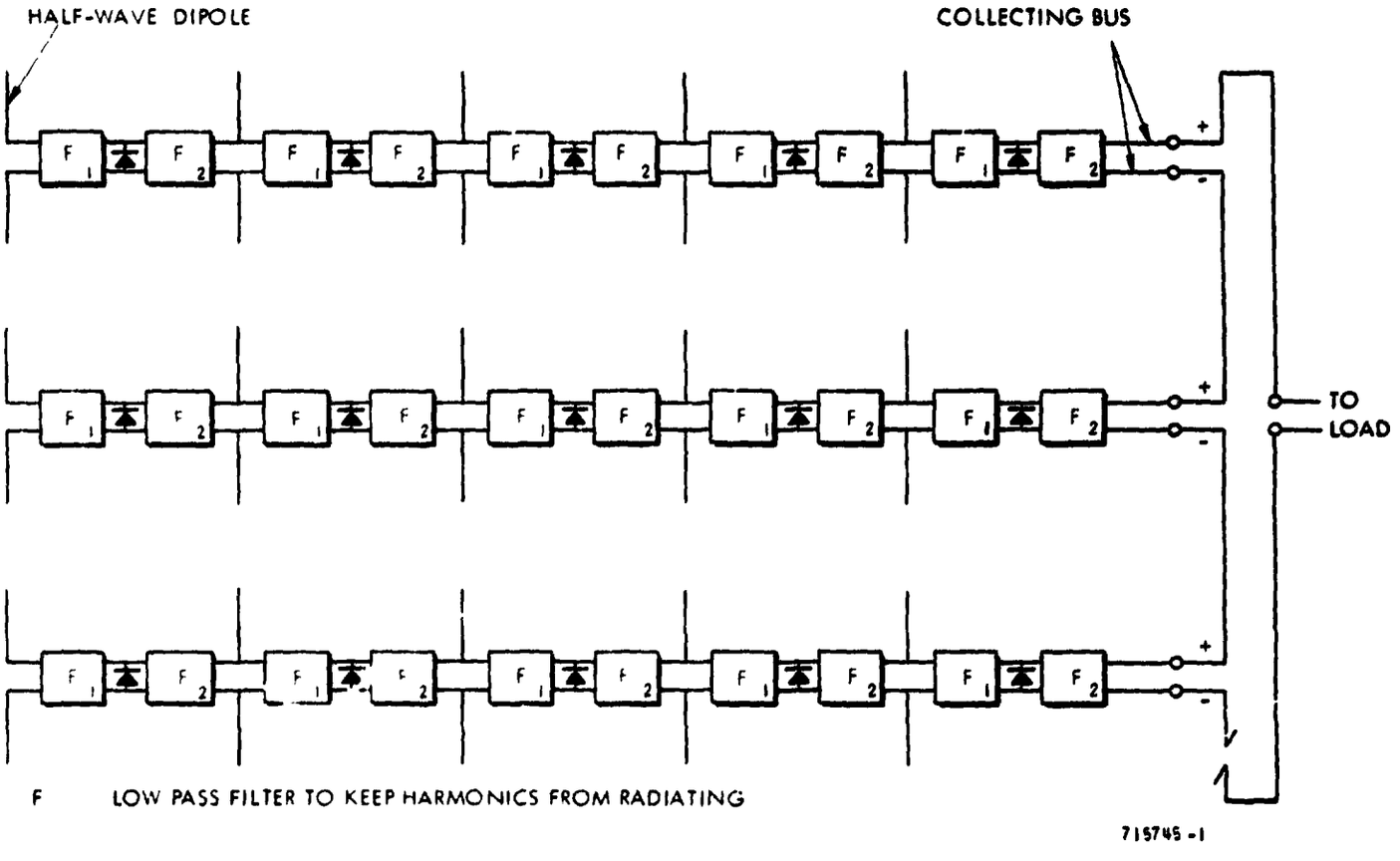

Figure 5-3. Schematic Arrangement of Rectenna Showing Half-Wave Dipoles, Low-Pass Filters, Diodes, and DC Power Collection Busses

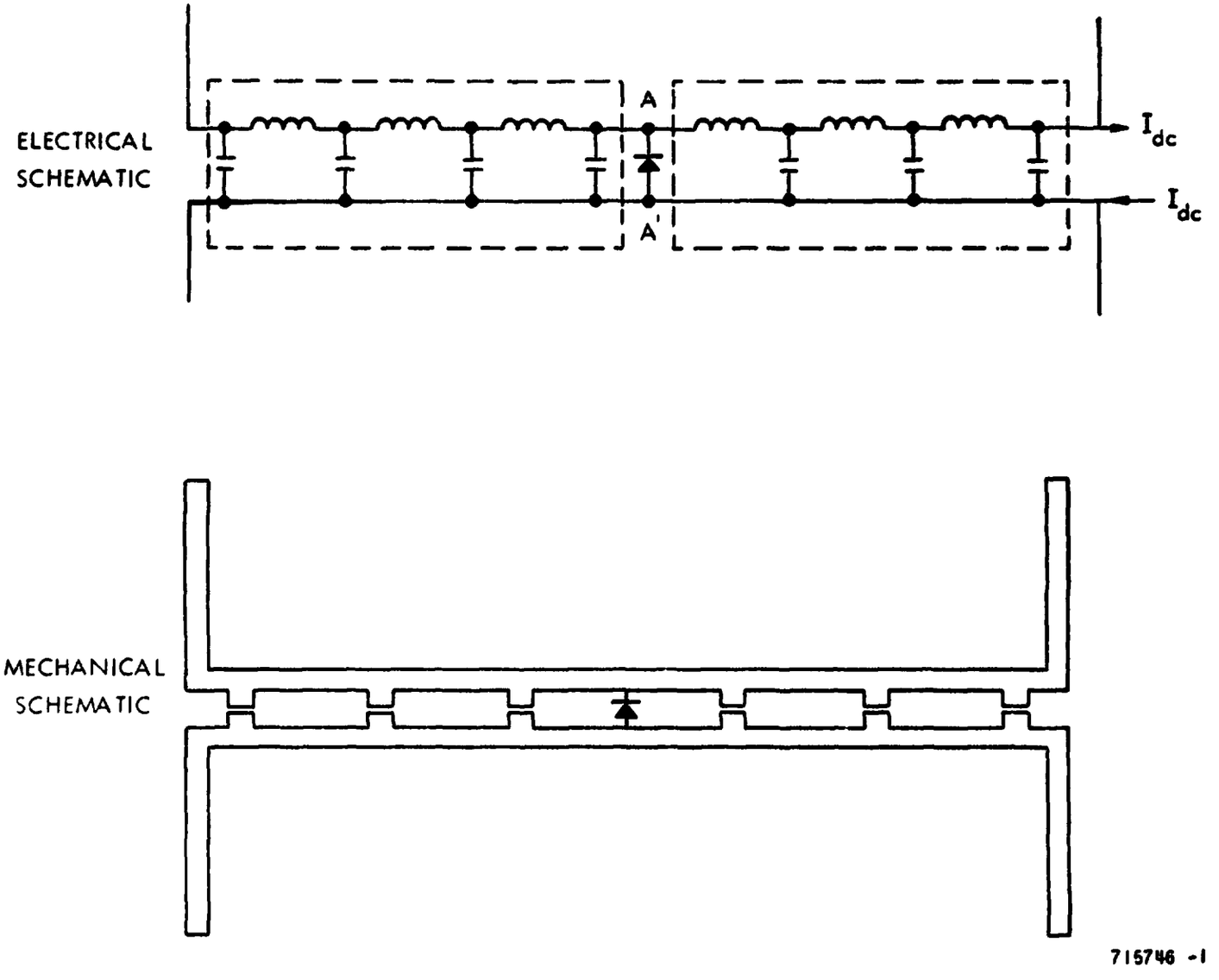

Figure 5-4. Electrical and Mechanical Schematics of Filter Sections

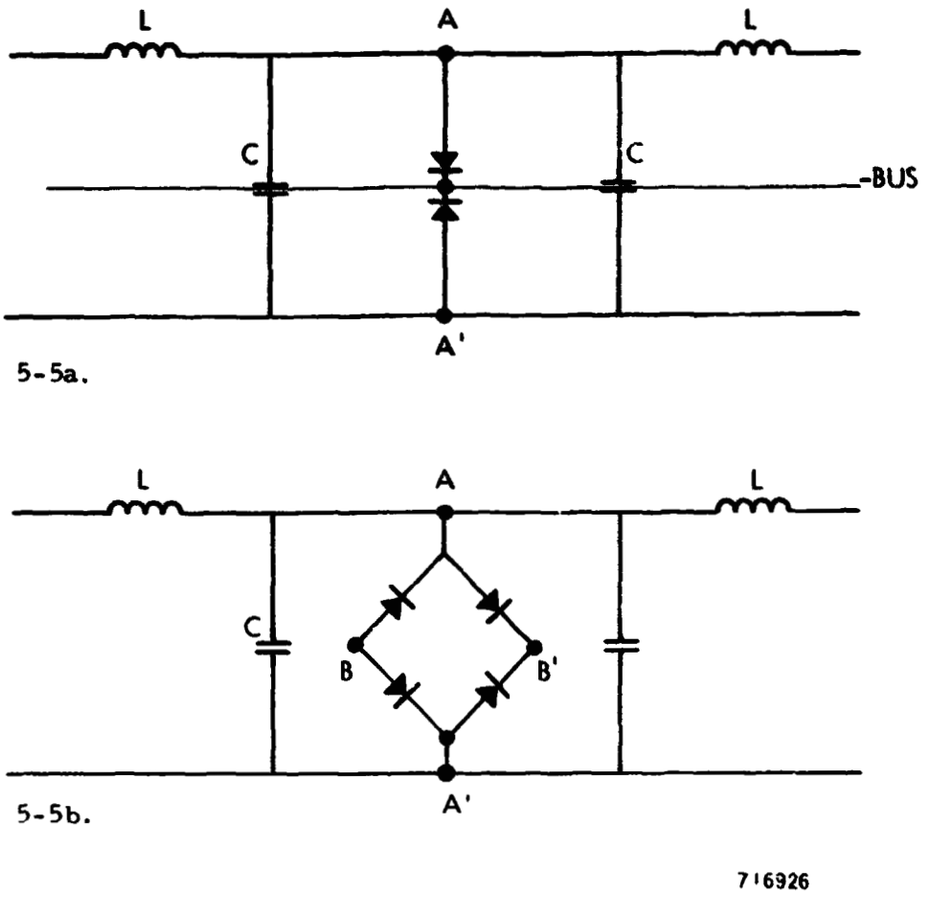

Figure 5-5. Full-Wave and Bridge-Rectifier Configurations in Relationshp to Wave Filter Terminals

the capacitances. This is probably not practical. If a full-wave bridge-type rectifier is used (as in Figure 5-5b), the problem becomes even more acute, since two additional terminals are created. If the terminals of successive rectifiers are connected in parallel, two additional busses will be required. Both the rectennas built internally at MSFC and those built at Raytheon have used bridge-type rectifiers and the power has been collected by a single dc bus, connecting the elements in series. But these rectennas contained no filters between the rectifiers and the dipole antennas. If filters were inserted, the schematic would then have to look like that of Figure 5-6 and there is no single-plane topological solution since the filter is a two-terminal pair device. There is also the problem of a strong second harmonic content at terminals B-B' and the suppression of its radiation from the series bus. It would therefore appear that if a full-wave rectifier or a bridge-type rectifier is to be connected to terminals A-A' an additional plane would be required for bussing the power. This does not necessarily rule out these configurations since there may be no disadvantage in using stripline configurations and there may be some advantages. This will require more detailed study.

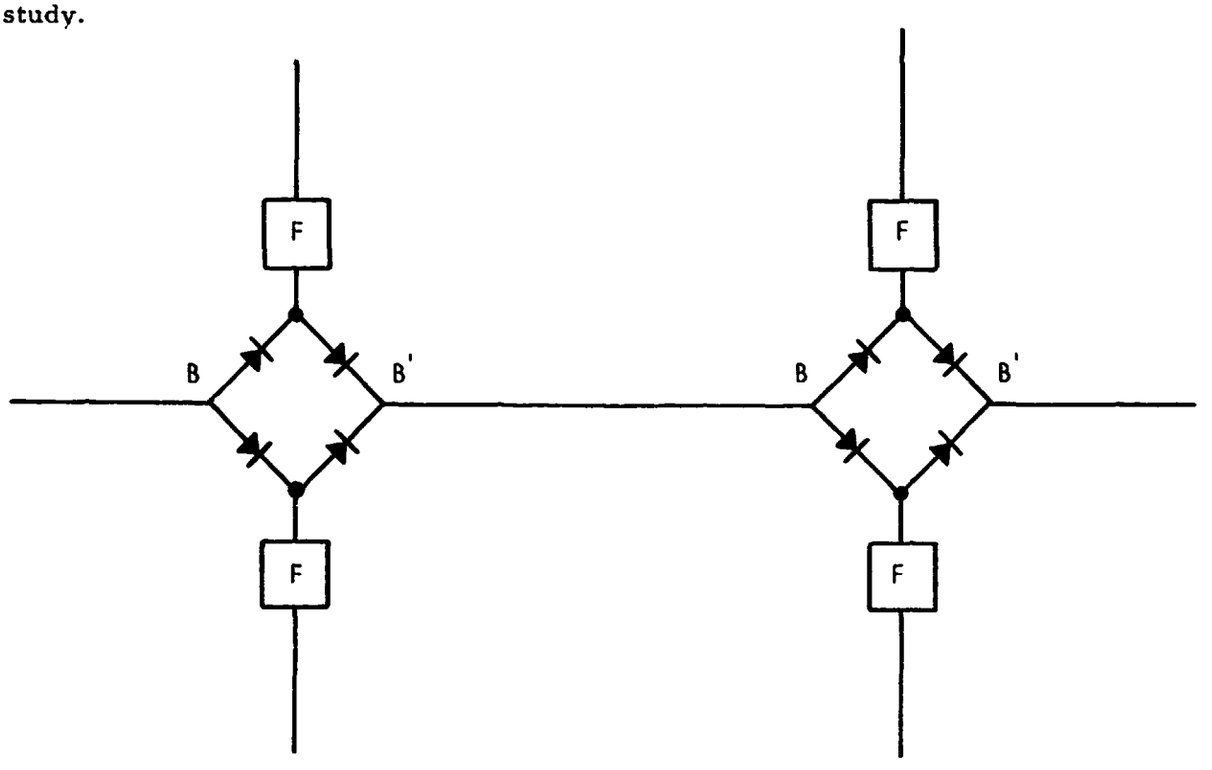

716927

Figure 5-6. Schematic Showing Difficulty of Incorporating Wave Filters, a Bridge-Rectifier, and Power Collection Busses on a Single Plane

Before ending the discussion of rectifier configurations, it should be noted that if the top and bottom conductors at A-A' are broken, a two-terminal pair network may be inserted and this can lead to an element that looks like a filter section. One example (shown in Figure 5-7) of a two-terminal pair structure that could be useful is a low-pass filter element made up of the capacitance of the diodes themselves with an intervening inductance whose value is such that the filter operates at or near the upper cutoff frequency. Under that condition, rectifier diodes are operating 180° out of phase. This filter section then behaves as a full-wave rectifier in the sense that current flows into the dc busses on both halves of the rf cycle. Such an element could have a considerable amount of energy storage, i.e., a significant Q. If the device were fed from one side only, the symmetry of the rectification process would be affected, being less affected with the higher Q values. The symmetry could be restored, regardless of the Q value, by feeding the network from adjacent half-wave dipoles assumed to be excited in the same phase.

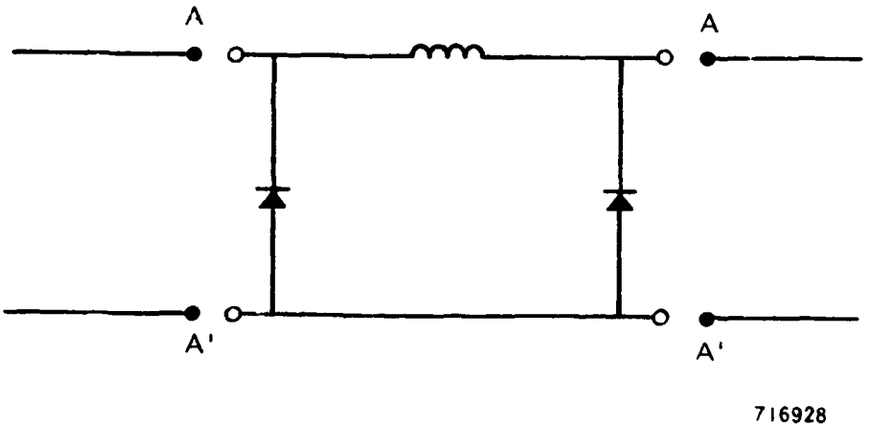

Figure 5-7. An Approach to an Effective Full-Wave Rectifier without Introduction of another Bus (Diodes are 180° out of phase)

Until now, a general discussion of whether the rectifying element is excited by one dipole or more than one dipole has been avoided. Referring to Figure 5-3, if F_1 and F_2 are identical then the rectifier will be excited by microwave power flowing from the left and right. Furthermore, all of the dipoles will have some mutual coupling to each other through the shared microwave circuitry and there will be some compromise in the desirable non-directive properties of the rectenna. On the other hand, F_2 can be a filter whose upper cutoff frequency is below the frequency of the incoming radiation so that it will not transmit the fundamental frequency either to the right or left, and hence the directive properties of the rectenna will be unaffected. The filter, of course, will look like a reactance above cutoff and this must be taken into account in the design of the circuitry. It is probable that the choice which is made in this matter will depend upon how important the non-directive property is in the intended application.

In most of our experimental work, we have assumed that only a single dipole is involved with the rectifier. This permits designing and testing a single element of the rectenna according to the procedure that we have used successfully in the past. This procedure makes use of a section of expanded waveguide into which the complete element is matched. Accurate measurements of efficiency can be made, and the cross-section of the expanded waveguide has been correlated with the area taken up by the element in the finished rectenna. The electrical and mechanical design of the element is such that it can be adapted to a printed circuit or stripline configuration.

5.4 Rectenna Element Improvement

5.4.1 Introduction

The task of improving the rectenna element efficiency was approached by determining the areas of loss within the element and by lowering the losses in the most critical areas. At the same time, it was necessary to maintain the high absorption efficiency of the element and avoid reradiation. Since preliminary calculations had shown that skin losses within the structure of the element should account for less than one-fourth of the experimentally measured values, the main focus of this effort was concentrated on a study of the semiconductor diode. This study was undertaken using the following different, but supportive tacks:

1. Mathematical analysis of the probable diode loss mechanisms.

2. Computerized transient analysis of the rectenna element performance with numerical output of waveforms and losses.

3. Experimental program of measuring diode efficiencies with parameter variations among individual diodes.

Preliminary tests (see Table 5-1) on a coaxial test fixture (Figure 5-8) showed that superior power handling capability and rectification efficiency could be obtained from Raytheon's Special Microwave Devices Operation's GaAs diodes as compared to Hewlett-Packard Associates' silicon diodes. Accordingly, further tests and analyses were confined to these GaAs devices.

5.4.2 Diode Selection and Characterization

The diodes tested were produced in a three-dimensional matrix of characteristics. The varying parameters were breakdown voltage, junction capacity, and back-contact type. The diode model chosen for analysis and

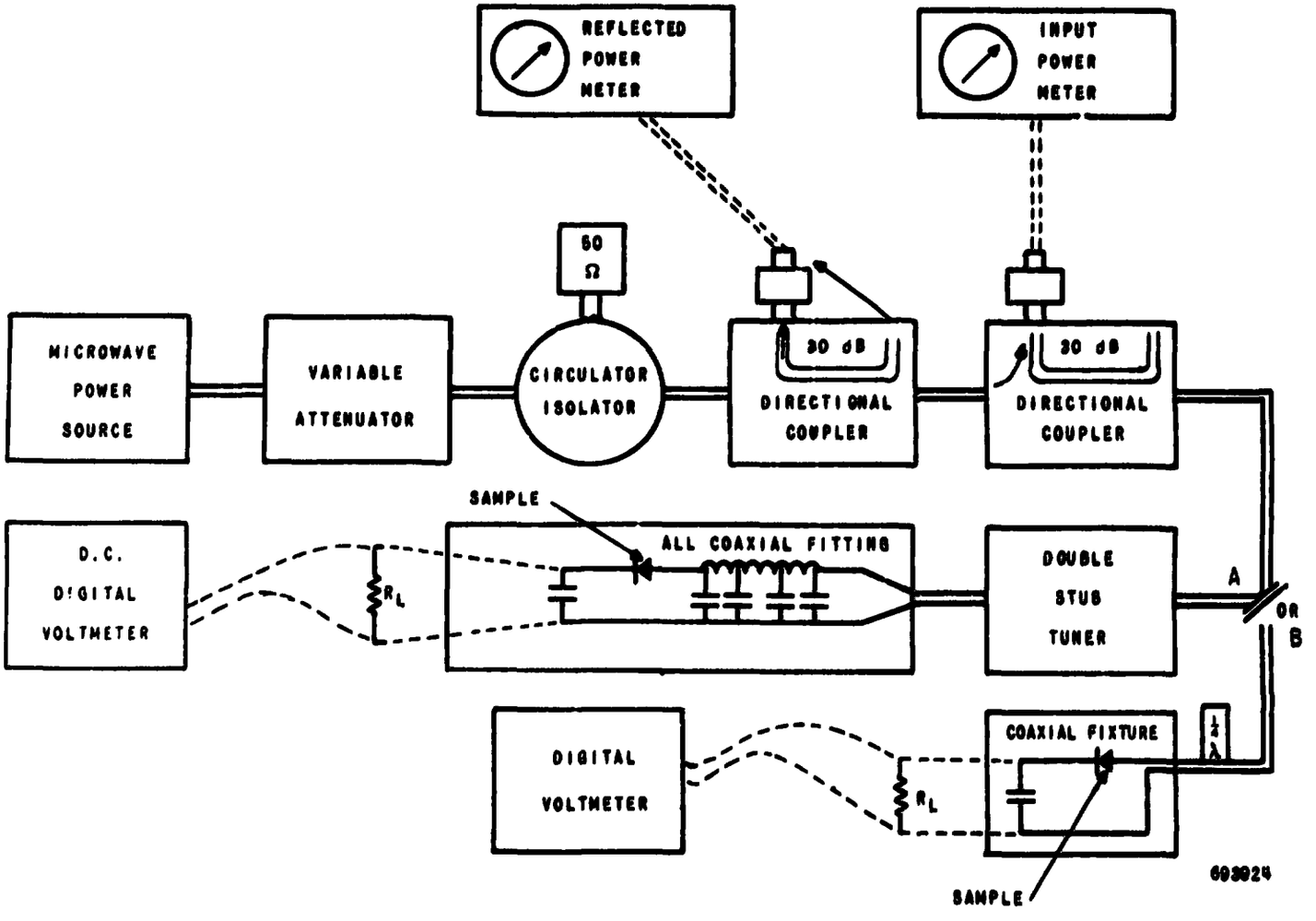

Figure 5-8. Coaxial Circuit for Preliminary Tests

Table 5-1. Preliminary Tests of Diode Efficiency

Micro State	Rs (Ω)	C (pF)	V_{br} (V)	R_L (Ω)	P_{in} (W)	η (%)
Group 1	4	1.5	80	800	1	78
				400	3	78
Group 2	5.8	4	63	200	3	78
				500	1	76
HPA5082 Series						
-2900	5	0.8	50	500	0.25	64
				600	1.0	55
-2565	2	0.8	15	[illegible]	0.25	69
				[illegible]	0.50	65
-2353	2	0.8	12	300	0.25	58
				200	0.50	59
-2800	25	1.0	80	Sampled only: only efficiencies less than 40% were found.		

computer characterization was determined by the diodes tested experimentally. The package in which the diode chip was encapsulated (see Figure 5-9) determined the parasitic case parameters. The junction parameters are uniquely determined by material used to set the breakdown voltage of the diode and by chip sizes into which it is cut (see Figure 5-10).

Figure 5-11, which will be referred to often in the following discussion, pulls together the diode model used. The elements denoted Cp and Lp (the package capacitance and inductance, respectively), are those determined by the encapsulation. Cj, the junction capacity, and Rs_4, the series resistance of the epitaxial region, are those parameters determined by the physical properties assigned to GaAs in Figure 5-10. Rs_3, Rs_2, and Rs_1 are further additions to the diode series resistance due to the substrate material, the back contact, and the leads interior to the case. These resistances cannot be objectively separated for measurement or analysis and are therefore lumped with

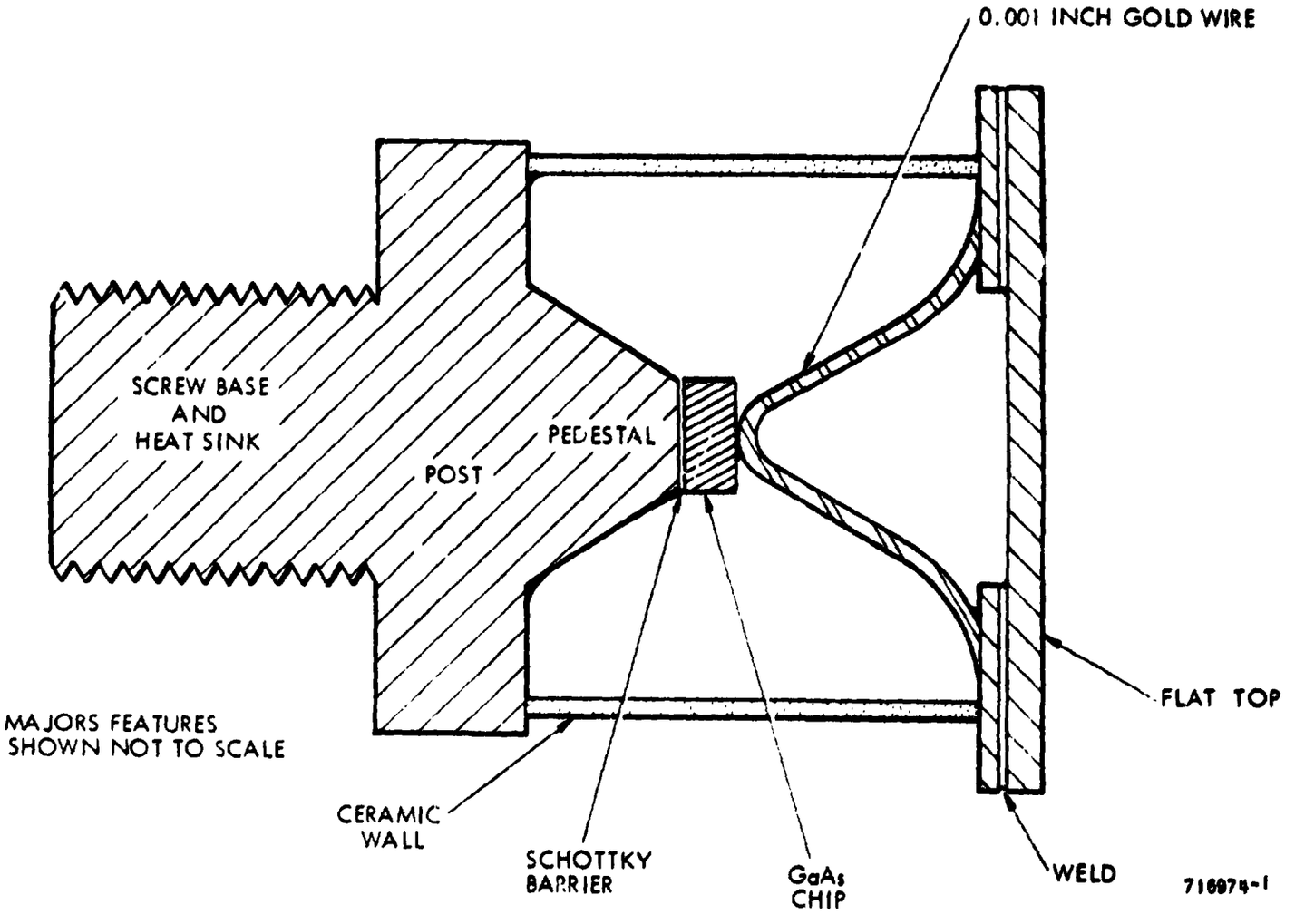

Figure 5-9. Cut-away View of a Micro State GaAs Schottky-Barrier Diode

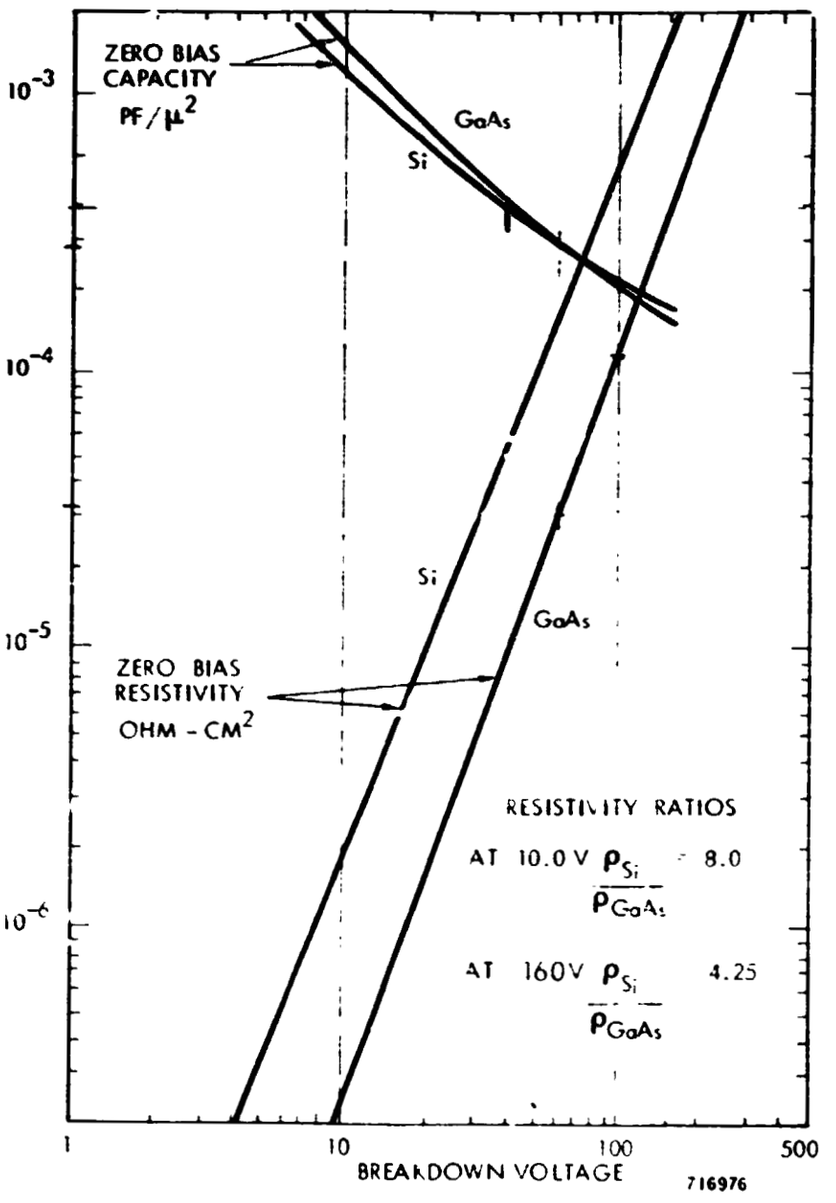

Figure 5-10. Junction Parameters as a Function of Breakdown Voltage

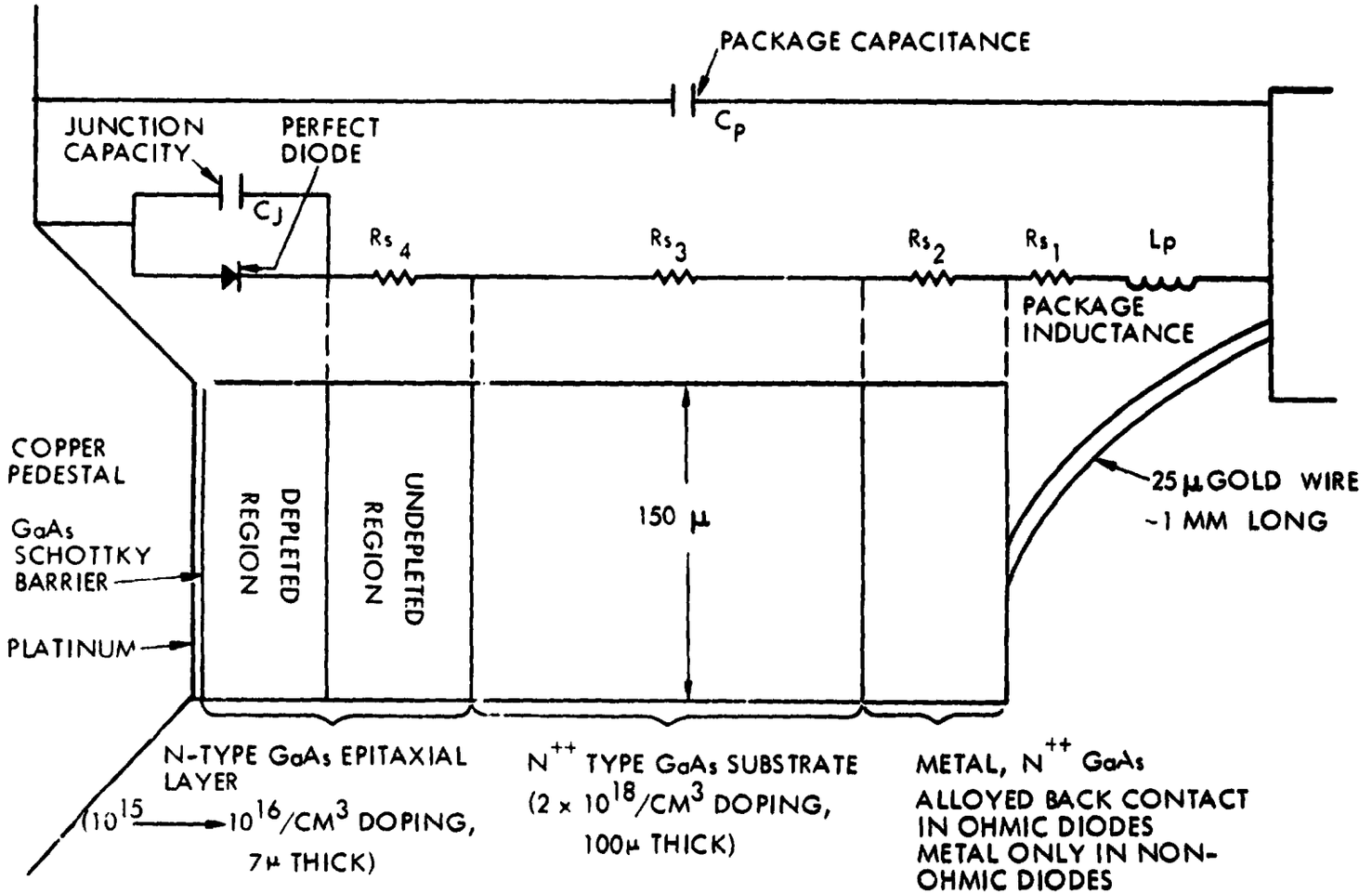

NOT TO SCALE

716979

Figure 5-11. "Working" Part of Diode Showing Materials and Sources of Electronic Circuit Model Parameters

Rs_4 and called simply Rs in the subsequent discussion. The perfect diode which models the Schottky-barrier is rigorously described by the relationship between the current through it and the voltage across it by:

$$I = Io\left(\exp\frac{qV}{nkt} - 1\right) \tag{5-1}$$

However, the GaAs-platinum junction used can be described as having no conduction below 0.5 volts forward bias and infinite conduction above that. The approximation is valid as long as a significant part of the cycle is not spent in the 5 mA to 50 mA conduction region.

The only factor which does not figure explicitly in the model is the diode reverse breakdown voltage. It, however, will be contained implicitly in the combination of diode capacity and, ideally, resistance chosen, due to the character of the epitaxial diode region. A brief explanation of those relationships is given in the following paragraph.

The diode junction breaks down in the reverse direction when the electric field gradient becomes too high in the epitaxial region. The steepness of this gradient is determined by impurity concentration. The greater that concentration, the sharper the gradient. If we denote the width of the region across which the gradient appears as w, then

$$w \cong \sqrt{\frac{K}{N}(V_B - V)} \tag{5-2}$$

where K = a collection of physical constants

N = the impurity concentration

V_B = the Schottky-barrier height

V = the voltage impressed on the junction

To the approximation that the maximum E-field the material can tolerate is constant (it changes by only a factor of 2 over 3 orders of magnitude changes in N in the region of interest), the breakdown voltage:

$$V_{BR} \propto \frac{1}{N} \tag{5-3}$$

The width, ω, called the depleted width of epitaxial material in Figure 5-11, can also be seen to set the capacity of the junction:

$$Cj \propto A/w \tag{5-4}$$

where A is the area of the junction. Substituting in the previous expression for w, as a function of impurity concentration and applied voltage:

$$Cj \propto A\sqrt{\frac{N}{K(V_B - V)}} \tag{5-5}$$

If we describe a new parameter, the zero bias junction capacity, Co

$$Co \propto A\sqrt{\frac{N}{K(V_B - 0)}} \tag{5-6}$$

then,

$$Cj = Co\sqrt{\frac{V_B}{V_B - V}} \tag{5-7}$$

The junction capacity then increases under forward bias and decreases under reverse bias and is generally higher for greater impurity concentrations.

The epitaxial resistance will also be influenced by the dopant level and the applied voltage. If w_o is the full width of the epitaxial layer and σ is the conductivity of the region, then

$$Rs_4 = \frac{1}{A\sigma}(w_o - w) \tag{5-8}$$

where σ in a semiconductor is described by

$$\sigma = q\mu N$$

where q = electron charge

N = appropriate carrier impurity level

μ = appropriate carrier mobility

Rs_4 will then decrease with increased reverse voltage and increase with decreased reverse voltage, and at any voltage be inversely proportional to carrier density.

In summary, increasing dopant density increases capacity and decreases resistance and breakdown voltage. Increasing the junction area increases capacity and decreases resistance, and also increases power handling capability. This pair of tradeoffs will be important in choosing diodes for optimum performance.

5.4.3 Diode Efficiency Analysis

Before beginning an analysis of the diodes, a set of impedance measurement, further described in section 5.4.5.3, was undertaken to establish the correspondence between the diode characterization and the experimental action of the devices obtained. Good agreement was found between measured and calculated Cj(V) and between published and measured Cp and Lp. The series resistance, Rs, while decreasing as predicted from forward to small reverse bias, increased under stronger reverse bias. Because the overall effect was neither very strong nor highly predictable, the diode resistance was considered to be independent of voltage (equivalent to assuming that undepleted epitaxial resistance did not dominate in the diode).

Historically[1, 2], the diode as a microwave rectifier has been considered to be dominated by its low frequency junction characteristics, with microwave frequency reactances acting as only perturbations to that picture. This view is difficult to justify in light of the changing impedances in the diode conduction process. The package inductance, Lp, in series with the junction capacity, Cj, combines for complex impedances varying from -j 200 to + j 10 in the diodes used. This appears in series with a resistance of only about 1 or 2 ohms.

During a cycle, the diode is still dominated as necessary by its junction. However, the effect is not to switch the diode from short to open but rather to determine which reactive element dominates. During most of the cycle, while reverse bias conditions prevail, Cj(V) dominates the diode performance. If one drives the diode sinusoidally and neglects the effect of harmonics, the diode will be self-biased to some dc level with the drive signal superimposed:

$$V_{in} = Vo\,Sin\omega t - V_{DC} \tag{5-9}$$

where V_{DC} is the output voltage.

To arrive at a simplified description of the reverse loss, neglect all other components with respect to Cj(V) and keep Rs as the lossy element. Then, for a forward conduction angle of 2θ and

$$Cj = Co\left(\frac{V_B}{V_B + V_{DC} - Vosin\omega t}\right)^{1/2} \tag{5-10}$$

where

V_B = Schottky-barrier voltage

Co = Zero bias junction capacity

the reverse loss

$$2 \int_{-\pi/2}^{\pi/2 - \theta} RsI^2(t)dt \tag{5-11}$$

may be written as

$$2\,Rs \int_{-\pi/2}^{\pi/2 - \theta} \frac{\omega^2}{2\pi} \frac{Co^2\, VB\, Vo^2 \cos^2 \omega t}{(V_B + V_{DC} - Vo \sin \omega t)} \quad (\omega dt). \tag{5-12}$$

If, as an additional step, one allows

$$V_{DC} \cong Vo \cos \theta \tag{5-13}$$

as a useful approximation of the output voltage in a well-matched case, the loss is

$$Rs\, Co^2\, \omega^2\, V_B\, V_{DC} \left\{ 1 - \frac{\theta}{\pi} + \frac{\tan \theta}{\pi} \left[1 + fn \left(\frac{2VDC \sin^2 \theta}{V_B \cdot \cos \theta} \right) \right] \right\} \tag{5-14}$$

in the reverse direction for angles, θ, in the range of 5° to about 60°.

To obtain the angle, θ, one must perform an operation to derive the current flow in the forward direction and from the equation of charge conservation in steady state solve for the angle θ. The literature advocates a strong simplification of this problem. This approximation states that all of the reactive components of the circuit are tuned out at the fundamental, and a pulse of charge flows, controlled by the remaining loss resistor (Rs)

$$Q = \int_{-\pi/2}^{3\pi/2} I_j dt = \int_{+\pi/2-\theta}^{\pi/2+\theta} I_j dt = \frac{1}{2\pi} \int_{\pi/2-\theta}^{\pi/2+\theta} \frac{Vo(\sin\omega t - \cos\theta)}{R_s} d\omega t$$

$$= \frac{V_{DC}}{RL} = \frac{Vo\cos\theta}{RL} \qquad (5\text{-}15)$$

$$\frac{Rs}{RL} \approx \frac{\tan\theta - \theta}{\pi} \approx \frac{\theta^3}{3\pi}$$

or $$\theta \cong \left(\frac{3\pi Rs}{RL}\right)^{1/3}$$

where RL = output resistor

V_{DC} = output voltage

I_j = junction current

Disregarding the series inductance, Lp, of the diode renders such a result invalid since that element will not pass the spikes of current th t analysis implies. This problem is so complex that only the computer numerical analysis detailed later is seen as a useful tool in solving the problem. The loss due to the junction offset is:

$$\int_{\pi/2-\theta}^{\pi/2+\theta} V_F \cdot I(t)dt = V_F \cdot \frac{V_{DC}}{RL} \qquad (5\text{-}16)$$

independent of the shape of the current pulse as long as the junction is turned on enough for the two line approximation to the diode characteristic to be valid.

Having determined what the diode losses should be, these values may be divided by the power input to give the loss as a percentage. By writing

$$P_{in} = \frac{V_{DC}^2}{\eta_{RL}}$$

where η = overal[l] element efficiency, one obtains, for reverse loss percentage,

$$100 \frac{\eta Rs\ RL\ Co^2\ \omega^2\ V_B}{V_{DC}} \left\{ 1 - \frac{\theta}{\pi} + \frac{\tan\theta}{\pi} \left[1 + \ln \left(\frac{2V_{DC}\ \sin^2\theta}{V_B \cos\theta} \right) \right] \right\} \quad (5\text{-}17)$$

and for forward junction loss percentage:

$$100 \left(\eta \frac{V_F}{V_{DC}} \right)$$

The forward conduction loss is still not known accurately enough for a diode which departs significantly from low frequency characteristics to be included here.

Without a statement of forward loss and conduction angle in closed form, one is in no position to rigorously optimize the interdependent characteristics of the diode: Co, Rs, and V_{BR}. Choosing the external operating levels, P_{in} and RL, presents a similarly complex problem. It seems likely that one would prefer to minimize both Rs and Co simultaneously – an operation which is invalid from both materials and chip sizing points of view. To minimize the product $RsCo^2$ would not be sufficient without taking into consideration the secondary effect on possible levels of V_{DC} as influenced by V_{BR}. The inclusion of the effect of forward loss, probably independent of Co but not of Rs, is also unlikely. It was decided therefore to undertake a digital computer analysis of the circuit.

5.4.4 Computerized Rectenna Element Analysis

To utilize a computer in the analysis of the rectenna element, a straightforward transient solution was sought. The rectenna element, including its semiconductor rectifying device, in use in the continuing experimental program (see Figure 5-12), was modeled as a set of idealized lumped elements (see Figure 5-13). The junction elements were made voltage dependent to yield the rectifying action. A set of differential equations is then written at each current node in the network in terms of voltages and element values. The equations are then digitized: the time differential equations are written in terms of small finite difference equations. Thus

$$\frac{dv}{dt} = f(v, t, \ldots) \qquad \text{becomes } v(t) = v(t - \Delta t) + f(v, t, \ldots)\,\Delta t \quad .$$

If a second degree equation is written at a node, it should be in terms of the first differential of the node variable, the variable itself if present, and the integral of the variable. That integral becomes simply the continuing summation of the product of the variable and the time interval.

The equation set must then be driven by a source and some determination must be made of when a steady-state condition is reached. To do this, the power output is integrated during each cycle and the achievement of steady-state is assumed when the change from one cycle to another becomes a small fraction of the total. This process may be shortened by introducing a dc bias to the structure to avoid waiting for the long charging constant of the high capacity employed to get the dc output. When steady-state has been achieved, the waveforms for a cycle are read-out and Fourier-analyzed if desirable.

In adopting the rather simplistic approach of solving a set of non-linear equations numerically, it is important that the time interval chosen be short enough so that it will not interact as a delay with any other time constants in the equations to cause physically non-existent oscillations. In the

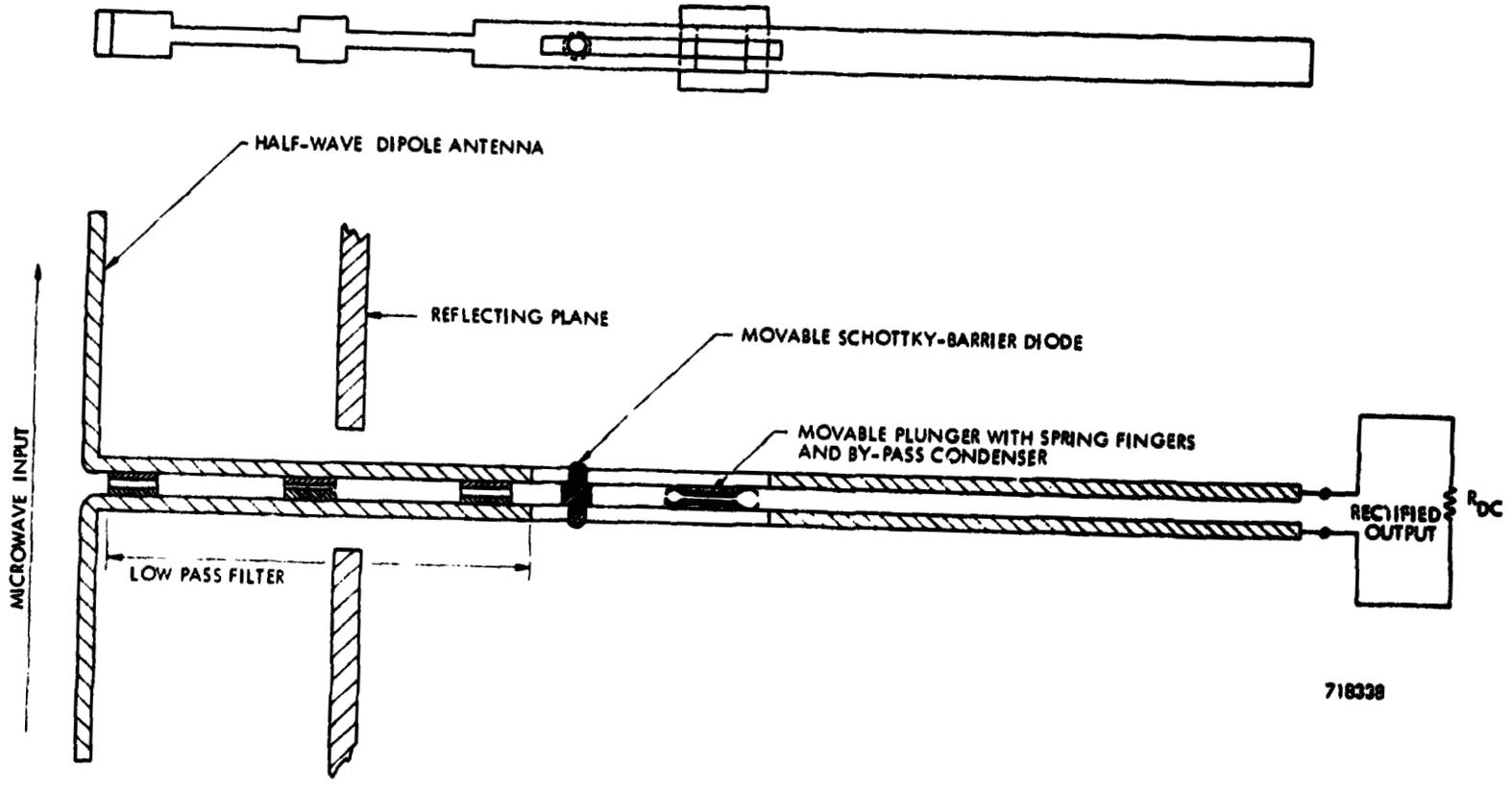

Figure 5-12. Experimental Rectenna Element (Element contains Schottky-barrier diode in half-wave mode of operation)

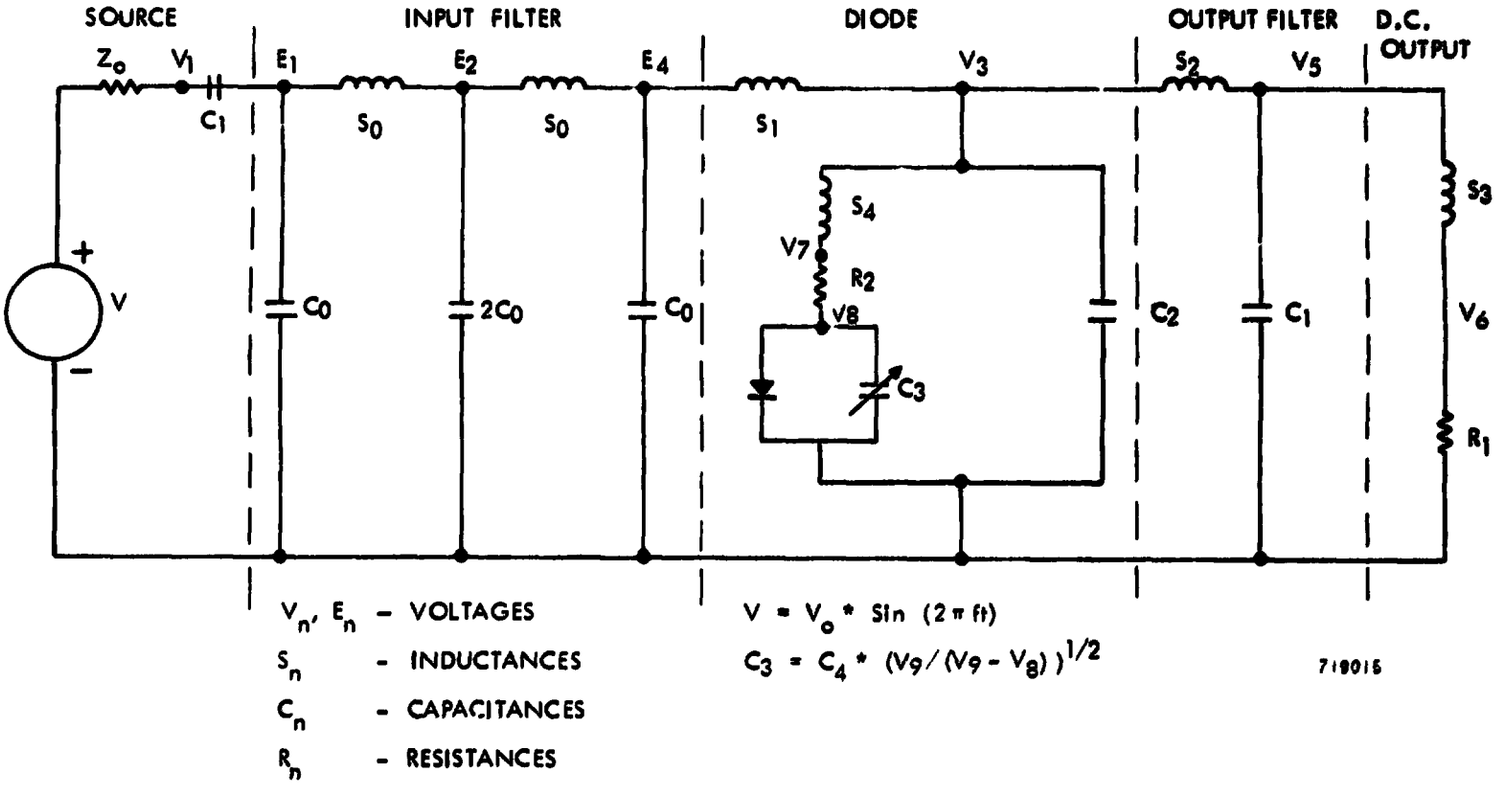

Figure 5-13. Element Model for Computer Analysis

case of a rectifying circuit generating many harmonics, the option of setting to zero time constants which are small with respect to the reciprocal of the drive frequency is not open, as those times may be comparable to harmonic time constants.

With this in mind, the computer program was written and run. The output waveforms departed substantially from those predicted by assuming low frequency operating conditions with losses as perturbations. In particular, the series inductance of the diode limits conduction in the forward direction to a low value. The diode generates a significant second harmonic output, apparently due to the non-linear junction capacity. The losses in the diode (modeled as having Rs = 1 ohm everywhere, Co = 5 pF, and breakdown voltage in excess of 120 V) amounted to about 10% with an excess of 8% in the reverse direction. The bulk of loss appeared to occur at just slightly negative voltages where low junction capacitive reactance, further reduced by the inductive reactance, allows large current to flow through the diode resistance.

It appears probable that losses elsewhere in the rectenna element must approach those in the diode itself, perhaps due to large circulating harmonic currents and resistive circuit losses. Resistive circuit losses other than in the diode itself were not taken into account in the first writing. This and several other problems have thus far made the computer model ineffective as a precise predictive tool. In particular, because of the much higher than expected harmonic content in current and voltage waveforms, even short lengths of lines must have their parameters distributed and not be modeled as the inductances they appear to be at the fundamental frequency.

Several valuable insights have evolved, however. The junction capacity variation with voltage has proved a powerful generator of second harmonic energy. The inductances present near the diode preclude a current spike of forward conduction and give a broad, relatively

settled, forward characteristic. The greatest currents and losses in the diode occur at just slightly reverse bias where the junction capacity is high. Losses are probably so dependent on the phases of the harmonics added in the diode that analyses at single frequencies are invalid. Reverse conduction losses are overwhelmingly predominant (diode modeled had Co = 5 pF, Rs = 1 Ω, $V_{DC} \approx 40$ volts), but the total diode losses calculated are only half the losses measured experimentally. Finally, the computer is a far more valuable analytic tool than any reasonable mathematical analysis could be.

A plot of junction current and junction voltage from a single run appears as Figure 5-14. The circuit was driven from a sinusoidal source with zero phase at zero degrees. The plot must be considered only representative of an approximation to these important parameters.

5.4.5 Experimental Investigation of Rectenna Element Efficiency

5.4.5.1 Introduction

Both mathematical and computer analyses were undertaken to draw together the results of an experimental diode efficiency test program. The program was undertaken to establish, by systematically varying diode parameters, a direction to move in selecting optimum devices. In particular, a correlation between the two physical diode parameters (dopant concentration and chip size) and microwave rectification efficiency was sought. In cooperation with Raytheon's Special Microwave Devices Operation, GaAs diodes of various chip sizes selected from materials of three impurity concentration levels were obtained. Their pertinent microwave circuit parameters were measured and efficiencies as functions of load resistance and power level were derived.

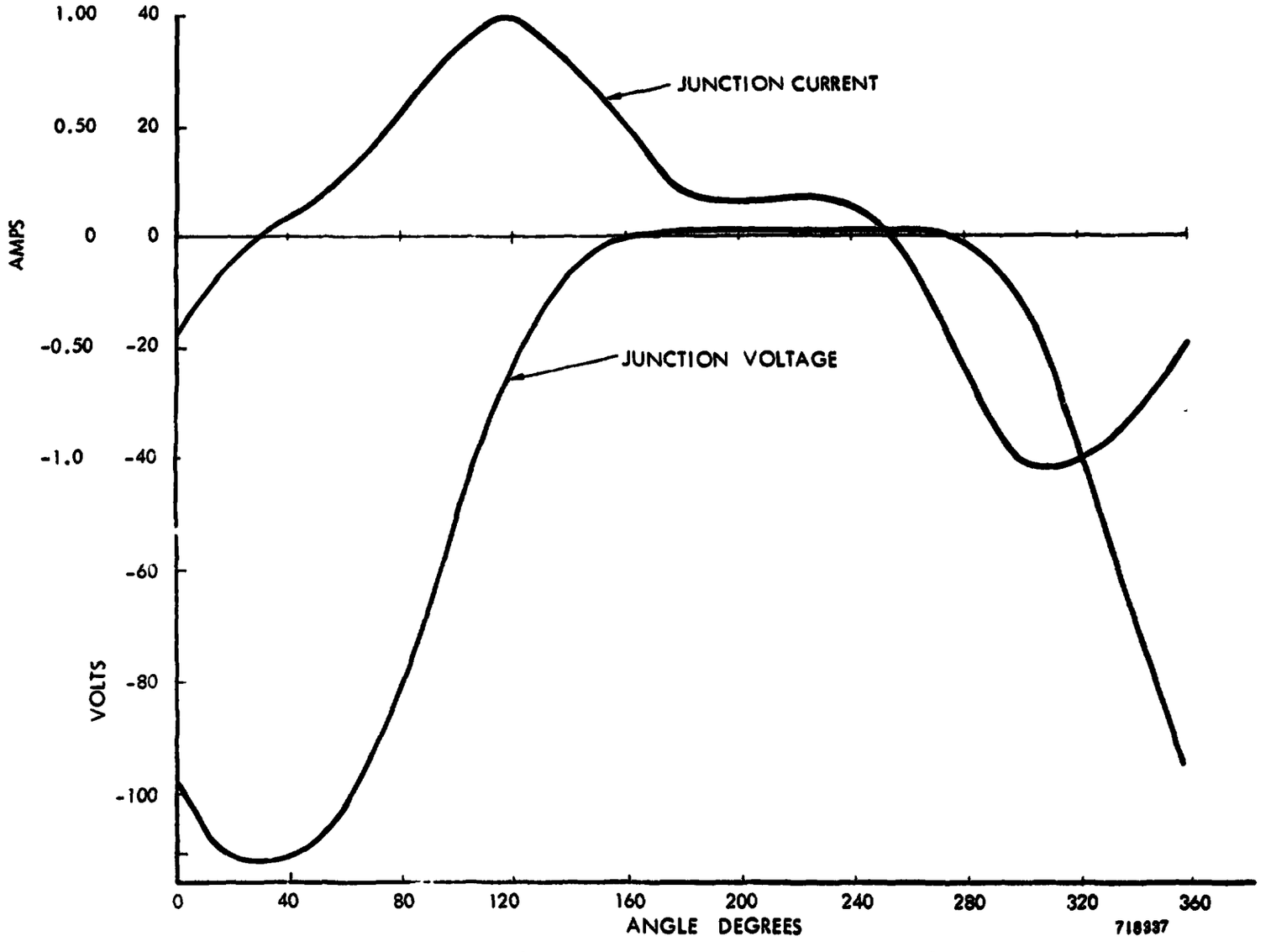

Figure 5-14. Plot of Computer Program Output

5.4.5.2 Description of the Sample Space

The diodes selected may be characterized by a matrix of three dimensions. One is the dopant level as indicated by breakdown voltage; another is the chip size as indicated by the zero bias capacity of a particularly doped material. The third dimension exists for only a partial set of the points determined by the first two selection characteristics; it is the type of back-contact made to the diode and is described as being either ohmic or rectifying. The rectifying back-contact is produced when the highly doped substrate material is plated to produce a contact to the fixture (see Figure 5-11). For IMPATT oscillations, the purpose for which the diodes are usually employed, this junction is biased far forward and is of no consequence. The ohmic junction is produced by alloying the substrate with the contact material and is apparently more difficult to employ. Accordingly, an initial comparison was made between diodes with both types of back-contacts.

The impurity concentration levels in the materials used gave reverse voltage breakdown levels of 160 volts, 95 volts, and 50 volts, approximately. Diode zero bias capacities for these three materials ranged from about 3 pF to about 10 pF with diodes in a given group within ± 10% of some central level. All sizes were produced by the normal method of etching a chip with around 12 pF capacity.

In manufacture, each diode is assigned a number. All digits preceding the "S" identify the particular wafer and, therefore, doping concentration. The following numbers, except for the last digit in parantheses, will identify diodes processed in the particular manner chosen. Table 5-2 is designed to identify representative diodes tested from each individual class. These diodes will be referred to in later discussion and have typically the best efficiency characteristics of any diode in their respective groups. In addition to the features just listed by which the diodes are classified, the measured series resistance is included.

Table 5-2. Diode Selection Characteristics

Diode No.		Breakdown Voltage (V_{BR})	Ohmic	Co (pF)	Rs* (Ω)
61319S12a2a	(1)	46	Yes	6.5	0.43
61319S1G	(6)	48	No	5.2	0.68
61319S4a	(1)	51	Yes	3.0	1.6
61319S4a	(6)	51	Yes	4.0	1.7
30118S2	(8)	95	Yes	9.3	0.50
30118S1b	(6)	95	No	5.4	0.50
30118S2d	(3)	92	Yes	3.1	2.7
30118S2d	(8)	91	Yes	4.1	1.6
30102S3Ba	(3)	160	Yes	5.6	0.77
30102S3Aa	(4)	160	No	6.5	0.62
30102S3B	(2)	162	Yes	2.9	2.7
30102S3B	(10)	160	Yes	4.1	2.0
135S9b	(6)**	64	No	3.4	0.60

* Measured at -10 V bias.

** Diode from chip in initial preliminary testing program.

5.4.5.3 Experimental Procedure

The diode microwave circuit parameters of the diodes listed in Table 5-2 and others of their type were measured in a coaxial fixture terminating a 50-Ω line. That fixture was a series connection of the diode and a large capacity across which a dc bias could be applied.

The minimum position and amplitude of the standing-wave ratio in the line were compared to those occurring with a short circuit at the diode position. A precision attenuator with a detector whose output was displayed on a digital voltmeter read the VSWR over a range of 0 to 50 dB with an accuracy of ± 0.2 dB. The position of the minimum in the standing-wave pattern was read from a vernier scale on the VSWR measuring carriage to an accuracy of ± 0.2 mm.

These measurements were taken over a large range of forward and reverse dc biases with small microwave signals used for measurement, since both average circuit parameters over a cycle and parameters at particular bias levels were sought. Preliminary testing indicated that the complex impedance changed rapidly at small values of bias voltage and more slowly at higher values. Accordingly, a somewhat logarithmic progression of test points was chosen (-0, -0.5, -1.0, -2.0, -5.0, -10.0... to breakdown) in the reverse direction. In the forward direction, points at typically 1 mA, 50 mA, and 100 mA were measured. The complex impedance was virtually the same at the 50 mA and 100 mA points and indications were that it would not change with greater forward bias. The amplitude of the sampling was typically on the order of 1 to 4 V. The greater signal levels were only used at greater dc bias levels where they were necessary to get a good reading. The change in model parameters with voltage should have been slow enough to avoid "smearing" the voltage minimum at the various bias levels.

The standing-wave ratio varied from 25 dB to 47 dB, depending on the diode and the bias. Due to the very small series resistance of the diode compared to the 50-ohm characteristic of the line, the phase angle with respect to the short position of the signal could be measured around the outside circle of the Smith chart. This accurately provided the reactive component of the complex impedance, a value referred to as X in the following calculations. For $R \ll Z_o$, as in all the measurements taken,

$$R \cong \frac{Z_o^2 + X^2}{Z_o \cdot VSWR} \qquad (5\text{-}18)$$

Using the diode model in Figure 5-11, a method for deriving junction capacity (Cj), series resistance (Rs), and series inductance (Lp) of the diode from VSWR measurements may be postulated. The only assumption made in the model is that the case capacitance (Cp) is constant around 0.3 pF. This value is that measured by Raytheon's Special Microwave Devices Operation on empty packages and is identified in the following expressions by its complex reactance, -Xc, of around -210 at 2450 MHz. The series resistance of the reference short circuit (Rc) was about 0.3 ohms and is carried through the calculation as if it were part of the diode resistance, and finally removed at the end.

The inductance of the diode is derived from the model of the diode in far forward conduction, which is a series connection of (Rs), and the case inductance (Lp). The resistance of the inductor ($X\ell$) is identified as the reactance of the diode at 50 mA or 100 mA of forward bias. With a forward bias,

$$Rs = R - Rc = Rf \tag{5-19}$$

In the reverse direction, the interaction between the shunt package capacitive resistance, in parallel with the series resistance, the junction capacitive reactance (-Xj), and the inductive reactance ($X\ell$) yields a more complex problem.

$$R + X = \frac{Rs}{\left(\frac{X\ell - Xj - Xc}{Xc}\right)^2} + j\,\frac{(X\ell - Xj)\,Xc}{(Xc + Xj - X\ell)}$$

or

$$Xj = \frac{-Xc \cdot X}{Xc + X} + X\ell \tag{5-20}$$

and

$$Rs = \left(\frac{Xc + Xj - X\ell}{Xc}\right)^2 = \left(\frac{Xc}{Xc + X}\right)^2 R$$

For the set of diodes listed in Table 5-2, Rs(V), Cj(V), and Lp were derived. That data was then used to derive analytic expressions for the diode junction capacitance as a function of instantaneous voltage by graphical methods. It fit very well the function

$$Cj = Co \left(\frac{0.8}{0.8 - V}\right)^{1/2} \qquad (5\text{-}21)$$

Lp and Cp were assumed to be constant. Reverse Rs was a slow function of voltage with a minimum of approximately -10 volts and a maximum at breakdown with a small rise toward zero bias. Forward series resistance (Rf) was typically between the extremes of Rs. The element values derived were used both as inputs to the mathematical model where approximations were necessary and to establish the numerical levels in the computer program.

A similar effort was undertaken to measure the efficiencies of these diodes in the rectenna element. The test fixture was that of Figure 5-12. The dipole antenna on its ground plane was mounted in an expanded waveguide fixture, designed to simulate placement of the element in an array. That waveguide was fed through an adaptor by a coaxial line containing the power monitoring equipment. Input and reflected power were read to within calibrated accuracies of 1% or 2%. The diodes were tested over a range of calibrated dc output resistance and dc output voltage was read to within less than 1% on a digital voltmeter.

Figures 5-15, 5-16, and 5-17 present the efficiencies at the 4-watt level of the rectenna element using diodes from Table 5-2. These figures depict the efficiencies of diodes in the 50-volt, 90-volt, and 160-volt breakdown chip groups, respectively. The performance of diode No. 135S9b(6) at an operating level of 4 watts is included on all for comparison. In Figure 5-18, the performance of the single diode (135S9b(6)) as a function of both dc resistance and power level is depicted. This is the best diode of a group taken from a GaAs wafer identified as being optimum in the preliminary tests in coaxial fixtures of GaAs diodes. The substrate material of this particular chip

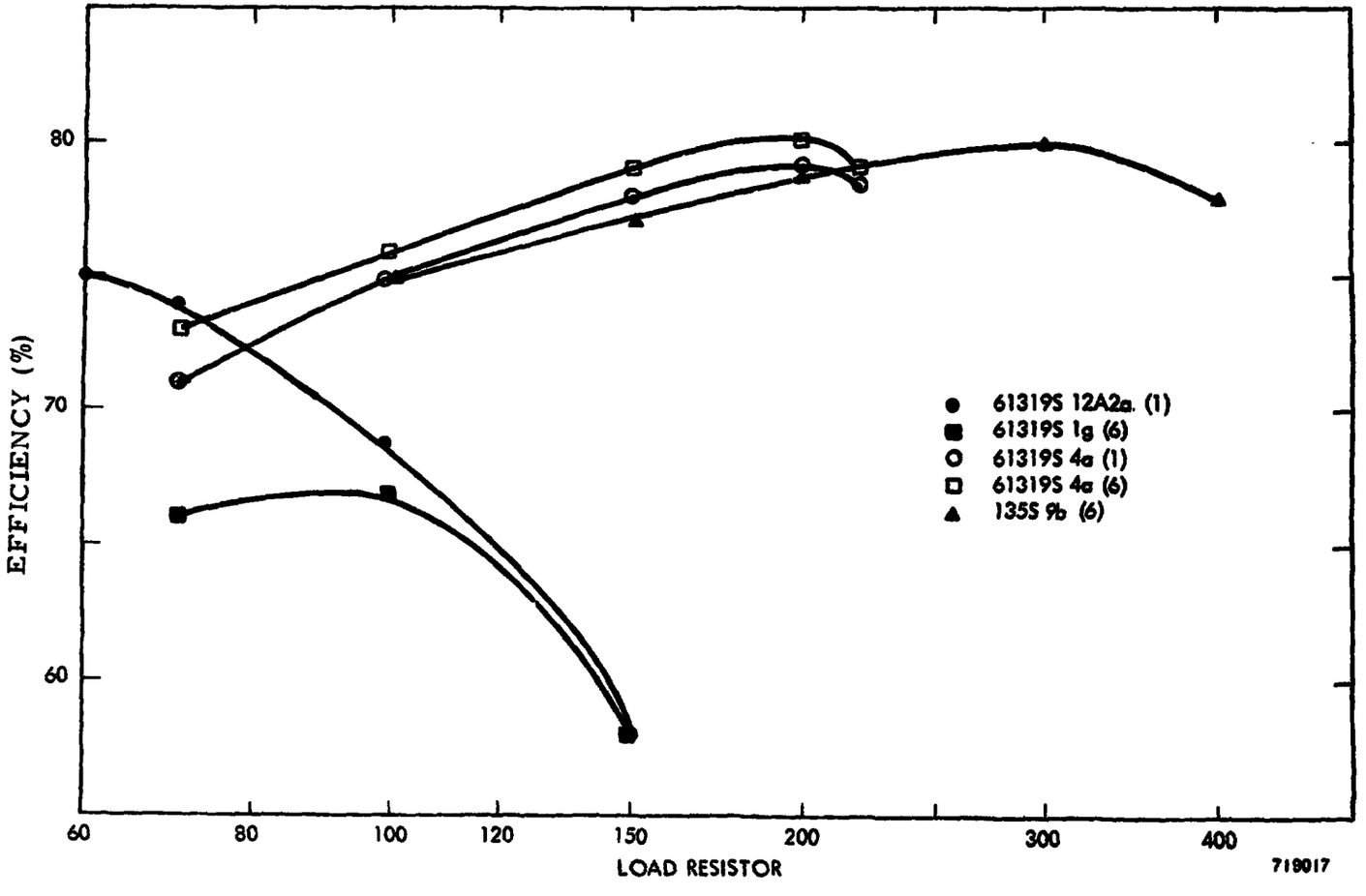

Figure 5-15. Efficiency vs Load Resistance for 50-Volt Breakdown Diodes

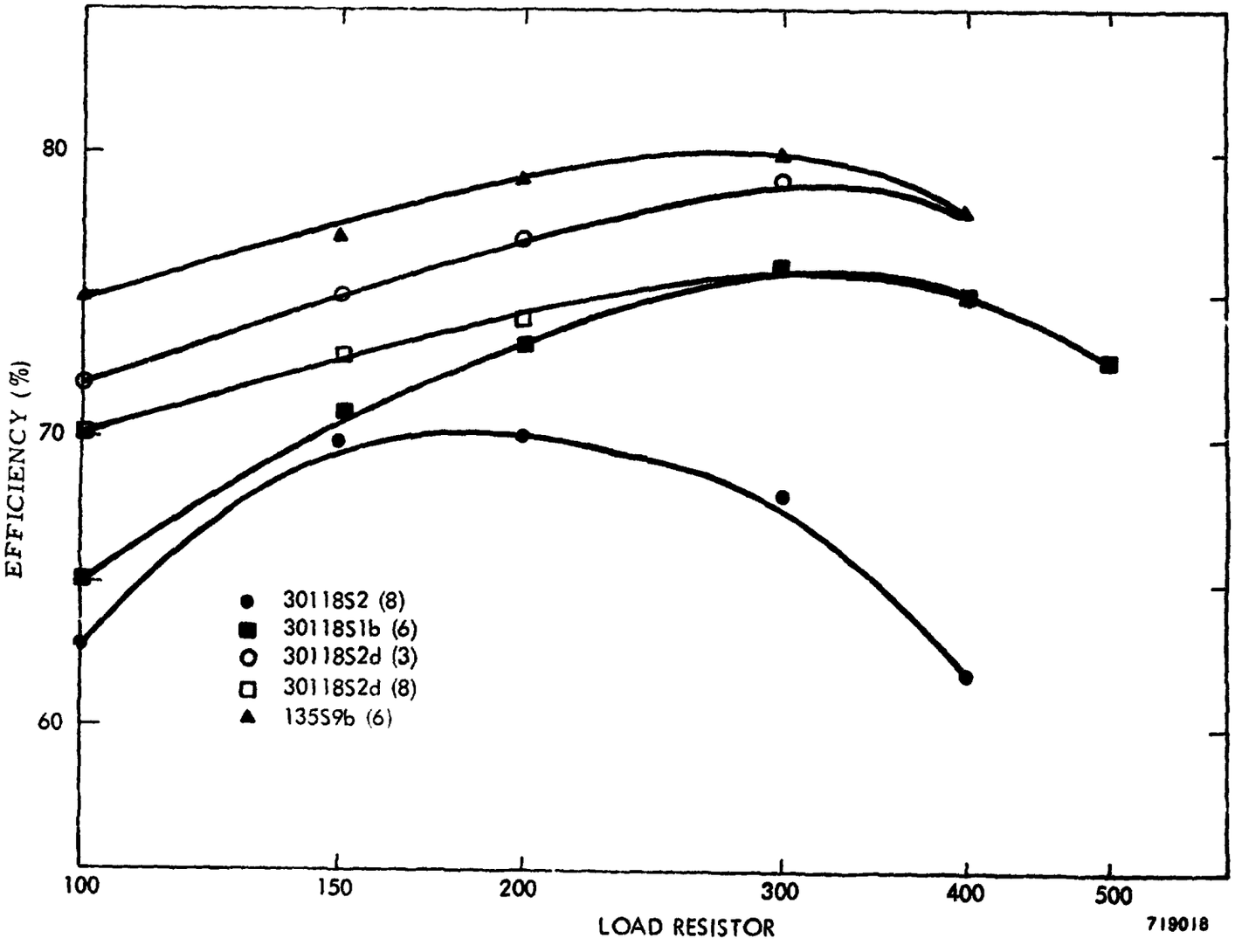

Figure 5-16. Efficiency vs Load Resistance for 90-Volt Breakdown Diodes

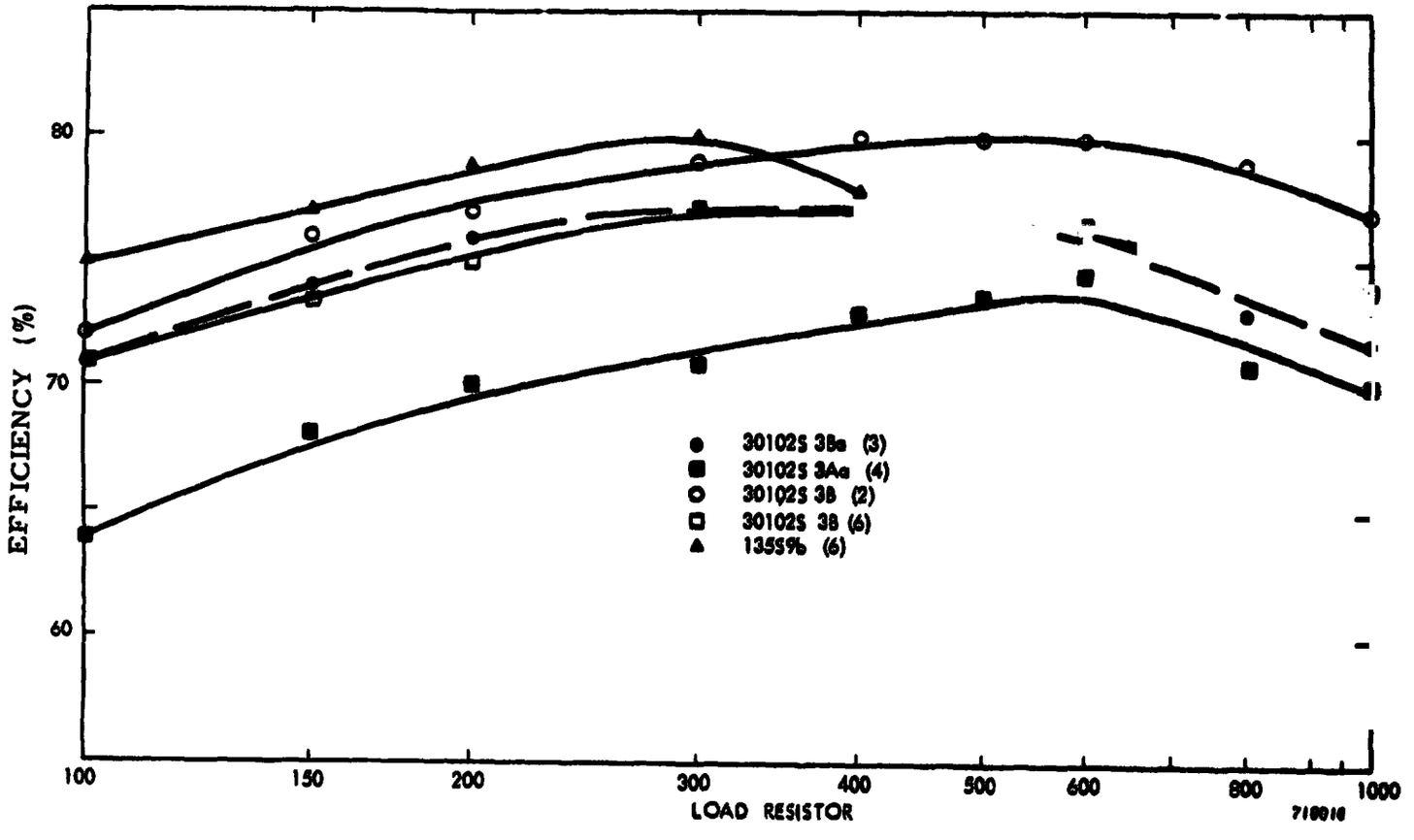

Figure 5-17. Efficiency vs Load Resistance for 160-Volt Breakdown Diodes

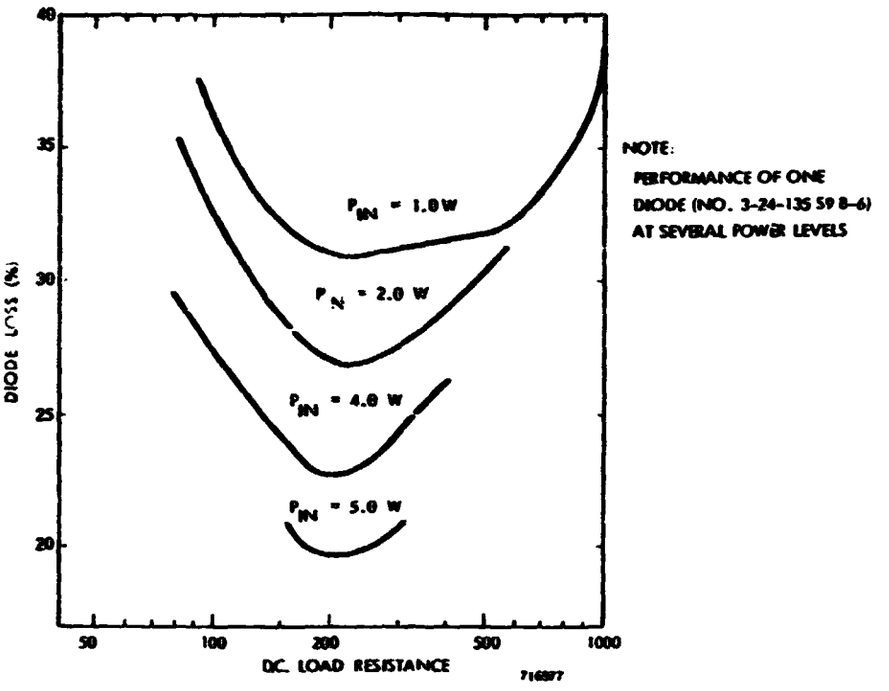

Figure 5-18. Diode Losses as a Function of DC Load Resistance

is superior to the substrate now in general use by Raytheon's Special Microwave Devices Operation. The material from which the chip was made was abandoned because of great variation in material properties and purity from one chip to another in a single wafer. The decrease in element losses with increase in power level is typical of all the diodes studied. The narrowing of the range of resistance studied with increasing power is due to the entrance of reverse breakdown into the diode characteristic. Note, however, that in all cases, a minimum of loss was found between the extremes of resistance used. A complete listing of the efficiency data on all GaAs diodes systematically tested appears in Appendix A.

From Figures 5-15 to 5-18, a few definite trends have been established. Ohmic back-contacts are definitely desirable. In the range of device capacitance examined, a general increase in efficiency with

decrease in capacity is present.* The change in material dopant concentration, while shifting the optimum operating point of a device, does not seem to affect maximum efficiency. In the groups of diodes tested there was enough individual variation to preclude prediction of the operation of a randomly-selected diode. Experimental results in conjunction with partial mathematical and computational results seem to indicate that losses are more nearly equally divided between the diode and the fixture than previously postulated.

5.4.6 Special Topics

5.4.6.1 Full-Wave Rectification with GaAs Diodes

Preliminary results were achieved in the construction and test of a two-diode, full-wave fixture. In that experiment, two diodes were inserted in shunt in the element of Figure 5-12. At power input levels of four and eight watts, efficiencies for the few diode pairs sampled were at least as good as the results with each diode taken individually. In one case, there was an increase to 79% from individual levels of 74% and 76%. These tests also appear in Appendix A. The rectenna element structure's range of circuit parameters is probably not as nearly-optimum for the full-wave rectifier as for the higher impedance half-wave rectifier.

5.4.6.2 High Power Rectification

One higher breakdown voltage diode was tested at 10-watt and 20-watt input levels and found to be about 80% efficient at those powers. The results of that test are given in Appendix A.

5.4.7 Summary

In the past year, the efficiency of the rectenna element has been raised from a previous maximum of about 74.5% without a low-pass filter to in excess of 80% with a low-pass filter. At the same time, the number

* A general decrease in yield with decrease in chip size seemed to occur, making the manufacture of still smaller diodes somewhat hazardous.

of diodes necessary has been decreased from four per element to one per element. The power handling capability has increased from about one watt per element to 20 watts per element, maximum. The maximum power level in general testing has been seven watts. While no consistent new predictive theory of microwave rectification performance has yet evolved, major steps have been taken to unsettle old inaccurate postulates, to create new bases, and to develop new analytical tools.

5.5 Incorporation of the Rectenna Element into the Rectenna and Matching the Rectenna to Space

In section 2.5, it was pointed out that an efficient rectenna design was a three-level hierarchy starting with the most efficient diodes, followed by the incorporation of these diodes into efficient rectenna elements, and concluding with arranging the rectenna elements in the rectenna so that the incoming microwave energy would be efficiently absorbed. It is this last step in the design procedure which will be examined in this section.

The rectenna, from an electrical circuit viewpoint, may be visualized as shown in Figures 5-19 and 5-20. In Figure 5-19, a small section of a rectenna array is shown, consisting of an infinite number of equally-spaced elements comprising an equal number of identical cells. Under these circumstances, all elements will have the same amount of incident microwave energy falling upon them. Assume that the portions of the rectenna elements consisting of the half-wave dipole antenna and their spacings to the reflecting plane are all identical. Further assume that the magnitude and phase of the power reflected from any mismatch from the combination of low-pass filter, rectifier circuit, and dc load are the same for all rectenna elements. It must follow then that any power reradiated from one half-wave dipole must be the same in magnitude and phase as from all other dipoles. The phase coherence will establish a reflected beam which can be compensated for by introducing a counter reflection, for example, by a sheet of plexiglass of the proper thickness and location. It follows that if all rectenna elements are identical, and spaced identically with respect to each other and the reflecting plane, the rectenna can be matched to absorb all incident power even though power is reradiated from the individual elements.

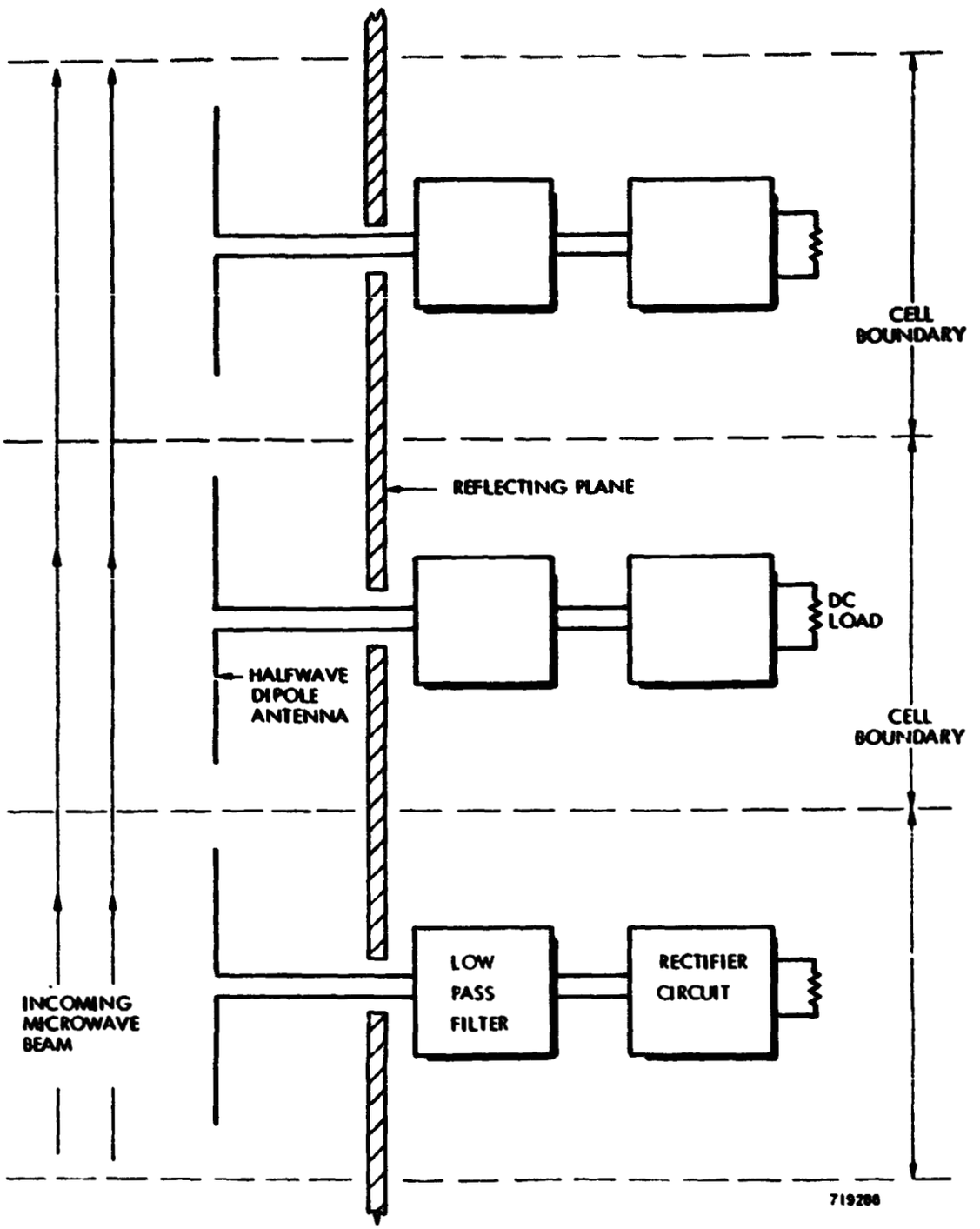

Figure 5-19. Section of Array Showing How Array May Be Broken-Up into a Large Number of Identical Cells

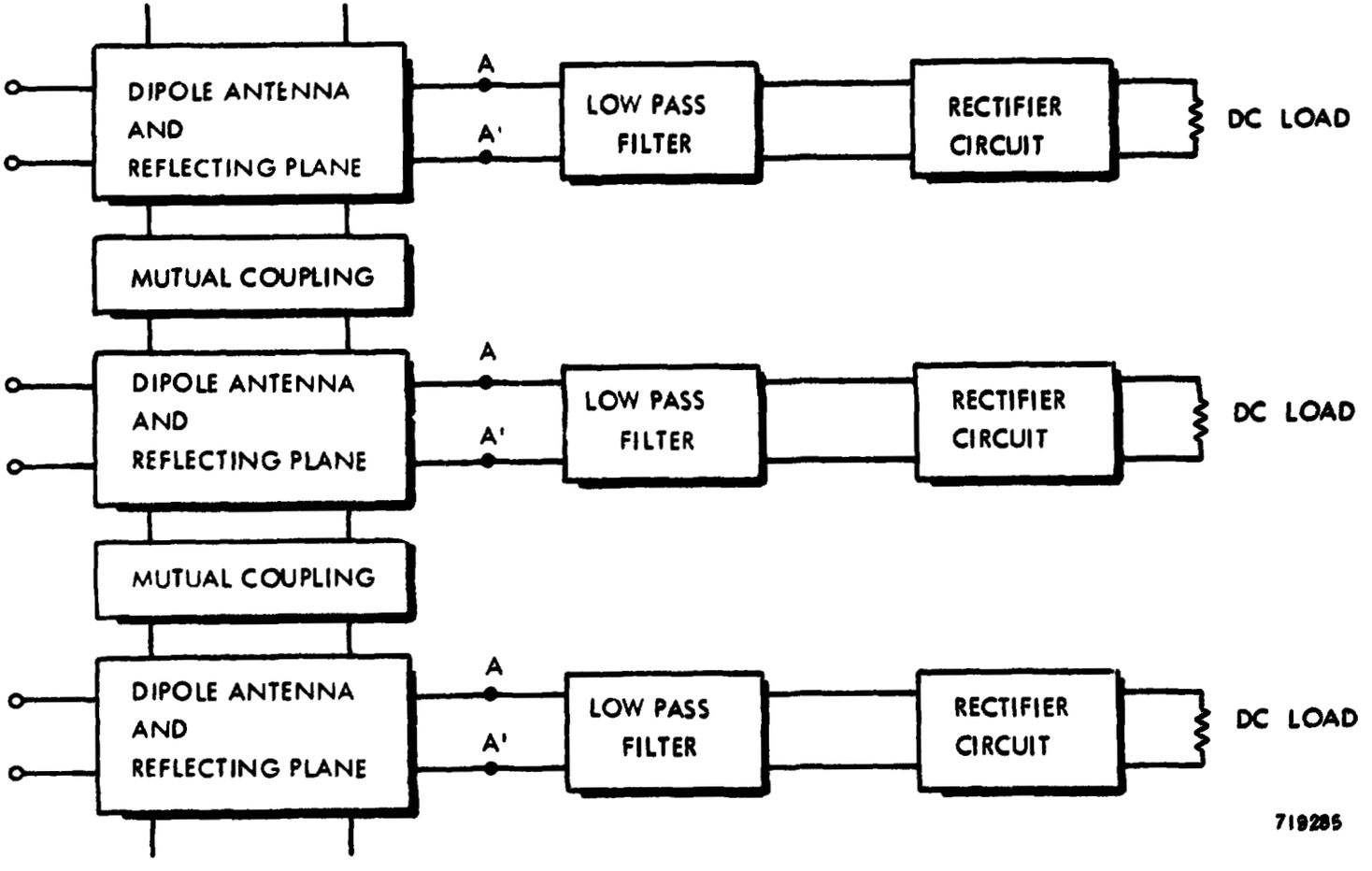

Figure 5-20. Electrical Schematic for the Array of Figure 5-19

Of course, it is hoped that each rectenna element would be so well matched to the incoming wave that no power would be reradiated since the use of a sheet of dielectric material in front of the rectenna is both lossy and expensive. We are, therefore, led to an attempt to design a rectenna which absorbs 100% of the incident power.

Returning to Figure 5-20, it is noted that the receiving dipole couples not only to the space in front of it, but also to the other dipoles in the near vicinity. In the arrangement of elements in the rectenna currently being used, there is significant coupling to six elements, although Figure 5-20 schematically shows coupling to just two other elements. Coupling to elements beyond the adjacent six is small and can be neglected.

The mutual coupling is sufficiently large to make a significant difference in the impedance transfer function between space and the input terminals to the low-pass filter, and it must be taken into account in designing the rectenna.

There are several approaches which can be used to arrange the rectenna elements so that there is zero reflection of power. In the subsequent material, we will discuss three approaches and make a relative evaluation of them.

The first approach to be discussed is one that we have used successfully in the effort discussed in section 3.0. First, the rectenna element is matched into a section of expanded waveguide which inaccurately simulates the infinite array. Although the simulation is very coarse, a good correspondence to an infinite array with low reflection has been determined with a single trial setting of the adjustable parameters available to the designer when the element is transferred into an infinite array. The confidence in being able to determine an excellent correspondence after additional trimming is very high.

In further support of the evolution of this approach, it is noted that one of the earliest prerequisites of the rectenna development was the development of a rectenna element of high efficiency. Furthermore, the rectenna element consisted of a half-wave dipole and a rectifier circuit located in a plane above the reflection plane. The dc power was collected in this plane. The efficiency evaluation necessitated a closed system and this, together with the physical arrangement of the rectenna element, led to the expanded waveguide fixture.

The use of this approach has been subsequently modified to develop a rectenna element configuration with the half-wave dipole in front of the reflecting plane, the rectifying circuit in back of the reflecting plane (as shown in Figure 5-12), and a transmission line and low-pass filter between. The development sequence for this circuit is as follows. With the half-wave dipole inserted into the expanded waveguide fixture, the input impedance at the input terminals of the half-wave dipole antenna is examined by S-curve measurements. The antenna length and penetration from the backwall is adjusted to eliminate any reactive component. The characteristic impedance of a parallel slab line is then designed to match the input impedance of the antenna. The low-pass filter is also designed to this characteristic impedance at the fundamental frequency. Then the rectifier circuit and dc load resistance are adjusted to give a match.

Unfortunately, the single rectenna element test fixture does not simulate the behavior of the same element in an infinite array. The infinite array which the test fixture does simulate is shown in Figure 5-21. The actual situation in the array currently being used is illustrated in Figure 5-22.

The process of relating the measurements of Figure 5-21 to Figure 5-22 is shown schematically in Figure 5-23. Here, the transfer function, which will transfer the rectenna element as matched out in the test fixture of Figure 5-10 to a matched-out condition in the environment of an infinite rectenna array, is seen to be a function of the cell dimensions

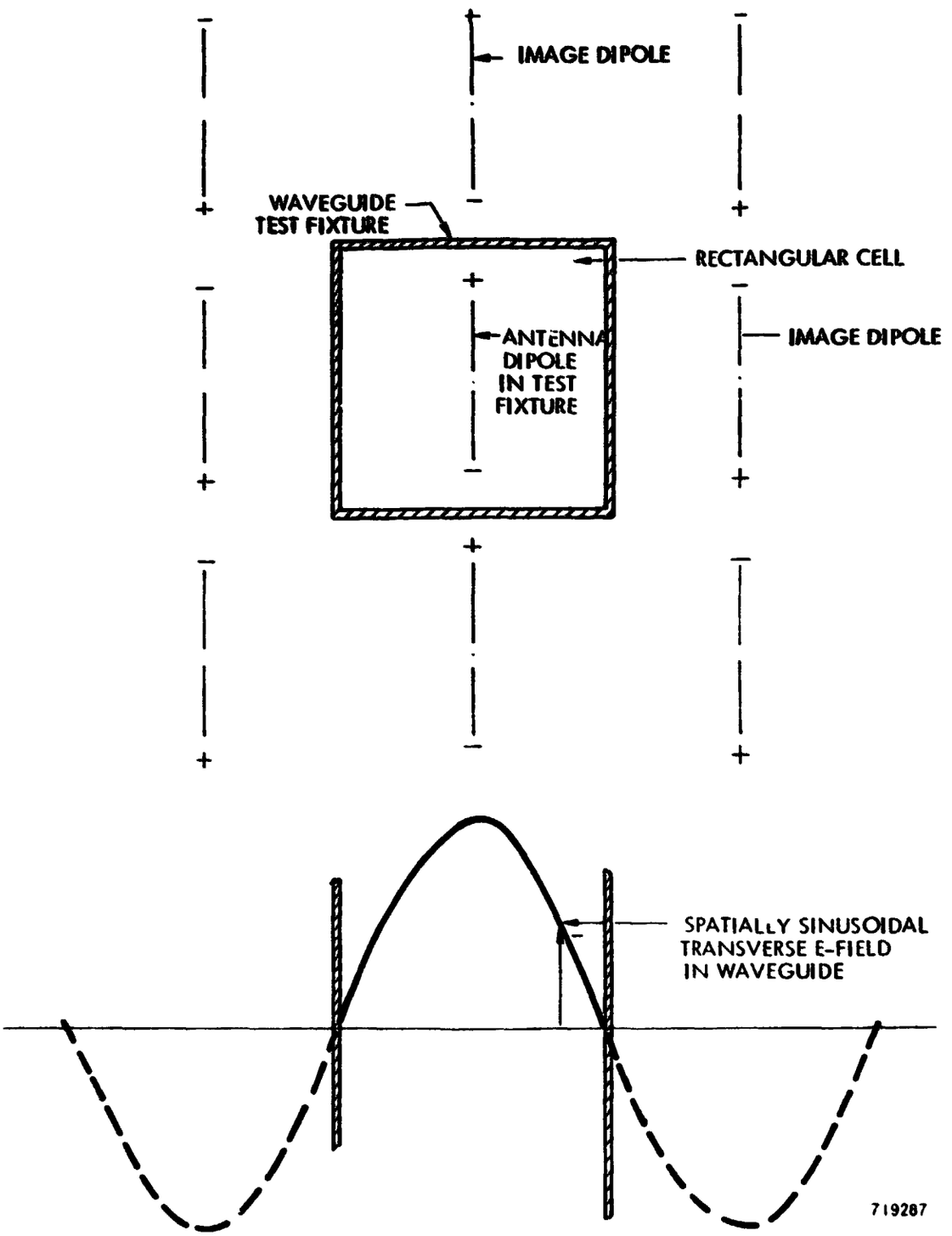

Figure 5-21. The Array and Illumination Pattern Simulated by the Waveguide Test Fixture

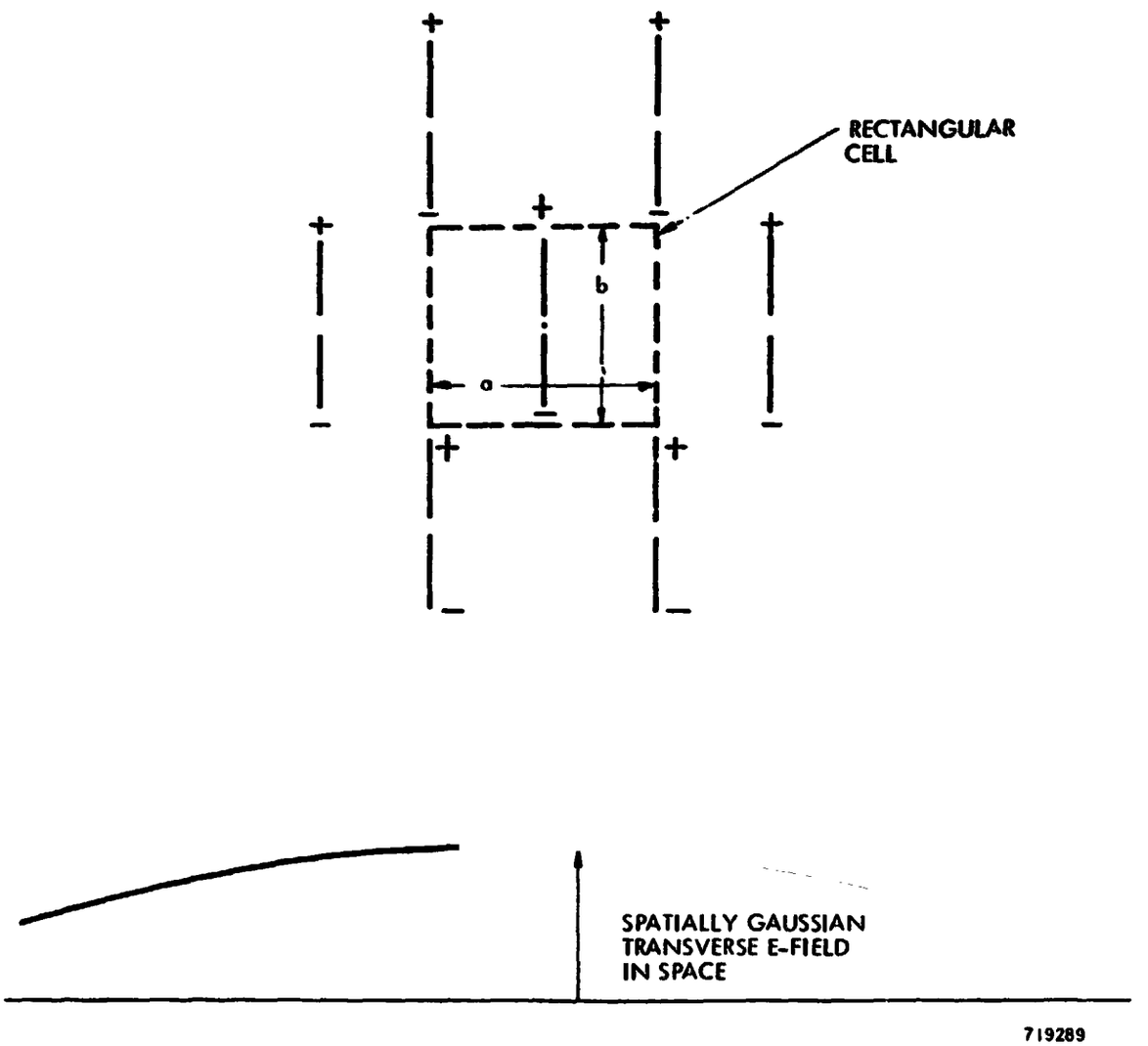

Figure 5-22. The Array Cell and Illumination Pattern for the Array of Figure 3-16.

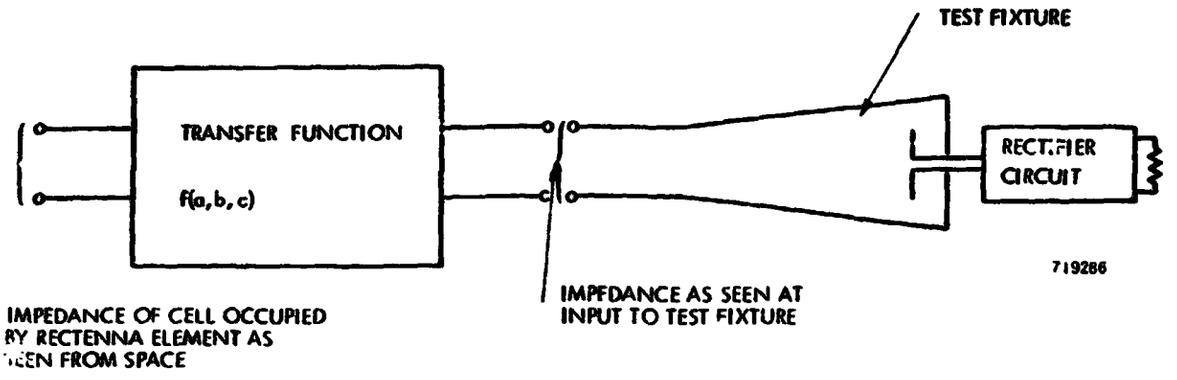

Figure 5-23. Electrical Schematic Indicating that the Spacing of the Elements on the Rectenna Effectively Provides a Transfer Function Between the Terminals of the Waveguide Fixture in Which the Rectenna Element is Developed and the Free-Space Wave Incident Upon the Area Occupied by the Cell

a and b in Figure 5-22 and the spacing, c, of the elements from the reflecting plane. The generality of the settings a, b, and c, to bring about a match to space for a single element tested in an arbitrary test fixture is in doubt. However, from the results of the work discussed in section 3. 3. 4, a transfer function in terms of physical spacings has been found which allows an estimated 94% absorption of the incident energy. This was achieved with only two trial settings of the a, b, and c parameters and with rectenna elements whose impedance input as determined by the waveguide test fixture varied considerably. It is the latter aspect which argues against further trial settings of a, b, and c, which can only be made with considerable effort, to effect a further improvement.

Another approach to the simulation problem is to utilize larger test fixtures such as those discussed by Hannan[3]. However, this approach has the following limitations:

1. Several rectenna elements are necessary (for example, 4 for an incoming beam inclined 12° from normal incidence or broadside for a rectangular-grid, rectangular-cell format).

2. A broadside simulation is not possible.

3. The waveguide test fixture can support higher order modes.

The latter limitation requires that the test fixture be constructed accurately and that all of the rectenna elements have identical input impedance. The difficulties that can be encountered in simulation with multiple element and multiple mode test fixtures are reviewed for another simulator in section 3. 3. 3. The waveguide simulation is additionally difficult for the triangular-grid, square-cell format used in the array of Figure 5-22 and which has decided advantages in matching the symmetry of a circular incident beam.

A preferable approach to the problem of arranging the rectenna elements in the rectenna for high absorption efficiency, η_{ra}, is to separate the development of an efficient rectifier circuit from the balance of the rectenna including the half-wave dipoles. This is now possible because the rf connection to each element is now brought back behind the reflecting plane. This arrangement can be explained with the aid of Figure 5-20. First, the filter, rectifier circuit, and dc load are developed to appear as a matched load looking to the right of the terminals A-A'. Next, the balance of the structure to the left of A-A' is developed to appear as a match looking to the left of terminals A-A'. This match must be obtained when the element whose impedance is being measured at A-A' is immersed in the array, with the array half-wave dipoles all excited in the proper phase, and with amplitude equal to that on the element whose impedance is being measured.

Another way of visualizing how the match is obtained is that the power coming into the antenna from the mutual coupling to other radiating antennas and the power being reflected by the antenna itself must add vectorially to zero so that there is no net power flow toward the terminals A-A'. It therefore follows that if the mutual coupling can be established between the element being measured and all other elements, if the self-reflection is known, and if the assumption is made that all elements are operating in time phase, the reflection coefficient can be established. Fortunately, the coupling between non-adjacent elements is nearly negligible, so a suitable test environment in which to measure the coupling would be the six adjacent elements with perhaps another ring of elements beyond for guard-ring purposes. From a practical point of view, only the measurement of mutual coupling to adjacent elements is necessary. This is further simplified by the symmetry of the structure, reducing the effort involved in the determination of the scattering matrix. The variables used to effect a match are the spacing of the elements from each other and their spacing from the reflecting plane. The 60° triangular-grid pattern requires a fixed ratio of vertical-to-horizontal spacing of the elements.

We are now in a position to discuss the relative merits of the three approaches to designing a rectenna with near 100% absorption efficiency. This is done with the aid of Table 5-3. From this table, it is seen that method No. 1 is preferred for a near-term objective of building an improved rectenna since the test fixtures for developing the rectenna element are available and the spacings of the elements in the rectenna have already been determined to a fair approximation. Method No. 3, however, would seem to be the best approach in the long run because it gives a much better insight into the amount of mutual coupling which exists and how this coupling varies as a function of element spacing. It may also provide a means of evaluating the effects of a rapidly varying power density as a function of radius. This occurs n the edge of a rectenna composed of a relatively small number of dipoles when the rectenna is illuminated with a gaussian beam which is only slightly truncated.

Table 5-3. Approaches to 100% Absorption Efficiency in Rectenna

Method No.	Method Description	Confidence	Effort Involved	Evaluation
1	Develop rectenna element in expanded waveguide fixture and determine spacing between elements in rectenna by experiment.	High – Has been successfully used. Does not depend upon indirect methods of determining spacing of elements.	Medium – Two or three rectennas have to be constructed before best match is obtained. However, same elements will be used so that only cost of additional mounting plates and labor for mounting are required.	Best approach if objective is to build improved rectenna in minimum time and with minimum financial support.
2	Simulation of array in waveguide	Low – Cannot simulate broadside. Subject to error because of higher order modes.	High – Construction of new test gear and several sets of identical elements.	Not recommended.
3	Separate rectifier circuit from rectenna element. Determine scattering matrix for element and reduce reflection factor to zero by varying spacing between elements experimentally.	Medium in near-term because indirect methods of determining spacings are subject to error. High in long-term	High – Construction of new test fixtures and development of new test methods.	Probably best approach for the long-term. Gives better insight into problem. Uses smaller number of elements to determine proper spacing.

APPENDIX II

PRELIMINARY INVESTIGATION OF A FLEXIBLE RECTENNA

Pages 80 - 82 reprinted
from PT-2931, the Phase I
Final Report

3.4.2.3 Preliminary Investigation of a Flexible Rectenna

The concept of a flexible rectenna was investigated as part of the study. In this area the help of the microelectronics laboratory of the Bedford Laboratory of the Raytheon Company was enlisted. This laboratory has equipment for the bonding of beam leads, normally to a substrate consisting of a thin application of gold to alumina.

The flexible rectenna involves the concept of a flexible printed circuit which consists of both microwave circuits and dc-buss circuits to which are bonded the diode rectifiers. The general concept of the flexible printed circuit is shown in Figure 3-28. The proposed rectifiers are beam leaded devices made by integrated circuit techniques. One common configuration would be a bridge circuit of four diodes on a single chip with four beam leads 90° apart. Two of the beam leads connect to the dipole antenna and two connect to the dc buss. The bonding process itself is essentially a combination of pressure and temperature. A wobbling motion is imparted to the bonding tool.

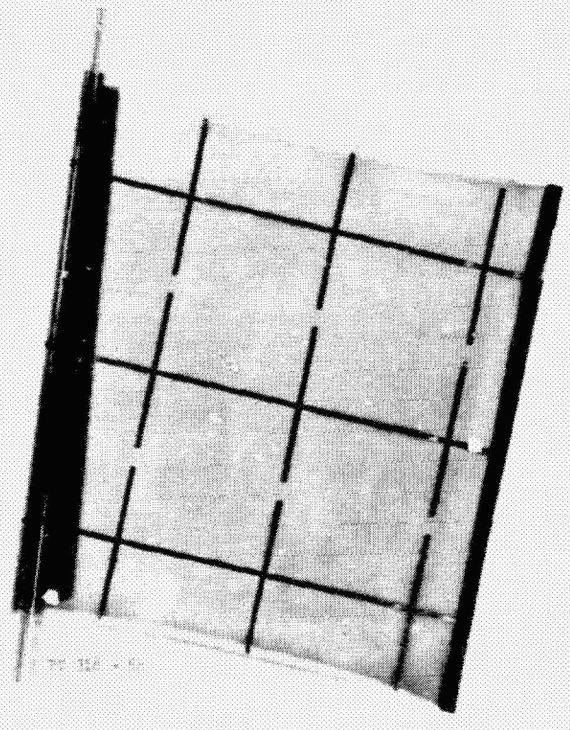

Figure 3-28. A possible physical configuration which future rectennas may assume. Rectenna is made in flexible form by employing printed circuit techniques on dielectric film material such as Kapton. Rectifiers perhaps made by integrated circuit techniques are bonded to the flexible printed circuit at appropriate points.

The first experiments involved attempting to bond mechanical samples of beam leaded devices to a substrate consisting of a 1/2 mil thick copper sheet laminated to two mil thick Kapton. This initial attempt was not successful because the force applied to the beam leads caused them to indent the copper, forcing the copper down into the Kapton substrate. The result was that the wobbling bonding tool rode on the surface of the copper as well as on top of the beam leads. In addition, it was felt that a gold plate on the copper would be desirable for future experiments.

To remedy the problem with respect to the indentation of the copper, a new Kapton-copper laminate was obtained in which the copper thickness was three mils, so that the copper would act as a heavy beam and would not bend. The Kapton, in this instance, was three mils thick. The surface of the copper was gold plated by the Techniques Laboratory in the Microwave Tube Operation of the Raytheon Company.

The experimental results with this new material were much more successful. A number of beam leaded devices were bonded. However, the bond fell short of perfection. In a standard test of the strength of the bond, in which a shear force is exerted on the beam lead device, only about 1/3 of the beam leads pulled away from the device and adhered to the gold plated surface of the copper. Upon inspection it was found that although the copper was not bonding, a coining operation was being performed in which the beam leads were actually being pressed down into the copper, the displaced copper flowing around the beam leads. Again, the limitation on the bonding was the riding of the bonding tool on the surface of the gold plated copper.

As a control experiment we then used the same pressure and temperature to bond a beam leaded device successfully to a "standard" substrate consisting of a gold film deposited on an alumina substrate. Because of the hardness of the alumina there was no coining of the substrate.

One way to overcome the coining difficulty would be to utilize a harder material, say, iron, on which a gold film had been deposited. The poor heat conductivity of the iron, however, might not be satisfactory from a heat dissipation point of view. Another better approach is to utilize a dispersion hardened copper which retains good heat conducting properties but which has a hardness level several times that of ordinary copper.

No doubt a suitable material in both hardness and heat conductivity could be found from which to construct the printed circuit. However, in subsequent discussion with D. Walters and R. Ilgenfritz of the Raytheon Bedford Laboratory, these experts in the bonding of beam devices expressed doubt as to the reliability of any assembly consisting of a flexible substrate with beam lead devices directly bonded to it. They highly recommended an intermediate step in which the beam lead device would be bonded to a thin small chip of alumina. This would not only solve the bonding problem, but the alumina chip would have a mechanical strength many times greater than the beam leads themselves. The alumina would have sufficient strength to help hold the flexible rectenna together so that large areas of the Kapton could be cut from the structure and more than make up for the additional small weight of the alumina. A good feel for the relative strength of the alumina chip versus the beam lead can be obtained by comparing the cross-section of the alumina chip which might be 0.060 inch square and ten mils thick with a beam lead which is 1/2 mil thick and 8 mils wide. The ratio of cross-sections is 150 to 1, and the alumina is probably stronger.

The information obtained from the experiments described above provides a basis for further investigation of the flexible rectenna concept.

APPENDIX III

EXPRESSION FOR LOSSES IN DIODE AS % OF MICROWAVE POWER INPUT THREE CASES

$$\frac{1.32}{V_{BR}}\sqrt{\frac{\eta Z_o}{2 R_L}} \quad (1 + \cos\theta) + \frac{\pi}{\theta}\frac{\eta}{R_L}\frac{1}{\text{Area}}\left(\frac{V_{BR}}{2500}\right)^{2.74} +$$

$$4.33 \times 10^{-22}\,(\text{Area})\left(V_{BR}\right)^{0.11}\omega^{2} V_B\,(1+\cos\theta)\sqrt{\frac{\eta Z_o R_L}{2}}$$

$$\left\{1 - \frac{\theta}{\pi} + \frac{\tan\theta}{\pi}\left[1 + \ell n\left(\frac{2}{1+\cos\theta}\frac{V_{BR}}{V_B}\sqrt{\frac{\eta R_L}{2Z_o}}\;\frac{\sin^2\theta}{\cos\theta}\right)\right]\right\}$$

where

V_{BR}	=	Reverse breakdown voltage
η	=	RF to DC efficiency
Z_o	=	Characteristic Impedance at Microwave Input to diode
R_L	=	DC load resistance
θ	=	1/2 conduction angle
Area	=	Area at junction in square centimeters.
V_B	=	Schottky barrier voltage

Case I Assume $\eta = 0.9$, $\theta = 45^\circ$, $R_L = 140$, $Z_o = 120$, $V_B = 0.9$, $\omega = (2\pi)(2.45 \times 10^9)$ and GaAs - PT

Then:

$$\% \text{ loss} = \frac{1.4}{V_{BR}} + \frac{(1.250 \times 10^{-11})(V_{BR})^{2.74}}{(\text{Area})} + 28.2\, V_{BR}^{0.11}\,(\text{Area}) + 8.4\, V_{BR}^{0.11}\,(\text{Area})\, \ell n\,(.66\, V_{BR})$$

Case 2 Assume $\eta = 0.9$, $\theta = 60^\circ$, $R_L = 140$, $Z_o = 120$, $V_B = 0.9$, $\omega = (2\pi)(2.45 \times 10^9)$ and GaAs - Pt

Then:

$$\% \text{ loss} = \frac{1.23}{V_{BR}} + \frac{(0.94 \times 10^{-11})(V_{BR})^{2.74}}{(\text{Area})} + 19.9\, V_{BR}^{0.11}\,(\text{Area}) + 4.3\,(\text{Area})\, V_{BR}^{0.11}\, \ell n\,(1.6\, V_{BR})$$

Case 3 (for Si- ω) Assume same values as Case 1, except $V_B = 0.5$

Then:

$$\% \text{ loss} = \frac{0.84}{V_{BR}} + \frac{(16.9 \times 10^{-11})(V_{BR})^{2.48}}{(\text{Area})} + 103\, V_{BR}^{-0.02}\,(\text{Area}) + 30.5\, V_{BR}^{-0.02}\,(\text{Area})\, \ell n\,(1.2\, V_{BR})$$